A study of selective vulnerability to diabetes of nerves supplying the ileum using *in vitro* models

Eleni Voukali

A thesis submitted for the degree of

Doctor of Philosophy

At the University College London

2013

Department of Cell and Developmental Biology

University College London

I, Eleni Voukali, confirm that the work presented in this thesis is my own. Where information has been derived from other sources, I confirm that this has been indicated in the thesis.

ELENI VOUKALI   21-05-2013

Abstract

Autonomic neuropathy is a complication of diabetes and, where the innervation of the gut is involved, results in disordered gut motility. *In vivo*, sympathetic nerves and subpopulations of enteric neurons supplying the ileum are differentially affected by diabetes. The overall of aim of this study was to establish whether such differential susceptibility could be reproduced i*n vitro* using wholemount preparations of myenteric plexus and sympathetic ganglion explants from the adult rat and to use such models to examine potential mechanisms underlying the development of neuropathy and its prevention. Preparations were exposed to a range of stimuli that mimic the diabetic environment including high glucose, advanced glycation endproducts (AGEs), carbonyl stress and oxidative stress. Evidence is presented that exposure of myenteric neurons to oxidative stress *in vitro* mimicked the effects of diabetes as reflected by increased expression of vasoactive intestinal polypeptide (VIP), decreased expression of neuronal nitric oxide synthase (nNOS) and unaltered calbindin expression. However, the mechanism underlying oxidative stress was not uniform, increased VIP expression only occurred on exposure to high glucose and carbonyl stress whereas decreased nNOS expression was only induced by AGEs. Neurons containing calbindin were resistant to all stimuli. Potential therapeutic agents produced differing effects depending on whether they primarily acted against oxidative or carbonyl stress. Using two photon microscopy and fluorescence lifetime imaging (FLIM), the effect of high glucose on reduced nicotinamide adenine (phosphate) (NAD(P)H) metabolism was investigated over time. Comparisons were made between sympathetic neurons from superior cervical ganglia (SCG), which are unaffected in diabetes, and from superior mesenteric/coeliac ganglia (CG/SMG) which develop axonal dystrophy. High glucose temporarily increased NAD(P)H levels selectively in the CG/SMG which coincided with a significant difference between the two ganglia in the fluorescence lifetime of free NAD(P)H. These results may explain the complex pattern of change that occurs in enteric nerves in diabetes.

Acknowledgments

I would like to thank Dr. Chris Thrasivoulou for his kind assistance and technical expertise on the expreriments with the multiphoton microscope.

I would like to acknowledge my gratitude to my supervisor and outstanding scientist Dr. Jill Lincoln, from whom I have learned much.

I would also like to acknowledge Dr. Hannah Shotton, Dr. Greg Campbell, Dave Blundell, Jane Pendjiky, Dr. Anthony Pullen for their invaluable assistance throughout this thesis.

Thanks also, to my family and friends for their support all these years.

Dedicated to my father

Abbreviations

5HT   **5-hydroxytryptamine (Serotonin)**

ACh   **Acetylcholine**

ACTION   **Chronic aminoguanidine treatment in overt diabetic neuropathy**

ADP/ATP   **Adenosine diphosphate/triphosphate**

AGE   **Advanced glycation end product**

AH   **After-hyperpolarisation**

ANS   **Autonomic nervous system**

B1   **Thiamine**

B3   **Nicotinamide**

BSA   **Bovine Serum Albumin**

CEL   **N6-(1-carboxylethyl)-lysine**

CGRP   **Calcitonin gene-related peptide**

CML   **N6-carboxymethyl-lysine**

CNS   **Central nervous system**

CG/SMG   **Coeliac/superior mesenteric ganglionic complex**

DCCT   **Diabetes control and complications trial**

DMSO   **Dimethylsulfoxide**

DNA   **Deoxyribonucleic acid**

DOLD	**3-deoxyglucosome-derived lysine dimers**
DRG	**Dorsal root ganglion**
ELAV	**Embryonic lethal, abnormal vision**
ENS	**Enteric nervous system**
FADH2	**Flavin adenine dinucleotide**
FLIM	**Fluorescence lifetime imaging microscopy**
GABA	**Gamma aminobutyric acid**
GI tract	**Gastrontestinal tract**
GOLD	**Glyoxal-derived lysine dimers**
GSH/GSSG	**Glutathione**
HbA1c	**Glycated hemoglobin levels**
HBSS	**Hanks balanced salt solution**
ICC	**Interstitial cells of Cajal**
IGF-1	**Insulin-like growth factor 1**
IMG	**Inferior mesenteric ganglion**
IPANs	**Intrinsic Primary Afferent Neurons**
LDL	**Low density lipoproteins**
MAPK	**Mitogen associated protein kinases**
MOLD	**Methylglyoxal-derived lysine dimers**
NA	**Noradrenaline**
NAD(H)	**Nicotinamide adenine dinucleotide**

NADP(H)   Nicotinamide adenine dinucleotide phosphate

NANC   Non-adrenergic non-cholinergic

NFκB   Nuclear factor κB

NGF   Nerve growth factor

NO   Nitric oxide

NOD   Non obese diabetic

nNOS   Neuronal nitric oxide synthase

NPY   Neuropeptide Y

PARP   Poly(ADP ribose)polymerase

PBS   Phophate-buffered saline solution

PFA   Paraformaldehyde

PI3K   Phosophoinositol-3-kinase

PKC   Protein kinase C

RAGE   Receptor for AGE

RNA   Ribonucleic acid

RNS   Reactive nitrogen species

ROS   Reactive oxygen species

S   Synaptic

SCG   Superior cervical ganglia

SOD   Superoxide dismutase

STZ   Streptozotocin

TCA   **Tricarboxylic Acid**

TCSPC   **Time correlated single photon counting**

TH   **Tyrosine hydroxylase**

TUNEL   **Terminal deoxynucleotidyl Transferase Biotin-dUTP Nick End Labeling**

VIP   **Vasoactive intestinal polypeptide**

Contents

List of Figures

plexus/muscle preparations.

List of tables

Chapter 1: General introduction

1.1 Diabetes and gastrointestinal problems

The incidence of diabetes mellitus is reaching epidemic proportions, particularly in the Western world. In addition to the control of the diabetic condition, the treatment of complications that arise as a consequence of diabetes represents a significant burden to health care costs. Complications due to diabetes involving the gastrointestinal tract (GI tract) are referred to as enteropathy or gastrointestinal neuropathy (Camilleri, 1996). Diabetic gastrointestinal neuropathy may cause symptoms such as dysphagia, heartburn, nausea, vomiting, abdominal pain, constipation, diarrhea and fecal incontinence. Epidemiological studies of diabetic gastrointestinal neuropathy provide conflicting results depending on the population studied. 76% of diabetic patients may present with a complex of gastrointestinal symptoms, the most common being constipation (Feldman & Schiller, 1983;Bytzer et al., 2001). Gastrointestinal symptoms can lead to dangerous complications such as ketoacidosis, infection and bezoar formation and further glycaemic deregulation (Feigenbaum, 2006). In many cases, these symptoms are due to abnormal gastrointestinal motility suggesting pathophysiology of the autonomic and enteric nervous systems (ANS, ENS) leading to motor and sensory abnormalities in the GI tract, the nature of which are not completely understood. At present there is an absence of markers that accurately predict which diabetic patients are at risk of developing enteropathy.

1.2 Diabetes and peripheral neuropathy

Diabetes mellitus is associated with a wide spectrum of neuropathy syndromes. Diabetic peripheral neuropathy has been defined as the presence of symptoms and/or signs of peripheral nerve dysfunction in people with diabetes, after exclusion of other causes (Boulton et al., 1998). It affects the sensory, autonomic or motor nerves and, in a subclinical form, the nerves are affected without overt symptoms. Depending on the nerves and the level that are affected, diabetic neuropathy can appear mild or asymptomatic or be disabling or painful, causing a serious decline in the quality of life of the diabetic patient (Greene et al. 1999).

Reports about the prevalence of diabetic neuropathy vary from 10% up to as high as 90% in a subclinical form, depending on the duration and severity of diabetes. This variability also derives from the difficulties in diagnosis and its early detection in routine diabetic care.

Many different classification systems have been proposed because of a wide range of clinical presentations. A broad separation into rapidly reversible or more persistent phenomena has been proposed by Thomas (Thomas, 1997). Rapidly reversible syndromes can be categorized as "hyperglycaemic neuropathy" and include minor sensory symptoms, reduced nerve conduction velocity and resistance to ischaemic conduction failure. Focal and multifocal lesions give rise to cranial, thoraco-abdominal, and limb neuropathies, including proximal lower limb motor neuropathy (diabetic amyotrophy). Diabetic amyotrophy, initially considered resulting from

metabolic changes, and later ischaemia, is now attributed to immunological changes. Focal neuropathies tend to occur after 50 years of age and mostly in patients with long standing diabetes. The overall prognosis of focal neuropathies is good.

Of the more persistent phenomena, distal symmetric polyneuropathies predominantly affect sensory and autonomic function and are the most common manifestation, accounting for 75% diabetic neuropathies (Bansal et al., 2006). Distal symmetric polyneuropathies are distal axonopathies of the dying-back type (Cavanagh, 1979). The fully expressed syndrome is a symmetrical distal lower limb sensorimotor polyneuropathy with a varying degree of autonomic involvement (Sinnreich et al., 2005). It is predominantly sensory, but in severe cases distal weakness and foot drop may be present. Almost with no exception sensorimotor involvement is restricted to lower extremities of the lower limbs. Large fiber dysfunction is assessed by nerve conduction velocity tests and small fibres dysfunction by skin biopsies. New diagnostic tools are appearing but need further evaluation (Papanas & Ziegler, 2011).

 Multiple clinical studies suggest that autonomic dysfunction is a common characteristic of both type 1 and type 2 diabetes. Autonomic neuropathy can affect the function of virtually every organ because typically it occurs as a system-wide disorder affecting all parts of the autonomic nervous system (Vinik et al., 2003). The cardiovascular, gastrointestinal and urogenital systems can all be affected leading in a range of debilitating symptoms. Somatic peripheral neuropathy is usually concurrent. Standard reliable non-invasive measures are used to identify autonomic failure and quantify disease severity. Diagnosis of diabetic autonomic neuropathy commonly includes tests on heart rate variability to measure the cardiovagal parasympathetic function, the Valsalva Maneuvre and various sudomotor tests to assess the sympathetic system

(Weimer, 2010). Tests to evaluate the function of the gastrointestinal motility require special expertise and are not standard practice.

1.3 Innervation of the GI tract

The proper function of the GI tract requires the integrated activity of the central nervous system (CNS), the ANS, and the ENS. The ENS is a neural subsystem of the ANS, incorporated in the walls of the gut. Because their cell bodies are located intramurally the neurons are termed enteric. Although, the activity of the ENS is to a large extent independent *in vitro* (Langley, 1921), the autonomic ganglia modulate the function of the ENS and, forming the extrinsic innervation of the GI tract, they serve as integrating centres between the ENS and the CNS. Sensory inputs from the GI tract enter the spinal cord via the dorsal roots and subsequently synapse on spinal cord neurons that supply higher centres in the brain. Higher brain centres include the frontal cerebral cortex, stria terminalis, paraventricular nucleus of the hypothalamus, and the central nucleus of the amygdala, all projecting into the vagal outflow centre in the medulla oblongata. The effector systems of the GI tract innervation are the musculature, mucosal epithelium, vasculature, immune cells, enteric neurons and interstitial cells of Cajal (ICC).

.

1.3.1 Extrinsic Innervation

The autonomic innervation of the GI tract comprises an efferent system sending signals from the CNS. Efferent neurons modulate motor and secretomotor functions in the GI tract operated by the ENS.

Generally, there are two types of efferent neurons in the ANS, the preganglionic neuron and the postganglionic neuron. Preganglionic cell bodies are found in the CNS and postganglionic cell bodies are located outside the CNS and their fibres end in the walls of the gut (see Jacobson & Marcus, 2008). The ratio of sympathetic preganglionic to postganglionic neurons is 1:10. Conversely, the divergence is considerably less for the parasympathetic neurons, which have a preganglionic to postganglionic ratio of about 1:3 neurons. Postganglionic autonomic fibres synapse with a vast amount of effector neurons. In this way, autonomic neurons function as command neurons that inhibit or stimulate neural circuits in the ENS. These circuits generate organised and repetitive behavioural patterns associated with gastrointestinal motility or secretion (Wood, 2008).

The GI tract receives dual extrinsic innervation, sympathetic and parasympathetic. In general, sympathetic nerves inhibit peristalsis and secretion and parasympathetic nerves stimulate these functions. Blood flow in the crypts and muscle layers, epithelial transport of fluids and electrolytes, motility and release of hormones from the enterochromaffin cells are activities that are controlled by the ANS (Lundgren, 2000). This occurs indirectly through postganglionic synapses with enteric neurons or directly as sympathetic and parasympathetic fibres interpenetrate the enteric plexuses and influence the crypt epithelium (Lundgren, 2000;Powley, 2000).

Different segments of the GI tract are innervated by different autonomic ganglia. The stomach as far as the proximal colon receives sympathetic input from the CG/SMG which is located on the celiac and superior mesenteric arteries. Renal ganglia lie laterally to the CG/SMG mass (Decktor & Weems, 1981). Preganglionic fibers of CG/SMG originate from thoracic levels T5-12 of the spinal cord to form the greater and lesser splachnic nerves. They bypass the sympathetic trunk without synapsing to activate the CG/SMG. Postganglionic fibres from there are distributed to the stomach, pancreas, small intestine, the ascending portion of the colon and the kidneys. Parasympathetic input to these areas comes from the dorsal motor nucleus of the vagus nerve and postganglionic cell bodies are located close to the viscera. Also, there is a different degree of innervation in the stomach and small intestine in comparison to oesophagus, showing a less direct parasympathetic control in these areas.

The distal colon as far as the rectum receives sympathetic input from the inferior mesenteric ganglion (IMG) found on the inferior mesenteric artery. The sympathetic preganglionic fibers originate from the first and second lumbar segments of the spinal cord to end in the IMG. From there, postganglionic fibres innervate the descending colon, the rectum, the urinary bladder, the ureter and the external genitalia. These areas receive parasympathetic input from neurons that originate in the second to forth sacral spinal cord levels, form the pelvic nerve and synapse with postganglionic neurons very close to the target organs (Snell, 2010).

Neuromuscular junctions in ANS have the following characteristics: 1) the autonomic effector is not a single cell; 2) the unmyelinated postganglionic fibres do not form specific pre- and postsynaptic sites but varicosities. These are up to 2 μm in diameter and packed with vesicles and mitochondria. And 3) neurotransmitters are released *en passage* from varicosities inducing excitatory or inhibitory junction

potentials to facilitate or prevent action potentials (see Milner et al., 1999). Parasympathetic postganglionic neurons release acetylcholine (ACh) and sympathetic postganglionic neurons release noradrenaline (NA). The action of these two neurotransmitters is often antagonistic. ACh is also a neurotransmitter in preganglionic autonomic neurons. However, there is also a multitude of non adrenergic non cholinergic (NANC) substances utilised as neurotransmitters such as peptides, purines and gases cotransmitted with and modulating the release of the classic neurotransmitters NA and ACh (Burnstock, 1976;Milner et al., 1999;Burnstock, 2004). For example, postganglionic sympathetic nerves in CG/SMG can co-release in varying proportions NA, somatostatin and neuropeptide Y (NPY) (Macrae et al., 1986). Postganglionic parasympathetic nerves can co-release ACh, VIP, adenosine triphosphate (ATP) and nitric oxide (NO). Besides different neurochemical properties (or chemical codes), different functional groups of autonomic nerves have distinct electrophysiological properties (Janig & McLachlan, 1992).

1.3.2 Extrinsic primary afferent/sensory innervation of the GI tract

Extrinsic afferent innervation from the GI tract involves extrinsic sensory neurons with receptors sensitive to multiple stimuli. Afferent fibres from the ENS send sensory information that are relayed in the vagus nerve or dorsal root ganglia and then sent to higher brain centres. This sensory input also affects the local processing circuit in ENS and the prevertebral sympathetic ganglia. Intramurally, the intestinofugal neurons project to prevertebral ganglia. Non-painful physiologic sensations that do not reach consiousness include responses to thermal or mechanical stimuli such as muscle

tension and mucosal brushing, or luminal chemical stimuli such as pH, osmolarity and the concentration of glucose, amino acids and long chain fatty acids. Sensory information also consists of nociceptive signals.

The visceral afferent neurons have their endings in the gut wall and their cell bodies, similarly to the somatic afferent neurons, are located in the dorsal root ganglia (DRG) ending in the spinal cord. Their fibres pass through the prevertebral CG, SMG or IMG and through the paravertebal ganglia, influencing the efferent transmission taking place in the autonomic plexuses. Sensory fibres are also contained in the vagus and pelvic nerves and terminate in the brain stem and lumbosacral spinal cord, respectively. The vagal afferents course from the nucleus tractus solitarius and innervate the GI tract from the esophagus to the transverse colon. Sensory fibres coursing from the lumbosacral spinal cord innervate the rest lower parts of the GI tract (Gebhart, 2000;Wood, 2007).

1.3.3 Intrinsic innervation

The ENS comprises the intrinsic innervation of the GI tract and involves as many neurons as found in the grey matter of the spinal cord (see Furness, 2005). The structure, function, and neurochemistry of enteric ganglia differ significantly from other autonomic ganglia. Unlike other autonomic ganglia, ENS ganglia are interconnected and, like in the brain and spinal cord, the ENS works with three functional categories of neurons identified as sensory, inter-, and motor neurons (see Wood et al., 1999;Hansen

2003b). The ENS is involved in a range of activities including motility, secretion, microcirculation and immunologic and inflammatory responses. Thus the effector systems of the ENS are the enteric neurons themselves, smooth muscle cells responsible for gastrointestinal motility; mucosal secretory cells; gastrointestinal endocrine cells; the gastrointestinal microvasculature that maintains mucosal blood flow during intestinal secretion; fibroblast–like cells; and the immunomodulatory and inflammatory cells of the gut that are involved in mucosal immunologic, allergic, and inflammatory responses. The ENS may influence these targets directly or may do so indirectly through intermediate cells, which include endocrine cells, the interstitial cells of Cajal (ICCs), and cells of the immune system, such as mast cells (see Hansen, 2003c).

The general structure of the ENS is similar from the oesophagus to the rectum. The neuronal cell bodies are grouped into small ganglia that are connected by bundles of nerve processes forming two major plexuses, called the myenteric (or Auerbach's) plexus and the submucosal (or Meissner's) plexus (see Furness, 2005). The neurons in the myenteric plexus lie between the outer longitudinal muscle and circular muscle layers and predominantly regulate motility. The neurons in the submucosal plexus lie in the submucosa near the inner surface of the circular muscle and predominantly regulate secretion of water and electrolytes across the intestinal epithelium.

Different types of neurons in the myenteric plexus project their fibres to neurons in the same plexus, the submucosal plexus and prevertebral ganglia, and to cells in the circular and longitudinal muscle layers (see Hansen, 2003a). The myenteric plexus provides motor innervation to the two muscle layers and secretomotor innervation to the mucosa. In the striated-muscle portion of the esophagus, the myenteric plexus innervates motor end plates with NO and calcitonin gene-related peptide (CGRP). This innervation is unique to the esophagus (Worl et al., 1994).

The submucous plexus is best developed in the small intestine, where it plays an important part in secretory control (see Goyal & Hirano, 1996). Besides innervating the glandular epithelium, neurons in the submucous plexus innervate the muscularis mucosa, intestinal endocrine cells, and submucosal blood vessels.

Glial cells are an integral component of the ENS, and they outnumber enteric neurons. Enteric glial cells resemble the astrocytes of the CNS; their laminar extensions cover most of the surface of enteric neuronal cell bodies. They participate in modulation of inflammatory responses in the intestine, the regulation of neurotransmission and information processing in the gut (Ruhl, 2005).

1.3.3.1 Coordination of enteric neurons

Enteric neurones work in assemblies and generate cyclic patterns of behaviour (motility, secretory etc.) (see Furness, 2005). Neural circuits formed by interneuronal synaptic connections called central pattern generators generate organized and repetitive motor patterns. The entire sequence of the motor program may be initiated by input signals from a single neuron called a command neuron (Wood et al., 1999;Kunze & Furness, 1999;Wood, 2008). Thus, subsets of neural circuits control distinct patterns of behaviour in each effector system and coordinate activity of multiple systems. Integration of the patterns of behaviour is the result of reflexes. Reflexes are a form of neural-mediated behaviour of effector systems as a response to stimulation of sensory neurons (Wood et al., 1999). For example, the peristaltic reflex is the response to distension or mucosal stroking in the wall of the intestine and involves contraction of the circular muscle coat above the site of stimulation and relaxation of the circular

muscle below the site. Reflexes involve both plexi and during normal motility the longitudinal and circular muscle layers are synchronously activated (Spencer & Smith, 2001).

1.3.3.2 Classification of enteric neurons

Different methods, including light and electron microscopy, immunohistochemistry, electrophysiological analysis, intracellular dyes, and retrograde tracing of neuronal projections have allowed the classification of enteric neurons with respect to morphological, neurochemical, electrical and functional criteria (see Wood et al., 1999;Hansen, 2003b).

a) Morphological and electrical classification

According to their morphology, neurons have been classified into Dogiel type I to type VII. Although these seven morphologic forms of neurons have been identified, the majority are types I-III. Type I neurons have many processes and a single long, thin process, whereas type II neurons are multipolar and have multiple long processes. Type III are similar to type I but with a shorter axon (Wood, 1994;Furness, 2000;Hansen, 2003b;Furness, 2005).

Synaptic (S) and after hyper-polarisation (AH) types are distinguished by their electrophysiological properties. AH type neurons have prolonged hyper-polarisation

after they fire an action potential that inhibits further excitation. AH neurons lack a

prominent fast excitatory synaptic input, but they do receive slow synaptic input, which

regulates their excitability. S Neurons with synaptic type electrophysiological behaviour

have the morphology of Dogiel type I neurons, whereas the AH after hyper-polarisation

type are most often Dogiel type II (Wood, 1994;Furness, 2000; Hansen, 2003b) .

b) Functional classification

The neurons that make up the ENS can be widely classified by functional

criteria as sensory, interneurons, motor or secretomotor neurons (Goyal & Hirano,

1996;Hansen, 2003b). Furness describes 14 functionally defined neuron types, each

with a characteristic combination of morphological, neurochemical and biophysical

properties (Furness, 2000;Furness, 2005). In general, sensory neurons connect with each

other primarily through slow synaptic excitation and thus constitute a self-reinforcing

network. Similarly, the ascending and descending interneurons form interconnecting

chains. Lastly, the muscle motor neurons and secretomotor neurons innervate muscle

and the mucosa, respectively (Hansen, 2003b).

Intrinsic Primary Afferent Neurons (IPANs)

Intrinsic and extrinsic sensory neurons have receptor regions specialized for

detecting changes due to thermal, chemical, or mechanical stimuli. The intrinsic sensory

neurons or IPANs are located in both the myenteric and submucous plexuses. Thermal,

chemical or mechanical changes in energy are transformed into signals that induce

action potentials. These are subsequently transmitted along sensory nerve fibers to stimulate other enteric or extrinsic neurons (Wood et al., 1999).

IPANs maintain numerous connections to the mucosa and fibres that run through the circular muscles. They make direct contact with motor neurons and interneurons projecting circumferentially to them in the surrounding myenteric and submucous plexuses, and with the postganglionic termini of extrinsic autonomic nerve fibers. IPANs also forward information from the enterochromaffin cells that are located in the mucosa, release serotonin (5-HT) and facilitate GI function. Connections finally include endocrine and immune cells located in the gut. Apparently the role of the interaction with immune cells is protective (Hansen, 2003a).

Electrophysiologically, IPANs are characterized as AH neurons and morphologically are type II. They typically contain calbindin, ACh, CGRP and substance P (see Goyal & Hirano, 1996).

Interneurons

Interneurons are located between IPANs and the motor or secretomotor neurons. They process sensory information and signals from other types of neurons to control the behaviour of motor neurons. Interneurons of the enteric nervous system form networks with numerous connections making multisynaptic pathways. Thus, the various groups of interneurons comprise integrative circuits that organize reflex responses to sensory inputs (see Goyal & Hirano, 1996;Wood et al., 1999).

At least one type of ascending and three types of descending interneurons have been characterised in guinea pig (Furness, 2000). Several subgroups of interneurons have been defined on the basis of their neurotransmitter content. The ascending interneurons are mainly cholinergic, whereas the descending ones have a complex

chemical coding typically including ACh, NO, VIP, 5-HT, and somatostatin. ACh/ NO/VIP/ somatostatin neurons are involved in local motility reflexes, whereas ACh/ 5-HT neurones are involved in the local secretomotor reflexes. Interneurons are both AH and S types and usually Dogiel type II neurons (see Hansen, 2003c;Smith et al., 2007).

Motor neurons

Motor neurons are the final pathways to the effector systems. There are five broad types, and many subtypes, of enteric motor neurons: excitatory neurons to gut muscle, inhibitory neurons to gut muscle, secretomotor / vasodilator neurons, secretomotor neurons that are not vasodilator and neurons innervating enteroendocrine cells, such as those innervating the gastrin secreting endocrine cells of the stomach (Furness, 2000).

Muscle motor neurons. The longitudinal and the circular muscle layers are innervated by both inhibitory and excitatory motor neurons. These are S/Dogiel type I neurones. The motor neurons project anally or orally to the muscle. Transmission is predominantly muscarinic cholinergic and tachykinergic (substance P and neurokinin A) in excitatory neurons. Inhibitory neurons typically utilise NO, VIP, ATP, and possibly pituitary adenylate cyclase-activating polypeptide, gamma aminobutyric acid (GABA), NPY and carbon monoxide as transmitters (see Goyal & Hirano, 1996;Wood et al., 1999;Hansen, 2003a;Hansen, 2003b).

Fibroblast-like cells and ICCs are cells concentrated in close apposition with the varicosities of enteric motor neurons and smooth muscle cells. The physiological role of fibroblast-like cells has not been established but they seem to participate in motor neurotransmission. ICCs are non neuronal cells that generate electrical slow waves and function as pacemakers. Action potentials of motor neurons and pacemaker potentials

spread rapidly to every smooth muscle cell in three dimensions. The activity of inhibitory motor neurons determines when the slow waves initiate a contraction, as well as the distance and direction of spread once the contraction has begun (Wood, 2007).

Inhibitory motor neurons fire continuously and release neurotransmitters to inhibit contraction (Wood, 2007). Contraction can only occur when inhibitory neurons cease to fire after input from interneurons. The opposite occurs in the sphincters where inhibitory motor neurons only fire in the appropriate timing for coordination of the opening of the sphincter. Inhibitory neurons are normally switched off orally, resulting in contractile activity that spreads in the anal direction. During vomiting, the inhibitory motor neurons must be switched off in the reverse direction, anally, for the propulsion to travel from the small intestine towards the stomach.

Secretomotor and vasomotor neurons. Secretions and blood flow are controlled by secretomotor and vasomotor enteric neurons, respectively. Most secretomotor neurons have their cell bodies located in the submucosal plexus. Other submucosal neurons innervate the muscularis mucosae. Vasomotor (dilator) neurons also have their cell bodies in the submucous layer. There are two main types of intestinal secretomotor/vasodilator neurons: cholinergic and non-cholinergic. ACh released from the cholinergic neuron acts on muscarinic receptors on the mucosal epithelium. The non-cholinergic neurons appear to mediate most of the local reflex responses and utilise VIP as a transmitter (see Furness, 2000;Hansen, 2003b).

c) Chemical Classification

Finally, neurotransmitter content may be used as a classification tool (Kunze & Furness, 1999;Hansen, 2003b). Enteric neurotransmitters are either small molecules

(e.g. ACh, GABA, 5-HT, ATP), larger molecules (neuropeptides) or gases (NO and carbon monoxide). Functional subtypes of neurons express particular unique combinations of transmitters and other molecules, a phenomenon known as *chemical coding*. Enteric neurons contain many combinations of transmitters, transmitter-related molecules, such as choline acetyltransferase, and other regulatory molecules, such as calcium-binding proteins (e.g. calbindin, calretinin) that can be considered and used as a chemical code for identification of functional subtypes. The chemical code of a functional group may vary depending on the species and the intestinal segment. ACh is the major excitatory transmitter of the enteric nervous system and neurons that contain VIP or nNOS are inhibitory motor neurons. Using colchicine to enhance VIP-immunolabelling, 90-100% of nNOS-containing myenteric neurons have been reported to contain VIP in the mouse and guinea-pig ileum (Costa et al., 1992; Qu et al., 2008).

1.4 Changes in intrinsic and extrinsic nerves due to diabetes mellitus

When neuropathy occurs, gastrointestinal functions (motility, secretion etc.) are disturbed, depending on the subpopulation of neurons affected. For example, loss or malfunction of inhibitory motor neurons is the pathophysiological starting point for random contractions spreading in the uncontrolled syncytium. These random contractions result in pseudoobstruction, spasticity and sphincteric achalasia (or failure to relax) (Wood, 2007). Secretomotor neuronal hyperactivity is associated with

neurogenic secretory diarrhea and hypoactivity is associated with decreased secretion and a constipated state. Primary causes of abdominal pain of digestive tract origin are hypersensitivity or lower sensory threshold of sensory mechanoreceptors to distension and extensively strong muscular contractions (however it may also reflect abnormal processing of more central pathways in the spinal cord or/and in the brain). Therefore, knowledge of the gastrointestinal innervation is required for understanding the pathophysiology of ENS due to diabetes mellitus.

1.4.1 Clinical diabetes

Neuropathologic studies of human diabetic autonomic neuropathy suggest a prominence of autonomic nerve terminal damage or degeneration in various end organs, in the absence of significant neuronal loss within sympathetic ganglia (Schmidt et al., 1993). In an extensive study of human biopsies, the neuropathologic hallmark of diabetic autonomic neuropathy was neuroaxonal dystrophy, markedly swollen structures originating as distal axonopathy, involving terminal axons (Schmidt et al., 1993; Schmidt, 2002). It was also noted that neuroaxonal dystrophy in diabetes preferentially involved the prevertebral CG/SMG and largely spared the paravertebral SCG.

In parasympathetic nerves, and specifically in the vagus nerve and its projections, axonopathy is also described but not with consensus. No morphologic abnormalities of the gastric wall or abdominal vagus were identified in diabetic gastroparesis using conventional histology techniques (Yoshida et al., 1988). This evidence was challenged by an ultrastructural study of vagus nerves from diabetic patients who had undergone vagotomy. The vagus nerve showed pathological changes

including: reduced myelinated fibre density, degeneration and regeneration of unmyelinated fibres, and capillary basement membrane thickening (Britland et al., 1990). In another study the conduction velocity of afferent vagal pathways were reduced, suggesting vagal neuropathology (Tougas et al., 1992).

Abnormal relaxation of the gastric fundus or excessive contraction of pylorus and small intestine of diabetic patients has been described as indicative of excitatory-inhibitory motor neuron pathology (Camilleri & Malagelada, 1984;Mearin et al., 1986;Samsom et al., 1998).

1.4.2 Animal models of diabetes

In humans, it is difficult to examine the nerves of autonomic nervous system, particularly those innervating the GI tract using non-invasive techniques (Samsom & Smout, 1997). In addition, the available information from diabetic patients is limited by the relatively small number of studies and the difficulties in obtaining biopsies and controlling for variables, such as the type and duration of diabetes and the adequacy of glycemic control. For this reason, research studies have extensively used rodent models to characterise and identify changes in intrinsic and extrinsic innervation in various segments of the GI tract during diabetes. Unlike many animal models of diabetic somatic sensory polyneuropathy, autonomic neuropathy in rodent animals shows many of the neuropathological features described in human subjects (Schmidt, 2002).

There are three main categories of animal models of diabetes: a) those in which type 1 diabetes is induced by a chemical toxin (streptozotocin, STZ, or alloxan) that selectively destroys the insulin secreting pancreatic islet cells. The STZ-induced

diabetic rat is the most commonly used animal model mainly for practical reasons (see sections 1.4.3.1 and 1.4.3.2); b) those in which strains of mice or rats that are genetically predisposed to developing either type 1 or type 2 diabetes are selectively bred and c) dietary models of diabetes (Lincoln & Shotton, 2008;DeAngelis et al., 2009).

Two spontaneously diabetic rat strains (BB/Wor and BBZDR/Wor), that are closely related genetically, enable the comparison of neuropathic changes in type 1 and type 2 diabetes since the BB/Wor rat is a hyperglycaemic, hypoinsulinaemic model of type 1 diabetes and the BBZDR/Wor rat is a hyperglycaemic, hyperinsulinaemic model of type 2 diabetes. The onset of diabetes is confirmed by glucosuria, weight loss and hyperglycaemia.

The non-obese diabetic (NOD) mouse is a model of insulin deficiency. Mice develop diabetes as the result of T-cell mediated autoimmune attack on the pancreatic islets, a process which begins at approximately 4–8 weeks of age (Sreenan et al., 1999). There is a greater incidence in females (80%) than males. NOD mice are hypoinsulinaemic and hyperglycaemic and require insulin replacement to survive. Another model for insulin deficient spontaneous diabetes is the Wistar Bonn/Kobori rat. These animals develop hyperglycaemia, glucosuria, hypoinsulinaemia and glucose intolerance (Nakama et al., 1985). The disease is prominent at 8–9 months and is seen only in males.

Models for type 2 diabetes are obese rodents with gene mutation(s) in leptin production or metabolism. For example, the Zucker strain, first described in the 1960s (Zucker, 1965), has a mutation in the leptin receptor gene resulting in impairment in the ability of leptin to suppress food intake. The genetically diabetic db/db mouse (BKS.Cgm+/+Leprdb/j) used as a model of insulin resistant type 2 diabetes also has a

leptin mutation resulting in hyperglycemia, insulin resistance and hyperinsulinemia (Chen et al., 1996). Other genetic obese models are KKAy and ob/ob mice.

Finally, the use of dietary methods for the induction of diabetic states is common, particularly because of the relevance to the human condition (DeAngelis et al., 2009). For example, the rationale for the use of high fructose as a test diet comes from the predominance of high fructose corn syrup in processed food and increased consumption of such food in Western society.

1.4.3 Experimental studies

1.4.3.1 Enteric neurons

Gastrointestinal dysfunction in diabetes has been extensively investigated in experimental studies based on the hypothesis that pathological changes in the enteric nervous system underlie gastrointestinal symptoms. There is considerable evidence for this hypothesis. However, reported changes do not give a straightforward conclusion.

One reason might be the different animal models used. For example, NOD mice have a short lifespan (5–8 weeks after onset of diabetic symptoms) and are difficult to study because of the rapid progression of the disease (Watkins et al., 2000). NOD mice show early onset and marked neuropathy in the prevertebral sympathetic ganglia. A comparative study demonstrated that the severity of the autonomic damage is much greater in NOD mice than in STZ treated animals (Schmidt et al. 2003). Also, in another study, STZ was suggested to be responsible directly for some neuronal reduction in the duodenum (Buttow et al., 1997).

In addition, using the STZ-induced diabetic rat, there is extensive evidence that enteric neuronal subpopulations respond differently to diabetes. Some exhibit

degeneration, for example VIP neurons and extrinsic NA-containing nerve fibresfibres (Lincoln et al., 1984, Belai et al. 1988). However, CGRP-containing nerve fibres (intrinsic and/or extrinsic) exhibit a loss of neurotransmitter without evidence of degeneration (Belai et al. 1988). Finally some are unaffected, for example Substance P containing enteric neurons (Belai et al. 1985). Similarly in Crohn's disease, a chronic disease that affects the intestine, the enteric neuronal changes in neurochemical composition are not homogeneous either (Belai et al., 1997). It is interesting to note that nerves that contain the same neurotransmitter but innervating a specific region of GI tract are also differentially affected in diabetes (Belai et al., 1991). Thus, neurochemical plasticity or morphometric changes not only depend on the animal model used but also depend on the GI region, diabetes duration and the age of the animal.

There is a relatively common agreement that inhibitory neurons are particularly affected in diabetes in comparison to intrinsic excitatory neurons. Numerous studies have investigated the expression of nNOS in the GI tract arguing that downregulation of the enzyme can be one of the main contributors of the dysmotility of the gut. Reduction in intestinal nNOS activity is associated with an impairment of the NANC relaxation (Martinez-Cuesta et al., 1995). Tagahashi et al. and Wrzos et al. in 1997 found reduction of NOS in gastric myenteric plexus of BB/Wor and STZ rats using various methods of analysis (Takahashi et al., 1997; Wrzos et al., 1997). Similar changes were found in NOD and obese mice in antrum and duodenum (Spangeus et al., 2000; Spangeus & El-Salhy, 2001). In the duodenum and ileum of STZ rats and the jejunum of BB/Wor rats, nNOS activity was also reduced (Martinez-Cuesta et al., 1995; Shotton & Lincoln, 2006;Zandecki et al., 2008). However, one study reported an increase in the tissue content of nNOS, but not the number of cell bodies in STZ-diabetic mice

(Adeghate et al., 2003) and another did not find any difference in nNOS levels in the small intestine and colon (Wrzos et al., 1997).

Differential effects of diabetes have also been reported in the intrinsic inhibitory motor nerves containing VIP. In the gastric and intestinal myenteric plexus, the number of VIP-containing neurons and/or levels of VIP protein and mRNA have been reported to be increased, unchanged or decreased in response to diabetes (Belai et al., 1985; Belai et al., 1988;Belai et al., 1991;Belai et al., 1993;Adeghate et al., 2001). Using electron microscopy, Loesch et al. reported disrupted structural integrity of VIP containing neurons with degenerative processes occurring within the axons (Loesch et al., 1986). A study of VIP release following nerve stimulation suggested that impaired release of VIP at the terminal site and/or defective axonal transport may account for the accumulation of VIP in the neuronal cell body (Belai et al., 1987). VIP mRNA is also increased in diabetic rats indicating either defective mRNA breakdown or increased synthesis (Belai et al. 1993). However, a longer duration of diabetes results in a decrease in the number of VIP-positive cell bodies and VIP levels in the ileum and proximal colon, together with a decrease in density of VIP-positive fibres. To date there is no information in the literature as to whether the changes in VIP occur in nNOS-containing neurons. The concentration of galanin, another inhibitory peptide, was reduced in the colon of obese diabetic mice (El-Salhy, 1998). However, an increase in galanin was observed in colon of NOD mice (El-Salhy, 2001) and ileum of 12-week-old STZ-induced diabetic rats (Belai et al., 1996).

In contrast, cholinergic, serotoninergic and substance P-containing nerves were intact in the ileum-myenteric plexus of 8 w STZ-induced diabetic rats (Lincoln et al., 1984). Also, endogenous release of the excitatory transmitters ACh, 5-HT, and substance P was unaffected by the diabetic state (Belai et al. 1985, Belai et al. 1987).

1.4.3.2 Sympathetic neurons

Sympathetic innervation to alimentary tract is also affected in experimental diabetes. Ileal mesenteric nerves show dystrophic axonopathy the frequency of which increases with the duration of diabetes (Schmidt & Plurad, 1986). In addition, the activity of tyrosine hydroxylase (TH), the rate limiting enzyme that modulates the synthesis of catecholamines in sympathetic nerves, increases in CG and SMG of diabetic STZ rats (Schmidt & Cogswell, 1989). Increased size of varicosities containing TH in the diabetic STZ rat ileum suggests neurodegeneration of the nerve fibres (Shotton et al., 2007). Increased activity of TH was accompanied with increased endogenous Neuronal Growth Factor (NGF) in CG /SMG (Schmidt et al., 2000). Neuroaxonal dystrophy in sympathetic nerves accompanied with diminished regenerative response has been reported in several diabetic animal models such as BB rat, NOD mice, STZ-induced diabetic rat and BBZDR/Wor rat (Yagihashi & Sima, 1985; Schmidt et al., 2003; Schmidt et al., 2004).

The selective distribution of lesions in sympathetic nerves occurs in experimental diabetes similarly to clinical diabetes. Paravertebral SCG or prevertebral IMG are relatively unaffected by diabetes compared to CG/SMG (Schmidt, 2002, Belai et al., 1991). CG/SMG of diabetic rats present identical ultrastructural changes with those observed in human studies. Experimental studies demonstrated accumulation of TH and increased NA levels in the CG and loss of NA in the ileum together with reduced TH-positive fibres with swollen varicosities (Belai et al., 1988, Schmidt & Cogswell, 1989, Shotton et al., 2007). Increased TH mRNA in mesenteric nerves is

accompanied by decrease in the level of dopamine-β-hydroxylase and NA in the ileum but not in the distal colon (Belai et al., 1991, Schmidt & Cogswell, 1989).

It has been suggested that this differential response occurs because the mesentery nerves are lengthier or the hypertrophic/ hyperplastic small bowel of diabetes evokes these degenerative responses (Schmidt & Plurad, 1986; Schmidt & Cogswell, 1989). However, the selective vulnerability of the prevertebral CG/SMG in diabetes was reproduced *in vitro* in response to glucose and oxidative stress challenge. CG/SMG showed a slower neurite regenerative capacity than SCG neurons *in vitro* after exposure to high glucose for 24 h. Low levels of oxidative stress selectively caused increased TH immunoreactivity in CG/SMG (Semra et al., 2004;Semra et al., 2006). These findings raise the question whether vulnerability in diabetes reflects properties of the neurons themselves.

1.5 Pathogenetic mechanisms

Important progress was made by the Diabetes Control and Complications Trial Research Group (DCCT) and the UK Prospective Diabetes Study Group, which confirmed that neuropathy is correlated with hyperglycaemia, and that strict glycaemic control can reduce the occurrence or progression of diabetic neuropathy (The Diabetes Control and Complications Trial Research Group, 1993). High glucose may affect neurons directly through several proposed metabolic pathways and indirectly through microangiopathy.

Glucose is the major energy molecule for neurons of both peripheral and central nervous systems. The uptake of glucose by glucose carriers (for example GLUT1,

GLUT8) is not an insulin dependent process and depends on the extracellular concentration of glucose (Tomlinson & Gardiner, 2008b). Glucose is not stored in the form of fat and glycogen intracellularly in neurons as occurs in adipose tissue and liver, but is phosphorylated straight away and enters into glycolysis. This fact makes neurons vulnerable to excess glucose concentrations.

Increased extracellular and intracellular glucose becomes toxic for the neuronal cell leading to various biochemical alterations. Thus, sustained or regular episodes of hyperglycaemia interfere with metabolic pathways (discussed below) that impact upon neuronal phenotype.

In addition, microangiopathy is an undoubted accompaniment to diabetic neuropathy and its mechanisms for development centre on endothelial damage with features that include impaired vasodilation by NO, damage from oxidative stress, and alterations generated by the polyol pathway. Overall, diabetic vessels have more prominent impairment of vasodilatory mechanisms, favouring excessive functional vasoconstriction. Microangiopathy is then exacerbated by alterations in local oxygen release, contributing to an eventual cascade of hypoxia and ischaemia. Neuropathy may therefore be associated with abnormalities of oxygen delivery (Cameron et al., 2001). These two forms of high glucose involvement in diabetic neuropathy, direct and indirect, may eventually become parallel and synergistic (Theriault et al., 1997; Cameron et al., 2001).

1.5.1 Metabolism of nutrients in neurons and cell respiration

The metabolism of glucose and fatty acids are non insulin dependent processes in neurons and, after entering the cell, they immediately undergo phosphorylation. After a series of catabolic biochemical processes, glucose and fatty acids are metabolised to acetyl CoA during the tricarboxylic acid (TCA) cycle in mitochondria (Campbell & Smith, 2000). The co-enzymes nicotinamide/ flavin adenine (NADH and FADH$_2$) are also produced during the Krebs cycle. NADH and FADH$_2$ oxidation occurs and the hydrogen atoms that are removed release energy and they serve as electron donors to molecular oxygen in the electron transport chain.

The electron transport chain is a series of enzyme complexes (oxidoreductase I, II & III and cytochrome c IV) in the inner membrane of mitochondria. The electron transport chain uses the energy released from the oxidation of NADH (complexes I, II & IV) and FADH$_2$ (complexes II & III) to pump protons across the inner membrane of the mitochondria. This causes protons to build up in the intermembrane space, and generates an electrochemical gradient across the membrane. The energy stored in this potential is then used by ATP synthase to produce energy in the form of ATP (Campbell & Smith, 2000).

The chemical energy stored in ATP is used to fuel most of the biochemical reactions of the neuron. For example, special proteins in the neuronal membrane use the energy released by the breakdown of ATP into ADP to pump certain substances across the membrane, to establish concentration differences between the inside of the neuron and the outside, for anterograde transport etc.

1.5.2 Oxidative stress, anti-oxidants and diabetic neuropathy

As an unavoidable by-product of these biochemical processes, chemical species that contain unpaired electrons, the free radicals, are produced. Unpaired electrons increase the reactivity of the molecules (or atoms). Free radicals then react with all biological macromolecules to form new radicals that react with further macromolecules. The toxicity of free radicals thus arises in chain reactions and may cause lipid peroxidation (and disruption of cell membrane), protein damage or eventually apoptosis. Most common free radicals, with a varying degree of reactivity, are the reactive oxygen species (ROS) such as hydroxyl radical, superoxide anion. Other reactive molecules are, for example, the transition metals such as iron and copper, and the reactive nitrogen species (RNS) such as NO and peroxynitrite (Betteridge, 2000).

The cell has defences to inhibit or delay these reactions, such as the anti-oxidant enzymes, dismutases, peroxidases and catalases. Superoxide Dismutase (SOD) in the mitochondrion converts the highly reactive superoxide to hydrogen peroxide and oxygen. Hydrogen peroxide is more stable than superoxide and it diffuses easier through the cell membrane. Catalase converts hydrogen peroxide to water and therefore its activity is required when SOD is active. The detoxification of hydrogen peroxide also occurs through glutathione peroxidases, present in the cytosol and mitochondria with the oxidation of glutathione (GSH). GSH is the most important cellular anti-oxidant for neurons. To regenerate GSH, glutathione disulfide is reduced by NADPH and glutathione reductase.

Vitamin C and vitamin E are dietary anti-oxidants. The anti-oxidants vitamin E (the generic name for the family of tocopherol related compounds), β-carotene and coenzyme Q are present in cell membrane and interrupt lipid peroxidation. Vitamin C (ascorbic acid) scavenges an array of ROS including, hydroxyl, alkoxyl, peroxyl, superoxide anion, hydroperoxyl radicals and reactive nitrogen species such as nitrogen

dioxide, nitric oxide, and peroxynitrite at very low concentrations. In addition, ascorbic acid regenerates other anti-oxidants such as α-tocopheroxyl, urate and β-carotene radical cation from their radical species (Vincent & Feldman, 2004).

When the balance between the production of free radicals and anti-oxidant defences is disturbed, oxidative stress is induced in the cell. During hyperglycemia, excess glucose metabolism evokes the overload of mitochondrial pathways and the over abundance of NADH and FADH$_2$. Thus, increased production of free radicals occurs with the parallel depletion of anti-oxidants leading to oxidative stress. The mitochondria, the main source of ROS and RNS production, are the first cellular compartments that are affected.

Oxidative stress is important factor but it does not necessarily cause the onset of neuropathy. It may be a consequence rather than a primary cause of broad-based dearrangements since ROS and RNS production is intersected with other pathways (Betteridge, 2000;Figueroa-Romero et al., 2008).

1.5.3 Altered NADPH and NADH metabolism

NAD(H) and NADP(H) are involved in numerous pathways regulating energy metabolism, calcium regulation, antioxidation, gene expression and cell death. NAD(H) is prominent in its oxidised form and thus is used by enzymes that catalyse substrate oxidation. In contrast, NADP(H) is more abundant in its reduced form, therefore used by enzymes that catalyse substrate reduction (Pollak et al., 2007;Ying, 2008). Under pathological conditions, the ratio of the reduced and oxidised form of NAD(H)

(NAD+/ NADH) and NADP (NADP+/ NADPH) -termed the redox state of the cell-may change. In diabetes, it has been proposed that the polyol pathway leads to depletion of NADPH and furthermore excessive activity of the TCA cycle in mitochondria leads to an increase in NADH (Ido et al., 1997;Ido, 2007).

The polyol pathway initiates a cascade of events, induced by the toxicity of intracellular glucose overload, in various cell types, including neurons. The enzyme aldose reductase metabolises the excess glucose in sorbitol and sorbitol dehydrogenase further metabolises sorbitol to fructose (Fig. 1.1).
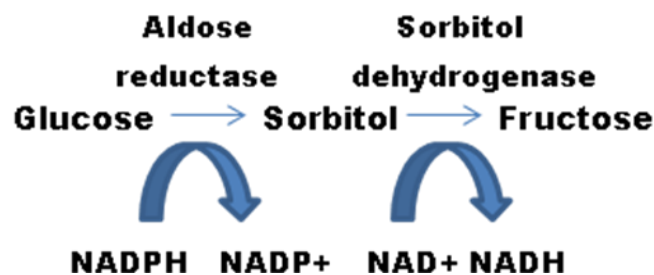
Figure 1.1: The polyol pathway

There are various signal transduction pathways that link the polyol intermediates with cellular stress but they are extremely complex. Among these is a metabolic flux that leads to the depletion of the anti-oxidant GSH. GSH depletion is linked with the deficiency of NADPH. Aldose reductase competes with glutathione reductase for NADPH which, of itself, participates in the production of GSH. Thus, one hypothesis is that coenzyme imbalances lead to anti-oxidant depletion and the cell is more susceptible to ROS. Another hypothesis is that the poorly membrane-permeable sorbitol accumulates in the cytosol and induces osmotic stress. This can also alter the anti-oxidant potential of the cell by the release of the osmolyte and anti-oxidant taurine. Although there is evidence supporting both hypotheses that possibly interrelate, there is

controversy between researchers (Oates, 2002; Obrosova, 2002). The polyol pathway has been the target of experimental studies in diabetes and aldose reductase inhibitors are currently undergoing phase III clinical trials (Schemmel et al., 2010).

Imbalances in the ratio of redox co-enzymes may have several consequences in cell metabolism. NADPH/ NADP+ ratio changes have a direct effect on the anti-oxidant capacity, affecting GSH/GSSG concentrations, inhibiting the reactivation of catalase and the pathway involved in the regeneration of thioredoxin. Abundance of NADH in mitochondria can increase the proton gradient across mitochondrial membranes and consequently potentiate ROS generation from the electron transport chain.

In summary, changes in the NAD+/ NADH equilibrium may facilitate a series of reactions requiring oxidation thus inducing reductive stress ("pseudohypoxia") and imbalance of NADP+/ NADPH may affect detoxification pathways. These mechanisms have been studied in vascular dysfunction in diabetes but there is little evidence in peripheral nerves.

1.5.4 Carbonyl Stress and AGEs

The AGE hypothesis proposes that chronic accelerated chemical modification of macromolecules by glycation in diabetes alters the structure and function of proteins, lipids and nucleotides contributing to pathophysiology and the development of diabetic complications. Glycation is the result of non-enzymatic addition of glucose or other saccharides to proteins, lipids and nucleotides. Glucose and other glycolytic

intermediates can bind to protein amino groups which first form a Schiff's base that then progresses to an Amadori product which is stable. This results in the irreversible formation of AGEs and the subsequent cross linking of proteins damaging their structure.

Dysfunction also arises through the increased production of the carbonyl species glyoxal, methylglyoxal, and 3-deoxyglucosone. These products are physiological α-oxoaldehydes formed by lipid peroxidation, glycation, and degradation of glycolytic intermediates (Abordo et al., 1999). Thus, α-oxoaldehydes are produced in the course of metabolism under normal conditions by both enzyme and non enzyme catalysed reactions. Their detoxification occurs mainly via the glyoxalase system that comprises two enzymes, glyoxalase I and II, and uses significant amounts of reduced glutathione. Increased production of α-oxoaldehydes or decrease of their detoxification systems results in the non enzymatic reaction and modification of various macromolecules. Depending on the macromolecule affected, these reactions cause a direct inhibitory effect to the affected macromolecules and the formation of AGEs leading to disturbance of cell function. This phase of toxicity is designated carbonyl stress. A second phase of toxicity leads to free radical production and oxidative stress (review by Kalapos, 2008).

AGEs are formed at an early stage in the disease process and the increase in their levels is systemic. AGE formation in cells leads to intra- and extracellular cross linking of proteins and protein aggregation. AGEs then interact with their receptor, RAGE, which is their main receptor appearing in several isoforms and in many cell types including neurons. RAGE alters intracellular signalling and has multiple specific downstream signalling targets including mitogen activated protein kinases (MAPK), p21 ras, nuclear factor κB (NFκB) and multiple other intermediates thus altering the gene expression (Tomlinson & Gardiner, 2008a; Tomlinson & Gardiner, 2008b).

1.5.5 Neurotrophic support deficiency and alterations in gene expression

Diminished neurotrophic support (NGF, insulin, C peptide, Insulin Growth Factor-1 (IGF1)) may also contribute to neurite and axonal degeneration in diabetic neuropathy. Deficiency of neurotrophic factors is implicated in defective interaction with surrounding cells and depressed axonal transport. Growth factors initiate signal transduction pathways to promote axonal and dentrite survival and regeneration. Genes may be upregulated or downregulated by the growth factor-promoted signal to generate a response to environmental stimuli or damage. Nevertheless, despite its efficiency in experimental diabetes, in phase III clinical trials, NGF administration failed to relieve neuropathy in diabetics (Apfel, 2002).

The activation of MAPK such as c-Jun N terminal kinase and p38, may arise from a combination of events (Tomlinson, 1999; Yang et al., 2003; Tomlinson & Gardiner, 2008b). Moreover, changes in the expression and activation of protein kinase C (PKC) has also been implicated in diabetic neuropathy occurring via the *de novo* synthesis of diacylglycerol (Eichberg, 2002). The main targets of kinases are transcription factors and the phosphorylation of these factors may occur post translationally leading to altered neuronal phenotype. Finally, the activation of the nuclear enzyme, poly(ADP-ribose) polymerase (PARP) contributes to early diabetic sensory neuropathy by mechanisms that may include oxidative stress (Ilnytska et al., 2006).

It would be useful to develop a model for diabetic gastrointestinal neuropathy to directly manipulate the immediate environment of myenteric or sympathetic ganglia, allowing the effects of altered metabolism or treatments to be observed. While *in vivo* studies provide physiological and cellular details of diabetic neuropathy, the complexity of the system obscures the details of molecular events under glucose stress. The use of simpler *in vitro* systems is hence very important to map these events. It is generally assumed that the mechanisms underlying diabetic distal sensory polyneuropathy also account for autonomic neuropathy but much of the work revealing pathological mechanisms has been carried out through the study of sensory neurons *in vitro*. Embryonic DRG neurons have mainly been utilised as an *in vitro* model of diabetic sensory neuropathy (Russell et al., 1999;Vincent et al., 2005a), but adult DRG neurons do not respond in the same way to high glucose *in vitro* (Tolkovsky, 2002;Huang et al., 2003). For example, apoptotic cell death has been reported as the response to high glucose *in vitro* but it is not a feature of diabetes *in vivo* (Schmidt, 2002; Tolkovsky, 2002). Furthermore, the effect of high glucose *in vitro* is greater when the neurons are dissociated prior to culture rather when explants are used (Semra et al., 2004). Thus, there is a requirement for a model of diabetic gastrointestinal neuropathy that allows the detailed study of the changes that occur *in vivo*.

Thus, the specific aims of this thesis are:

1) to establish *in vitro* models of diabetic gastrointestinal neuropathy and study subopulations of adult myenteric neurons in wholemount preparations following exposure to stimuli that mimic the diabetic environment;

2) to use the *in vitro* models to investigate the ability of therapeutic agents to prevent diabetic gastrointestinal neuropathy;

3) to investigate the effect of high extracellular glucose on NAD(P)H metabolism in living neurons from explants of sympathetic ganglia that either undergo degeneration in diabetes or are resistant to change.

Chapter 2: Establishment of the *in vitro* models

2.1 Introduction

A causative role of hyperglycemia for the pathology of diabetic complications, including neuropathy, was demonstrated about 20 years ago. The DCCT study for type 1 diabetes and UK prospective study for type 2 diabetes correlated hyperglycaemic blood glucose levels, measured by glycated hemoglobin levels (HbA1c) with diabetic complications (The Diabetes Control and Complications Trial Research Group, 1993;UK Prospective Diabetes Study Group, 1998). Intensified insulin treatment reduced the neurological deficits of diabetic polyneuropathy. Patients with intensified insulin treatment for 4 years (HbA1c levels of 7%) showed a clinically relevant and statistically significant improved nerve function when compared to the conventionally treated group with HbA1c levels of approximately 9%. Hence, hyperglycaemia *per se* has been proposed as the pathogenic factor for the onset and progression of diabetic

neuropathy. However, hyperglycaemia induces a complex interaction between metabolic and vascular abnormalities suggesting multifactorial pathways in the pathogenesis of diabetic neuropathy.

2.1.1 AGEs & methylglyoxal

The toxic effect of hyperglycaemic fluctuations has been linked with the formation of AGEs. Increased glucose and other sugar derivatives in plasma undergo the Maillard reaction, a cascade of non enzymatic reactions with amine substrates of proteins, lipids and nucleic acids. The predominant early product of these reactions is fructosamine (N6-fructosyl-lysine) that degrades slowly to form more stable advanced glycation adducts. Considering the numerous molecules that sugars can attach to via the Maillard reaction, there are a wide variety of AGEs recognised using chromatographic and immunochemical techniques. Hydroimidazolones, N6-carboxymethyl-lysine (CML), N6-(1-carboxylethyl)-lysine (CEL), pyrraline, bis(lysyl) imidazolium cross-links glyoxal-, methylglyoxal- and 3-deoxyglucosome- derived lysine dimers (GOLD, MOLD and DOLD respectively) are among recognised forms of AGEs (Thornalley, 2002). Some of them fluoresce and have a characteristic brown colour, for example, pentosidine and argipyrimidine. Some AGEs however, are short lived and their concentration depends on proteolysis and protein turnover (Ahmed & Thornalley, 2007).

Additionally, in the cytosol of cells like neurons that accumulate increased levels of glucose, concentrations of dicarbonyls increase and they can also lead to AGE formation (Brownlee, 2001). Dicarbonyls have low molecular weight and extremely

high chemical activity, even at low concentrations. Methylglyoxal is of particular importance in diabetes because its biogenesis derives not only as a parallel product of the Maillard reaction but also from glycolytic intermediates or from lipid peroxidation as well (Thornalley, 2005). Glycolytic intermediates and subsequent triose phosphate formation or threonine catabolism can accelerate significantly the formation of methylglyoxal. Methylglyoxal can diffuse passively in cell membranes. Its biological form is of two kinds; the unbound form that has very short survival and it is particularly difficult to quantify; and the bound form which is found on protein residues as a major glycation adduct (Turk, 2010). In order to protect the cell from methylglyoxal toxicity, its physiological levels are kept low mainly by the glyoxalase system, using reduced GSH as a rate limiting factor. Inefficiency of the related scavenger system (for example GSH depletion) and alterations in cell metabolism can provoke carbonyl stress (Thornalley, 2003a).

Carbonyl stress is an acute metabolic event characterized by accelerated tissue damage. Free amino groups of amino acids, phospholipids, peptides or nucleic acids react non enzymatically with the carbonyl group of methylglyoxal to form various modified macromolecules or carbonyl adducts. Hydroimidazolones, CEL and MOLD are important AGEs, derived from methylglyoxal -induced irreversible modifications of deoxyribonucleic acid (DNA), ribonucleic acid (RNA) and amino acids (Turk, 2010). Endogenous AGE formation and carbonyl stress can promote the pathology of diabetic complications but their impact has not been yet clarified in diabetic gastrointestinal neuropathy.

2.1.1.1 Functional effects of AGEs on neurons

Axonal atrophy and defective axonal transport is a characteristic feature of diabetic neuropathy and several lines of evidence have linked impaired cytoskeletal function with the formation of AGEs. A significant increase in the amount of pentosidine was found in both the cytoskeletal and myelin fractions of sural nerve biopsies of diabetic patients (Ryle & Donaghy, 1995). Similar changes occur in sciatic nerves of STZ-induced diabetic rats (Ryle et al., 1997). In contrast, in the same study, the cytoskeleton of CNS nerves was more resistant to non enzymatic glycosylation. Actin and tubulin in CNS neurons are increasingly glycosylated *in vitro* (Williams et al., 1982; Pekiner et al., 1993). The formation of amorphous α and β tubulin aggregates and the inhibition of guanosine diphosphate-dependent tubulin polymerisation may compromise microtubule formation and neuroaxonal regeneration. Vlassara and colleagues found a three fold increase in amino acid glycosylation–(especially lysine) from sciatic and femoral nerves of diabetic rats and dogs in comparison to controls (Vlassara et al., 1981).

Functional effects of AGEs in neuronal cells arise also from the modification of the peripheral nerve myelin, endoneurial microvessels and extracellular matrix. Sugimoto et al. found extensive CML immunoreactivity in biopsies of sural, peroneal and saphenous nerve tissue of patients with diabetic neuropathy. CML staining was located in the perineurium, axons and Schwann cells of myelinated fibres, in unmyelinated fibres, in endothelial cells and pericytes of endoneurial microvessels, and in interstitial collagen and basement membranes of the perineurium (Sugimoto et al., 1997). It has been suggested that glycation of the extracellular matrix proteins of the perineurium, laminin and fibronectin, accompanied by a reduction in neurotrophic

factors, contributes in neuroaxonal degeneration and failing attempts of the nerve cones to regenerate in diabetic neuropathy (King, 2001;Duran-Jimenez et al., 2009).

Furthermore, extracellular AGEs interact with their receptor, RAGE and this interaction activates a cascade of signal transduction pathways that can cause oxidative stress (Vincent et al., 2007a). RAGE is expressed predominantly in lung, endothelial cells and Schwann cells (Wada & Yagihashi, 2005). In neurons, RAGE mRNA was increased in peripheral epidermal axons, sural axons, and sensory neurons within ganglia of STZ diabetic rats and this increase was related with pathological changes (Toth et al., 2008). Expression of RAGE has also been demonstrated in enteric neurons (Korenaga et al., 2006; Jeyabal et al., 2008).

2.1.1.2 Correlation of AGEs with HbA1c levels

Higher HbA1c levels were correlated with decreased performance in autonomic and sensory neurological tests during DCCT trial (The Diabetes Control and Complications Trial Research Group, 1993). This shows that increased glycosylation is a significant risk factor to diabetic neuropathy. However, HbA1c measurements can only indicate the glycosylation of circulating haemoglobin and cannot indicate intracellular glycosylation levels.

2.1.2 Oxidative stress and accelerated ageing

Oxidative stress has been implicated in neurodegenerative diseases and ageing and has also been investigated extensively in diabetes. It has been associated with the pathogenesis of diabetes causing destruction of β cells and of the secondary complications of diabetes (Rosen et al., 2001). Clinical and experimental evidence demonstrates that generation of free radicals is increased in both type 1 and type 2 diabetes (Traverso et al., 1998). The end products of free radical attack are reliable indicators of oxidative stress. Thus, DNA damage, modified proteins and increased lipid peroxidation have been documented in various types of cells. Oxidized proteins have been reported to be significantly higher in diabetic patients with complications, than in those without complications (Rosen et al., 2001). Endothelial cells constitute major sites for the production of reactive species (Brownlee, 2001) and in neurons, hyperglycaemia is associated with oxidative stress, mitochondrial swelling and deregulation of inner membrane potential (Vincent et al., 2002;Vincent et al., 2004a;Vincent et al., 2005a;Yu et al., 2006). Contributory factors like endoneurial hypoxia, transition metal imbalances and hyperlipidemia are additionally linked with increased free radical generation in neurons (Low et al., 1997;Pop-Busui et al., 2006;Vincent et al., 2009).

Multiple pathways cause excess free radical production (Feldman, 2003;Vincent et al, 2004b;Pop-Busui et al., 2006;Figueroa-Romero et al., 2008). Increased metabolic flux of glucose through the polyol pathway induces NAD(P)H redox imbalances; reactive species can also be generated as a result of auto-oxidation of glucose, glucose metabolism, formation of AGEs and the action of AGEs on RAGE. PKC activity is regulated through the redox status; mitochondrial functional impairment and swelling are associated with oxidative stress. In addition, the sensitivity to oxidative stress due to anti-oxidant or reductant deficiencies has been extensively described. For example, colons from diabetic patients had decreased amounts of the non-enzymatic anti-oxidant

GSH and this correlated with higher HbA1C levels and diabetes duration. There was also an increased expression of SOD, possibly as a compensatory mechanism (Chandrasekharan et al., 2011).

In conclusion, oxidative stress plays a significant role in the onset and progression of diabetes. Whether oxidative stress has a causative role in diabetic gastroenteropathy has received less attention. In addition, it is not known if the proposed pathways described above contribute to changes in different neurons within the enteric nervous system. This is an important consideration since it is known that subpopulations of enteric neurons are affected differently in diabetes (see below). Studies in sensory neurons suggest that oxidative stress is a unifying mechanism (Vincent et al. 2004b), but this has yet to be examined in the enteric nervous system.

2.1.3 Culture models for the study of diabetic neuropathy

Much of the evidence concerning the mechanisms underlying diabetic neuropathy derives from *in vitro* studies. *In vitro* studies provide useful disease models to map molecular events of pathologic and neuroprotective mechanisms in more detail. It is also important to investigate the pathways involved under diabetic conditions excluding the vascular abnormalities as a contributing factor and the use of *in vitro* models facilitates this attempt. Thus, the *in vitro* approach allows the investigation of mechanistic questions that are not possible in animal models. Experimental models and genetic manipulations to animals then allow the study of the relevance of these mechanisms *in vivo* (Vincent et al. 2005a).

Primary cultures from DRG neurons are the most common *in vitro* model of diabetic sensory polyneuropathy (Hattangady & Rajadhyaksha, 2009). Most of the significant findings come from studies using primary DRG dissociated neurons from normal untreated rodent embryos in which the first step was to examine the defects in neuronal metabolism produced by high glucose. It was shown, using electron microscopy, that high glucose affected not only neurite outgrowth but also the percentage of cultured neurons that die (Russell et al., 1999). Programmed cell death was also demonstrated by immunohistochemical techniques examining the activation of caspase 3 and Terminal deoxynucleotidyl Transferase Biotin-dUTP Nick End Labeling (TUNEL) staining. Under high glucose concentrations, apoptosis occurred through the induction of ROS and mitochondrial degeneration with enlargement and swelling, disrupted inner cristae, mitochondrial membrane depolarization and decrease of absolute levels of ATP (Russell et al., 2002).

Using the same model, a series of studies shed light on oxidative stress, mitochondrial dysfunction, changes in morphology, anti-oxidant systems, together with the time course of changes and feedback mechanisms. Short term hyperglycemia induced superoxide formation and lipid peroxidation in 1 h, oxidative stress and apoptosis in 2 hrs and by 3-6 hrs, increase of anti-oxidant potential, but insufficient to protect DRG (Vincent et al. 2005a). RAGE expression was demonstrated in DRG after exposure to ligand but not high glucose. Downstream pathways such as transient activation of MAPK and PI3K/Akt, subsequent NADPH oxidase activation and oxidative stress were also shown (Vincent et al., 2007a). Intrinsic and extrinsic anti-oxidants and uncoupling proteins have all been shown to be protective (Vincent et al., 2004a; Vincent et al., 2005b; Vincent et al., 2007b).

However, the extrapolation of the above findings using embryonic cultures may be problematic because the developmental stage of neurons can influence the results. A study with primary cultures of sympathetic ganglia using neonatal and adult dissociated neurons showed that the age of neurons affects the response to high glucose and the ability of NGF to protect against the effect of high glucose (Semra et al., 2009). Adult rat sympathetic and sensory neurons differ significantly from embryonic neurons. Immature neurons have an absolute requirement for NGF for survival and need 30 mM glucose for optimal growth. In contrast, adult neurons can survive in the absence of NGF and at lower concentrations of glucose (7-10mM). Explants from newborn and older human myenteric plexus in culture showed differences in growth patterns, and specifically a different degree of neurite outgrowth and glial proliferation (Schafer & Mestres, 1997).

Interestingly, in primary cultures of adult vagal and DRG explants from diabetic animals, high glucose induced a regenerative effect, challenging the notion of glucose-induced cell death (Sango et al., 1991; Sango et al., 2002). When the morphological features and the neurite regeneration ability were investigated, no apoptotic cell death was found by light and electron microscope techniques or TUNEL staining. In contrast, there was enhanced neurite regeneration and upregulated expression of variable growth factors. In another study, hyperglycemia did not induce apoptosis of adult DRG neurons or Schwann cells but restricted axonal regeneration and Schwann cell proliferation (Gumy et al., 2008).

In vitro studies investigating diabetic gastroenteropathy have used various models. Studies from this laboratory, using two sources of adult rat sympathetic dissociated neurons, demonstrated that neurons from the prevertebral CG/SMG that supplies the upper GI tract are particularly sensitive to high glucose in comparison to

neurons from the paravertebral SCG (Semra et al., 2004;Semra et al., 2009). Using explants of the same ganglia it was also found that low levels of oxidative stress induced by menadione selectively caused the accumulation of TH that also occurs selectively in prevertebral ganglia *in vivo* (Semra et al., 2006). Enteric neuronal murine cell lines have also been used to show that treatment with high glucose increased cleaved caspase 3, decreased the survival pathway PI3K/Akt, and that an anti-oxidant reversed these responses (Chandrasekharan et al., 2011). Similar results were also found using primary cultures of embryonic enteric dissociated neurons. Hyperglycemic insult induced apoptosis, decreased Akt phosphorylation and these responses were inhibited by Glial cell line-derived neurotrophic factor (Anitha et al., 2006). Recently, dissociated enteric neurons from neonatal rats have been used to assess the effect of oxidative stress *in vitro* and hydrogen peroxide was shown to cause neuronal cell death (Korsak et al., 2012).

A model introduced by Korenaga et al. (2006) was whole mount preparations of longitudinal muscles with adherent myenteric plexus from the duodenum of adult male rats exposed to AGEs. AGEs induced RAGE expression in myenteric neurons and suppressed the expression of nNOS. However, this study was restricted to the nNOS myenteric subpopulation. We aim to use a similar *in vitro* model to study different subpopulations of myenteric neurons that respond differently in diabetes. The use of a wholemount preparation has the advantage of maintaining the normal environment of the myenteric neurons and avoiding the disruption associated with dissociation of the neurons. In addition, the use of cell lines does not allow the investigation of the different subpopulations of neurons that occur within the myenteric plexus *in vivo*.

2.1.4 Heterogeneity of enteric neuronal responses in diabetes

Previous studies from this laboratory using the STZ-induced diabetic rat model have shown that subpopulations of myenteric neurons are affected differently in diabetes. Changes include alterations in cellular morphology and chemical coding. Some enteric neuronal subpopulations exhibit degeneration, some undergo change in neurotransmitter content without degeneration while some are unaffected. It has been shown previously that the main intrinsic inhibitory motor neurons are particularly affected in diabetes resulting in abnormalities in smooth muscle relaxation, accompanied by increased excitatory messaging (Chandrasekharan & Srinivasan, 2007). In particular, it has been shown that VIP-containing neurons degenerate with accumulation of VIP in the cell body, while diabetes causes a reduction in the expression of nNOS in myenteric neurons (Shotton et al., 2004; Shotton & Lincoln, 2006;Shotton et al., 2007). Recently, in this laboratory, the subpopulation of myenteric neurons that contains calbindin has been shown to be resistant to change in diabetes (Voukali et al. 2011). Yet, it is not known if individual subpopulations are more or less susceptible to specific pathways implicated in the development of neuropathy.

Therefore, the aim of this study was to investigate whether the pattern of change that occurs in myenteric neurons in diabetes *in vivo* can be reproduced *in vitro* using a myenteric plexus/muscle preparation from the adult rat ileum. We chose representative enteric subpopulations that are differently affected by diabetes. The responses of VIP-, nNOS- and calbindin-containing neurons to oxidative stress, carbonyl stress, high glucose and AGEs were examined to investigate their potential contribution to the development of neuropathy.

2.2 Materials and methods

2.2.1 Culture preparations

Adult male Sprague-Dawley rats (275-350 g, 9-12 weeks old) were killed by CO_2 asphyxiation. All procedures described were in compliance with Home Office regulations. The ileum was dissected, cleaned, and stored in a dissecting buffer of Hank's balanced salt solution (HBSS) containing 10 mM glucose and 1% penicillin-streptomycin. Approximately 4 cm of the gut were put on a 2 ml stripette, scored gently with forceps and the myenteric plexus and the muscle layers were peeled away under a dissecting microscope. The myenteric plexus/muscle preparations were then washed in antibiotic wash solution (HBSS containing 1% penicillin-streptomycin, 2% gentamycin and 2% 5mg ml^{-1} metronidazole). The tissue was cut into segments approximately 1cm², stretched and pinned onto Sylgard (VWR, Buffalo Grove, IL, USA). The samples were cultured in defined culture medium containing 10 mM glucose (M199, supplemented with 1% L-Glutamine, 1% Hepes Buffer, 1% penicillin-streptomycin , 0.35% Pathocyte-4- bovine serum albumin (BSA), 60 ng ml^{-1} progesterone, 0.016 mg ml^{-1} putrescine, 400 ng ml^{-1} l-thyroxine, 38 ng ml^{-1} sodium selenite, 340 ng ml^{-1} triiodothyronine, 100 μg ml^{-1} transferrin).

The myenteric plexus/muscle preparations were exposed to a range of different stimuli in order to mimic the diabetic environment: a) for oxidative stress, 1 μM menadione sodium bisulfite was added to the medium, b) for hyperglycaemia, the medium contained additional glucose to give a final concentration of 30 mM., c) for carbonyl stress, a range of different concentrations of methylglyoxal (1, 10, 50, 100 and 500 μM) were examined and d) for AGEs 250 μg ml^{-1} BSA-AGE (Biovision Research

Products, CA, USA) was added. Control preparations were maintained in 10mM glucose in parallel. All preparations were maintained for 24h at 37°C gassed with 95% O_2 and 5% CO_2.

The samples were fixed in 4% paraformaldehyde (PFA) for 18-24h at 4 °C. Samples that had not been subjected to culture (*in situ* preparations) were also included in the immunohistochemistry experiments. Myenteric plexus/muscle preparations were washed and stored in phosphate buffered saline (PBS) merthiolate (0.05%) at 4 °C before processing. All chemicals mentioned above were obtained from Sigma, Poole, UK unless stated otherwise.

2.2.2 Immunofluorescence procedures: double staining for VIP, nNOS, or calbindin with HuC/D.

The myenteric plexus/muscle preparations were placed, longitudinal muscle uppermost, onto microscope slides and processed for immunohistochemical localisation of nNOS, VIP, and calbindin. In order to evaluate the relative frequency of the positive cell bodies, anti-Human Neuronal Protein (anti-HuC/D) was used to label all neuronal cell bodies in the myenteric plexus. The myenteric plexus/muscle preparations were incubated for 1 hour in blocking solution containing 10 % normal horse serum (Gibco-Invitrogen, Paisley, UK) and 0.1% Triton X100 in PBS merthiolate. Primary antisera were diluted in the above blocking solution (rabbit polyclonal anti-nNOS, epitope corresponding to amino acids 2-300 mapping at the N-terminus of nNOS, Santa Cruz, CA, USA, 1:500, rabbit polyclonal anti-VIP, Immunostar Inc., Hudson, WI, USA, 1:500, rabbit polyclonal anti-Calbindin D28k, Swant, Bellinzona, Switzerland, 1:1000). The myenteric plexus/muscle preparations were incubated with the primary antisera

overnight. After being washed in PBS containing 0.1% X100 Triton, the preparations were incubated in blocking solution containing 10% normal goat serum (Gibco-Invitrogen, Paisley, UK) and 0.1% Triton X100 in PBS merthiolate for 1 hour. Samples were then incubated overnight with mouse monoclonal anti-HuC/D (Molecular Probes Probes, Eugene, OR, USA) diluted 1:200 in the above solution. Finally, the samples were washed, incubated for 1 hour in the dark at room temperature with Alexa 488 Donkey anti-Rabbit (Molecular Probes, Eugene, OR, USA) and Cy3 Goat anti-Mouse (Jackson ImmunoResearch Laboratories, West Grove, PA, USA) diluted 1:100 in PBS Triton, washed, mounted and the coverslips sealed. All procedures were carried out at room temperature.

2.2.3 Analysis and statistics

The samples were processed in parallel and analysed on a Zeiss fluorescence microscope (Carl Zeiss Ltd., Welwyn Garden City, UK). For each sample, a minimum of 200 cell bodies positive for HuC/D was assessed for the presence or absence of nNOS, VIP or calbindin. The proportion of positive nNOS, VIP or calbindin cell bodies were expressed as a percentage of the number of HuC/D-immunoreactive myenteric neurons. In addition, the average number of HuC/D-positive neurons per ganglion was assessed by counting the number of HuC/D-positive neurons in six ganglia per preparation.

The data were analysed with GraphPad Prism 3 software using one way analysis of variance followed by Neumann-Keulls post hoc comparisons, or using an unpaired Student's t test, where $P < 0.05$ was taken to indicate statistical significance. The samples were also photographed using a Canon EOS Elan II digital camera and micrograph pictures were produced using Photoshop Elements 8.0 software.

2.3 Results

2.3.1 Effect of culture

Comparisons were made between the immunohistochemical staining of preparations that had been fixed immediately (*in situ*) and those that had been maintained for 24h *in vitro* to examine the effects of culture *per se* and the results are given in Table 2.1A. The number of HuC/D-positive neurons/ganglion was unaffected by culture. However, the percentages of HuC/D-positive neurons that contained VIP, nNOS or calbindin were all significantly increased following 24h in culture under control conditions.

Before assessing the effects of the stimuli *in vitro*, preliminary experiments were carried out to establish that, at the concentrations used, the stimuli did not affect the number of HuC/D-positive neurons per ganglion. The results are given in Table 2.1 B. Exposure of myenteric plexus/muscle preparations to oxidative stress, high glucose, carbonyl stress (explained below) or AGEs for 24h had no significant effect on the number of HuC/D-positive neurons per ganglion.

Table 2.1: Characterisation of myenteric plexus *in vitro*.

A. Effect of Culture	*In Situ*	Control Culture (10mM glucose)	
VIP (% HuC/D-positive neurons)	3.18 ± 0.18 (10)	10.13 ± 0.82 (12)	$p < 0.001$
nNOS (% HuC/D-positive neurons)	22.87 ± 1.96 (10)	31.94 ± 2.13 (10)	$p < 0.01$
Calbindin (% HuC/D-positive neurons)	19.30 ± 2.46 (10)	30.47 ± 4.03 (10)	$p < 0.05$
HuC/D-positive neurons (No. per ganglion)	50± 1 (6)	45 ± 3 (6)	NS
B. Effect of Stimuli *in vitro* (No. HuC/D-positive neurons per ganglion)	**Control Culture (10mM glucose)**	**Plus Stimulus**	
Oxidative Stress (1µM Menadione)	45 ± 3 (6)	42 ± 1 (6)	NS
High Glucose (30mM)		40 ± 2 (6)	NS
Carbonyl Stress (10µM Methylglyoxal)		43 ± 2 (6)	NS
Advanced Glycation Endproducts (250 µg ml⁻¹ BSA-AGE)		42 ± 2 (6)	NS

Data have been given as the mean ± SEM and the numbers of separate culture preparations used to provide the data are given in brackets.

2.3.2 Effects of stimuli on VIP-, nNOS- and calbindin-positive neurons *in vitro*

In all cases, control preparations (10 mM glucose) were maintained in parallel with preparations exposed to the stimuli mimicking aspects of the diabetic environment for comparison.

2.3.2.1 Oxidative stress

Representative micrographs demonstrating immunohistochemical staining for HuC/D together with VIP, nNOS or calbindin, with and without exposure to menadione to induce oxidative stress, are given in fig. 2.1 A-C. As has been reported previously, HuC/D labelled the cell bodies of all myenteric neurons without staining the nerve fibres providing a pan-neuronal marker with which numbers of neurons were easy to assess (Lin et al., 2002). Double labelling enabled the number of VIP-, nNOS and calbindin-containing neurons to be assessed as a percentage of the HuC/D-positive neurons and the results are given in fig. 2.2. Relative to control preparations maintained for 24h in 10 mM glucose, exposure to menadione caused a significant increase ($p < 0.01$) in the proportion of HuC/D-positive neurons expressing VIP and a significant decrease ($p < 0.01$) in the proportion of HuC/D-positive neurons expressing nNOS. Calbindin expression was unaffected by exposure to oxidative stress.
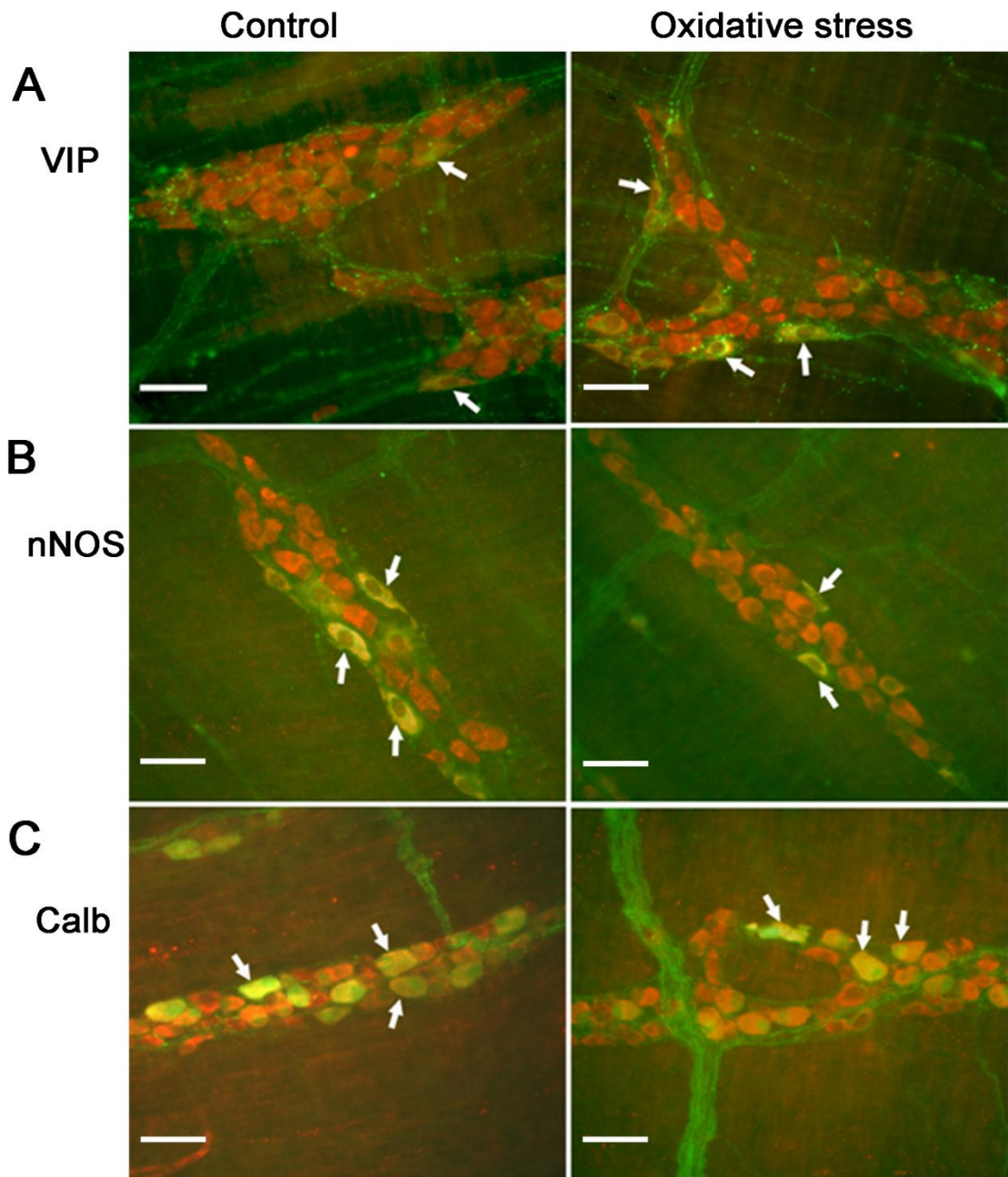
Figure 2.1: Effect of oxidative stress on myenteric neurons. Photomicrographs show the immunoreactivity of VIP (A), nNOS (B) and Calbindin (C) double labelled with the neuronal marker HuC/D. Left panels depict staining of control preparations maintained for 24h *in vitro* and right panels depict samples after exposure to menadione to induce oxidative stress. Green fluorescence indicates VIP, nNOS or Calbindin labelling and red fluorescence HuC/D. The arrows indicate co-localisation with HuC/D (yellow). Scale bars represent 50 μm.
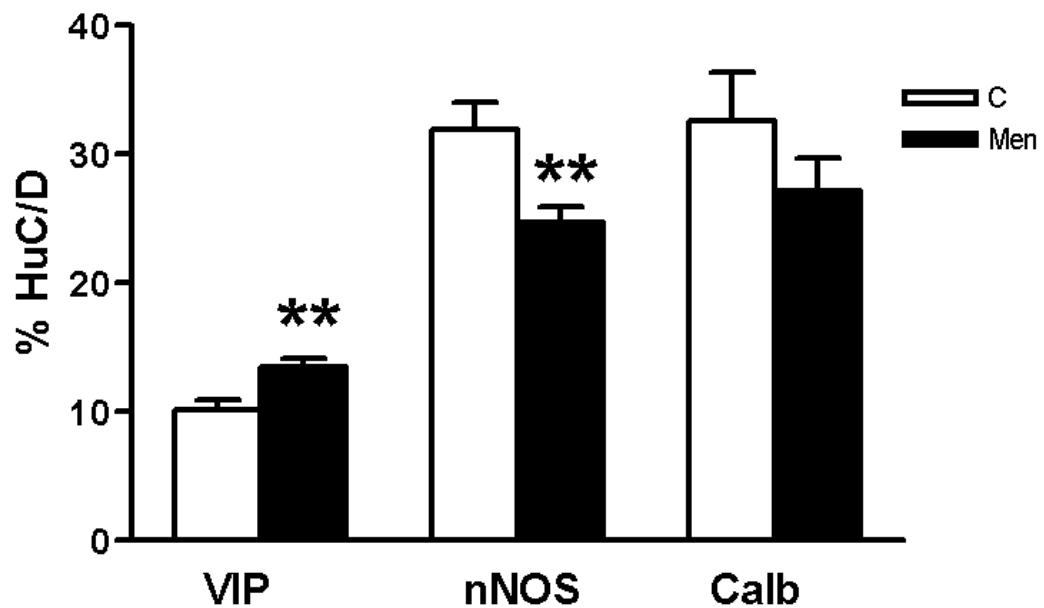
Figure 2.2: Effect of oxidative stress on the relative number of VIP, nNOS and Calbindin immunoreactive cell bodies. Neurons containing VIP, nNOS or calbindin are expressed as a percentage of the number of HuC/D-positive neurons. Clear bars represent data from controls and black bars represent data from preparations after exposure to menadione (Men). Note the significant increase of VIP positive cell bodies and decrease of nNOS positive cell bodies following exposure to menadione while calbindin-positive neurons were unaffected. Data are expressed as the mean ± SEM, n = 10, (** $p < 0.01$, by non paired Student's t-test).

2.3.2.2 Effect of different methylglyoxal concentrations

Myenteric plexus/muscle preparations were exposed to a range of different methylglyoxal concentrations in culture. The higher concentrations of methylglyoxal (50 μM, 100 μM, 500 μM) resulted at a significant loss of HuC/HuD positive cell bodies (fig. 2.3). Since diabetes does not cause a significant loss of HuC/HuD positive cell bodies (Voukali et al., 2011) a concentration of 10 μM was chosen for subsequent studies of the effect of methylglyoxal on VIP-, nNOS- and calbindin-containing neurons.

2.3.2.3 High glucose, carbonyl stress and AGEs

The effects of exposure to high glucose levels, methylglyoxal to induce carbonyl stress and of AGEs on VIP, nNOS and calbindin are shown in figs. 2.4, 2.5 and 2.6 and in the graph given in fig. 2.7 A-C, respectively. In the case of VIP-containing neurons, exposure to high glucose and to carbonyl stress caused a significant increase ($p < 0.01$, for both) in the proportion of HuC/D-positive neurons expressing VIP while exposure to BSA-AGE had no significant effect (fig. 2.4, 2.7A). In contrast, exposure to high glucose and carbonyl stress has no significant effect on nNOS-containing neurons while exposure to BSA-AGE resulted in a significant decrease ($p < 0.05$) in the proportion of neurons expressing nNOS (fig. 2.5, 2.7B). The proportion of HuC/D-positive myenteric neurons expressing calbindin was unaffected by exposure to high glucose, carbonyl stress or BSA-AGE (fig. 2.6, 2.7C). Preliminary control experiments demonstrated that exposure to BSA, at the same concentration as that used for BSA-AGE, had no effect on any of the subpopulations of myenteric neurons studied.
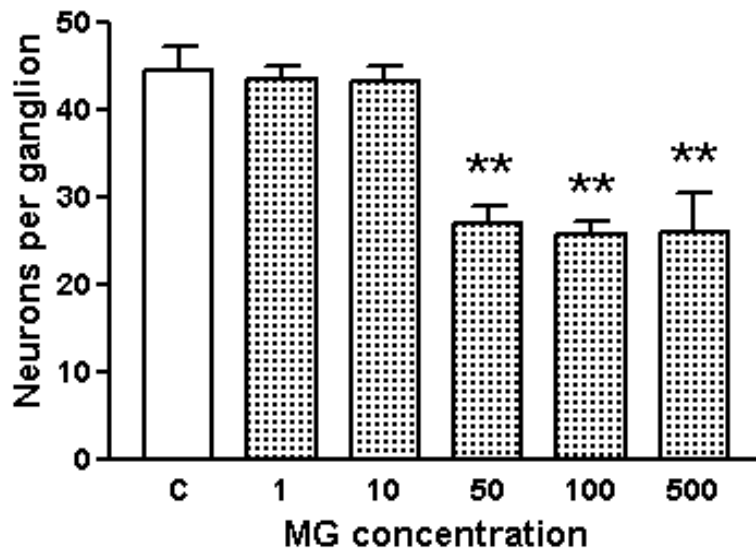
Figure 2.3: Effect of different methylglyoxal (MG) concentrations on the neuronal viability *in vitro* measured with the number of HuC/D positive neurons per ganglion. Clear bars represent data from controls and shaded bars represent data from preparations after exposure to the various methylglyoxal concentrations. Note the decrease in HuC/D immunoreactive neurons following exposure to higher methylglyoxal concentrations. Data are expressed as the mean ± SEM, n = 6, (** $p < 0.01$, by ANOVA).
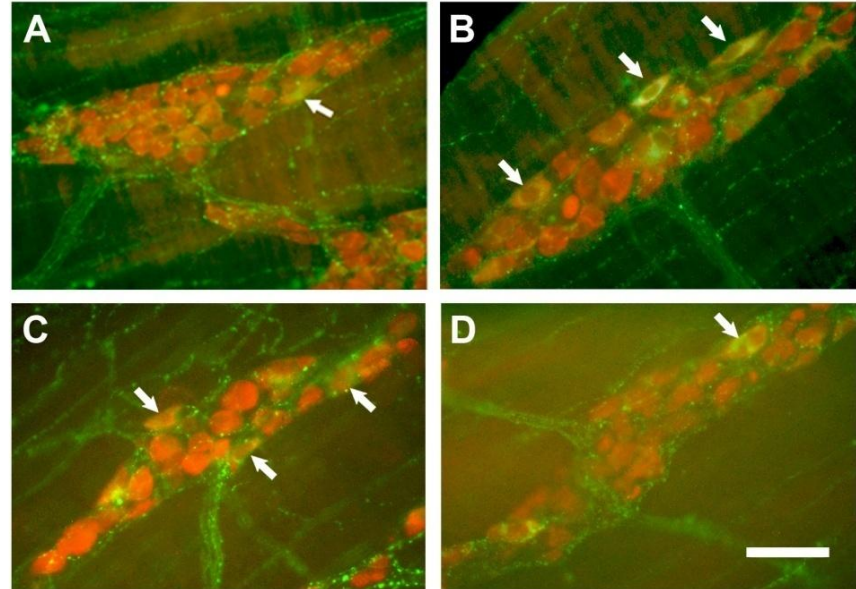
Figure 2.4: Effect of diabetic stimuli on VIP-containing myenteric neurons. Photomicrographs show the immunoreactivity of VIP double labelled with the neuronal marker HuC/D. Left top panel (A) depicts staining of control preparations maintained for 24h *in vitro* and the remaining panels depict samples after exposure to high glucose (B), methylglyoxal (C) or AGEs (D). Green fluorescence indicates VIP labelling and red fluorescence HuC/D. The arrows indicate examples of VIP in co-localisation with HuC/D staining (yellow). Scale bar represents 50 μm.
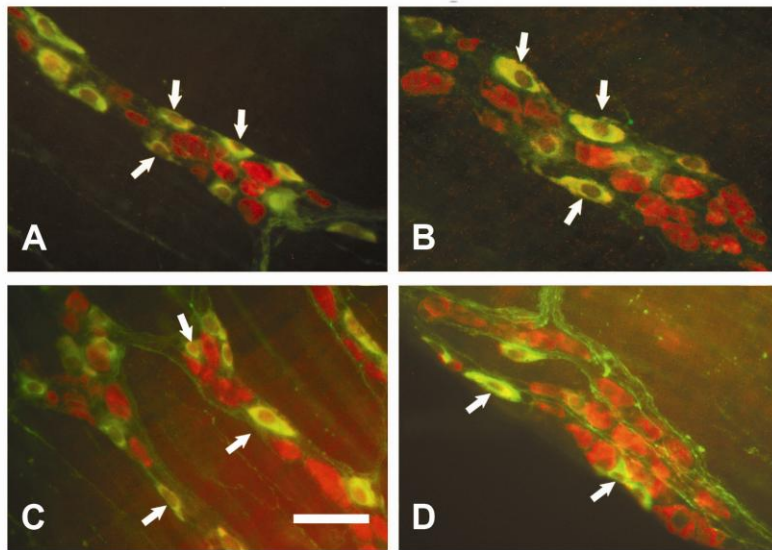
Figure 2.5: Effect of diabetic stimuli on nNOS-containing myenteric neurons. Photomicrographs show the immunoreactivity of nNOS double labelled with the neuronal marker HuC/D. Left top panel (A) depicts staining of control preparations maintained for 24h *in vitro* and the remaining panels depict samples after exposure to high glucose (B), methylglyoxal (C) or AGEs (D). Green fluorescence indicates nNOS labelling and red fluorescence HuC/D. The arrows indicate examples of nNOS in co-localisation with HuC/D staining (yellow). Scale bar represents 50 μm.
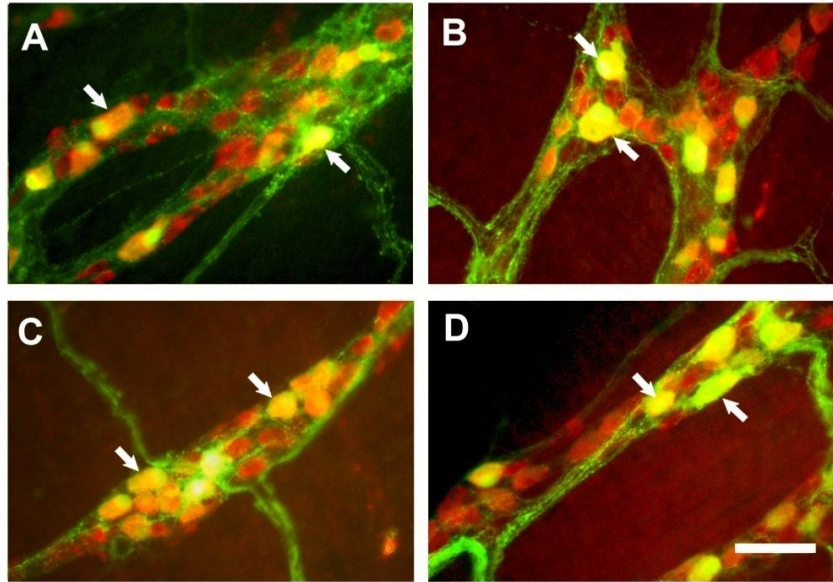
Figure 2.6: Effect of diabetic stimuli on Calbindin-containing myenteric neurons. Photomicrographs show the immunoreactivity of Calbindin double labelled with the neuronal marker HuC/D. Left top panel (A) depicts staining of control preparations maintained for 24h *in vitro* and the remaining panels depict samples after exposure to high glucose (B), methylglyoxal (C), or AGEs (D). Green fluorescence indicates Calbindin labelling and red fluorescemce HuC/D. The arrows indicate examples of Calbindin in co-localisation with HuC/D staining (yellow). Scale bar represents 50 μm.
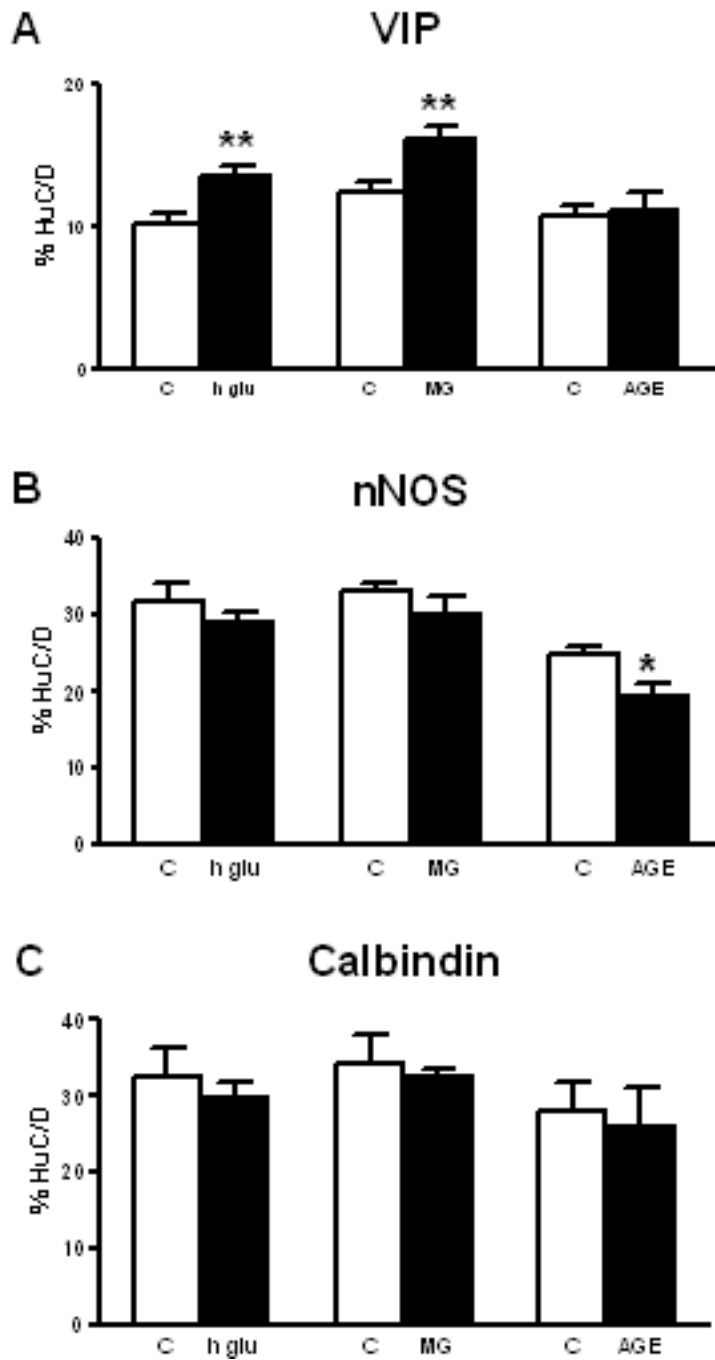
Figure 2.7: Effects of high glucose (h glu), methylglyoxal (MG) and AGEs on the relative number of VIP, nNOS and Calbindin immunoreactive cell bodies. Neurons containing VIP, nNOS or calbindin are expressed as a percentage the number of HuC/D-positive neurons. Clear bars represent data from controls and black bars represent data from preparations after exposure to the stimulus. (A) Note the significant increase of VIP positive cell bodies following exposure to high glucose and methylglyoxal but not AGE (h glu, n = 9; C, n = 12; MG, n = 7; C, n = 7; AGEs, n = 7; C, n=7) (B) Note the significant decrease of nNOS-positive cell bodies occurred only following exposure to AGE (h glu, n = 11; C, n = 10, MG, n = 7; C, n = 7, AGEs, n =5; C, n = 6) (C) Calbindin-positive neurons were unaffected by all stimuli (h glu, n = 11; C, n = 10; MG, n = 6; C, n = 6; AGE, n = 4; C, n = 5). Data are expressed as the mean ± SEM (** $p < 0.01$, * $p < 0.05$ by non paired Student's t-test).

2.4 Discussion

The results of the present study demonstrate that it is possible to replicate the effects of diabetes *in vivo* in an *in vitro* model using a myenteric plexus/muscle preparation from the adult rat. A number of pathways have been suggested to lead to neuropathy in diabetes and *in vitro* models are required in order to examine each pathway separately. This is the first *in vitro* study that uses explants of myenteric plexus/muscle to investigate different subpopulations of myenteric neurons involved in diabetic gastroenteropathy. The segment of the gut taken was always ileum since it has been shown that it is particularly susceptible in diabetes (Shotton et al., 2003).

Diabetes affects many subpopulations of the intrinsic and extrinsic nerves of the gut. Investigating the myenteric plexus has the advantage that it contains a number of different subpopulations of neurons that are not all affected in the same way in diabetes. We used wholemounts with the mucosal and submucosal layers stripped, in order to focus on three representative neuronal subpopulations in the myenteric plexus that show differential response to diabetes, the VIP, nNOS and Calbindin-containing neurons.

Previous studies from this laboratory have demonstrated that STZ-induced diabetes in rats causes an increase in the percentage of myenteric neurons containing VIP in the ileum (Belai et al. 1985; Shotton et al., 2004;Shotton et al., 2007) . This change is associated with failure to release VIP on electrical stimulation and degenerative changes in the nerve fibres (Belai et al., 1987).

In contrast, nNOS expression decreases. For example, the percentage of neurons expressing nNOS is significantly decreased in diabetes (Shotton & Lincoln, 2006; Shotton et al., 2007). However, there is some conflicting evidence possibly due to the

different time course of diabetes and the animal model examined (Adeghate et al., 2003;Pereira et al., 2008). There is a general consensus that dysfunction of NOS-containing neurons and decreased expression of nNOS are important contributing factors of impaired NANC smooth muscle relaxation and the gut dysmotility symptoms of diabetic gastroenteropathy (Takahashi, 2003). It has been reported, that nNOS myenteric neurons are particularly susceptible in diabetes (Cellek et al., 2004) and neuropathy in nNOS-containing neurons occurs in two phases. The first phase, with the loss of nNOS in the neurons is reversible on insulin replacement. The second phase occurring late in diabetes is characterized by neuronal apoptosis and is irreversible on insulin replacement (Cellek et al., 2003). Nevertheless, the mechanism by which the nNOS myenteric neurons are altered in diabetic complications is at present unclear.

The colocalization of nNOS with VIP has been reported in myenteric neurons throughout the GI tract in a range of species including rat, mouse, guinea-pig, pig, and human (Ekblad et al., 1996; Sang & Young, 1996; Costa et al., 1992; Timmermans et al., 1994; Porter et al., 1997;Qu et al., 2008). In the guinea-pig and mouse 90-100% of nNOS-immunoreactive neurons are positive for VIP (Costa et al., 1992; Qu et al., 2008). This overlap was determined in colchicine-treated tissue in order to enhance VIP immunoreactivity. Colchicine blocks axonal transport by disruption of microtubules causing peptides to accumulate within the cell bodies. However, according to Ekblad et al. (1996), colchicine treatment itself alters the expression of neuropeptides and nNOS in enteric neurons and extrapolation of data after colchicine treatment may give rise to misinterpretation of colocalization data. Double-labelling for VIP and nNOS has not been performed on the myenteric plexus of diabetic rats. Therefore it has not been determined if the increase observed in VIP occurs in nNOS-containing neurons.

In this study we also wished to examine whether resistance to change in diabetes could be replicated *in vitro*. Previously, it has been reported that substance P-containing nerves are unaffected in diabetes (Belai et al., 1985). However, it is not possible to quantify the number of intrinsic Substance P-containing neurons in the myenteric plexus without the use of an axonal transport inhibitor such as colchicine (Domoto et al., 1984). Therefore, we identified a population of myenteric neurons that were amenable to quantitation and were unchanged in diabetes. Calbindin-containing myenteric neurons were also unaffected after 12 weeks STZ-induced diabetes and provided a subpopulation with which to compare the responses of VIP- and nNOS-containing neurons (Voukali et al., 2011).

Calbindin belongs to a family of calcium binding proteins such as calretinin, parvalbumin, calmodulin, S100 etc. Calbindin is found in enterocytes and other types of cells and is also dispersed in various types of neurons. It has been extensively used as a neuronal marker, since it is localised in distinct neuronal subpopulations in the central and peripheral nervous systems and stains the cytoplasm and even the thin processes of neurons facilitating studies of neuronal shape and connectivity. The presence of calbindin in mammalian ENS was first shown by Buchan and Baimbridge (Buchan & Baimbridge, 1988). In rat ileum myenteric plexus calbindin neurons are not involved in the control of smooth muscle and they do not colocalise with VIP or nNOS forming a distinct subpopulation of neurons (Buchan & Baimbridge, 1988; Mann et al., 1999, Furness, 2005, Qu et al., 2008). They can be interneurons connecting the myenteric or submucosal plexus or may have sensory function with their afferent fibres leading to sympathetic ganglia. About 40% of calbindin-containing rat myenteric neurons are cholinergic (Mann et al., 1999). VIP or galanin nerve fibres were shown to terminate on calbindin-containing neuronal cell bodies. In other species, including human, the

distribution of calbindin in ENS is similar (Walters et al., 1993; Quinson et al., 2001;

Denes & Gabriel, 2004).

2.4.1 Apoptosis and cell death

Throughout this study we used anti-HuC/D as a pan-neuronal marker. Anti-

HuC/D recognises the neuronal proteins HuC and HuD. HuC/D are human members of

the embryonic lethal, abnormal vision (ELAV), Drosophila family of proteins (ELAV3

and ELAV4, respectively). The expression of both is restricted to neurons, where they

act as mRNA stabilizers and are involved in neuronal differentiation during

development. Their expression is also maintained in the adult (Schenes-Furry et al.,

2006; Bolognani & Perrone-Bizzozero, 2008). Anti-HuC/D has been used widely as a

neuronal marker in peripheral nervous system (Lin et al. 2002). It has been reported to

be preferable to PGP 9.5, tubulin β III isoform and Neuron Specific Enolase for neuron

staining in the myenteric plexus in wholemounts (Lin et al., 2002, Phillips et al., 2004).

The application of anti-HuC/D as a histochemical marker is advantageous because it

reliably labels all neurons. In addition, it provides accurate counts of neurons in ganglia

because immunostaining of anti-HuC/D is restricted to neuronal perikarya and does not

include the extrinsic and intrinsic neuronal fibres in wholemount preparations.

Loss of HuC/D coincided with TUNEL staining in CG/SCG in samples of

horses with equine grass sickness indicating that the latter stages of apoptosis are

associated with decreased HuC/D expression (Shotton et al., 2011). Other authors have

considered absence of HuC/D staining as an indication of cell loss (Izbeki et al., 2008;

De Mello et al., 2009).

Culture *per se* did not significantly affect the number of HuC/D neurons per ganglion indicating that the culture conditions did not result in significant neuronal loss. It cannot be excluded that culture altered neuronal metabolism or function. However, none of the stimuli investigated *in vitro* affected HuC/D expression relative to control culture preparations at the concentrations used. Thus any changes in VIP, nNOS or calbindin expression that were observed in this study could not be attributed to loss of HuC/D-positive neurons. In preliminary experiments to test the effect of various methylglyoxal concentrations in myenteric ganglia, a dose of 10 μM was selected, because higher concentrations induced neuronal loss.

Previous *in vivo* studies have reported the loss of myenteric neurons in STZ-diabetes. Counts of the number of enteric neurons per unit area in the STZ-induced diabetic rat have shown a wide range of reduction from 1% to 50% with some regional differences in the response (De Mello et al. 2009). On the other hand, in a study in this laboratory, quantification of the average number of HuC/D-positive neurons per ganglion demonstrated that there was no significant loss of neurons after 12 weeks STZ-induced diabetes in the ileum (Voukali et al., 2011). These contradictory results may be due to the difference in the methodology of quantification since measurement of the number of neurons per unit area will be susceptible to influence by the distension of the gut that occurs in diabetes *in vivo* (Schmidt, 2002). It is possible that the quantification of six ganglia was not sufficient to demonstrate a small loss of neurons. However, these results do demonstrate that any changes observed in the percentage of HuC/D-positive neurons containing VIP or nNOS were due to significant changes in the expression of VIP or nNOS rather than alterations in the pan neuronal marker.

Several groups have reported apoptotic neuronal cell death as a feature of diabetic neuropathy in other types of peripheral neurons (Russell et al., 1999; Russell &

Feldman, 1999; Srinivasan et al., 2000;Kishi et al., 2002;Schmeichel et al., 2003), but the evidence is controversial (Tolkovsky, 2002). Studies of the counts of the total number of neurons did not support the presence of significant neuronal cell death (Schmeichel et al., 2003;Guo et al., 2004). For example, in the study of Guo et al. neuronal counts in sensory, autonomic and myenteric ganglia demonstrated the reduction up to 2%. Activation of caspase 3 was proved to occur without evidence of DNA fragmentation and consequently caspase 3 activation does not necessarily imply apoptotic cascade (Cheng & Zochodne, 2003; Guo et al., 2004). Thus, neuronal cell death is not a prominent feature of sensory and autonomic neurons in diabetes *in vivo* (Schmidt et al., 1993; Schmidt et al. 1997; Schmidt, 2001; Zochodne et al., 2001). Apoptotic stresses are induced, but the final execution of apoptosis is prevented by the induction of counter regulatory elements (Kamiya et al., 2005). A slow progression of the disease with an axonal dying back phenomenon of axonal loss and neuronal atrophy takes place rather than apoptosis.

2.4.2 Effect of culture *per se*

All results were expressed as a percentage of HuC/D-positive neurons. Under control conditions, there was a significant increase in the percentage of myenteric neurons expressing VIP, nNOS and calbindin after 24h in culture, relative to myenteric plexus/muscle preparations that had not been exposed to culture. These results imply a direct effect of axotomy and culture.

An increase of VIP and nNOS in myenteric and submucous neurons after culture has been reported previously (Lin et al., 2003; Lin et al., 2004). Interestingly, in the

study of Lin et al., the increased expression of VIP-containing neurons occurred within the nNOS-containing myenteric neurons. Culture-induced changes in VIP synthesis within nNOS neurons were also explained as a need to enhance intestinal inhibition or an attempt to control excessive proliferation of smooth muscle cells during culture. Increased expression of VIP within the nNOS myenteric neurons has been found in several pathophysiological situations such as axotomy and colchicine treatment, hypertrophy of smooth muscle and in Crohn's disease (Ekblad et al., 1996;Belai et al., 1997; Ekblad et al., 1998). These alterations in chemical coding are referred as "cell body reaction", a response to injury or stressful conditions, to promote regeneration and survival (Zigmond & Sun, 1997). These changes reflect the shift from synaptic transmission to regeneration.

VIP, apart from its function as a neuromodulator, promotes neuronal survival and some authors identify VIP as a neurotrophic factor (Klimaschewski, 1997). Increased expression of nNOS is controversial in terms of survival and neuroprotection. Exogenous supplement of VIP and a NO donor improved the survival of myenteric cultures (Sandgren et al., 2003; Arciszewski & Ekblad, 2005). Hence, our results underline the role of calbindin, nNOS and VIP in neuronal plasticity. Whether VIP protects specifically the nNOS-containing myenteric subpopulation or NO and VIP act in collaboration are significant questions yet to be answered. Therefore, in the present study, the effects of all stimuli *in vitro* were assessed relative to preparations maintained in culture under control conditions in parallel throughout.

2.4.3 Effect of oxidative stress and diabetic stimuli

None of the stimuli investigated here caused a significant loss of HuC/D-positive neurons per ganglia. Recently, a significant loss of enteric neurons has been reported when dissociated enteric neurons were exposed to hydrogen peroxide *in vitro* which could be prevented by pre-incubation with neurotrophin-3 (Korsak et al., 2012). It is possible that myenteric neurons in wholemount preparations are better able to survive oxidative stress in culture than dissociated neurons since they have undergone less disruption and the normal supportive environment is maintained. Oxidative stress was induced by menadione in this study. Menadione is a quinone that undergoes a redox cycle resulting in the production of superoxide radicals and hydrogen peroxide (Briere et al., 2004). It can interfere with oxidative phosphorylation, diverting electrons from complex 1 (Chiou et al. 2003), inducing mitochondrial membrane depolarisation and disrupting calcium homeostasis activating apoptotic factors (Gerasimenko et al., 2002).

Only oxidative stress produced the same pattern of change *in vitro* that was observed in diabetes with a significant increase in the percentage of VIP-containing neurons and a significant decrease in nNOS-containing neurons. Furthermore, we demonstrated that resistance to change in diabetes was also reflected by resistance to oxidative stress *in vitro* since calbindin-containing neurons were unaffected under both conditions. Thus, oxidative stress appears to be a common element in neuropathic changes in myenteric neurons in diabetes.

A number of pathways have been suggested to lead to oxidative stress in diabetes including mitochondrial dysfunction induced by high glucose (Leinninger et al., 2006), carbonyl stress due to increased production of carbonyl species such as methylglyoxal (Thornalley, 2005), and activation of the RAGE receptor by AGEs (Yan

et al., 1994). When the effects of high glucose, methylglyoxal and AGEs were examined individually, an interesting differential pattern emerged. Exposure to high glucose and methylglyoxal caused an increase in the percentage of VIP-containing neurons but had no effect on nNOS-containing neurons. In contrast, exposure to AGEs decreased the percentage of nNOS-containing neurons but had no effect on VIP expression. Thus, the relative contribution of different pathways to change in diabetes appears to differ depending on the subpopulation of neurons involved. A decrease in the expression of nNOS in myenteric neurons on exposure to AGEs *in vitro* has been reported previously (Korenaga et al. 2006). Furthermore, vulnerability to AGEs in a neuronal cell line only occurred when the cells were induced to express nNOS (Cellek et al., 2004). RAGE expression has been demonstrated in myenteric ganglia (Jeyabal et al. 2008; Korenaga et al. 2006). However, it remains to be determined if RAGE is selectively expressed in nNOS-containing neurons. We were unable to answer such a question because of technical difficulties. Also, activation of RAGE in sensory neurons induces oxidative stress that can be prevented by α-lipoic acid (Vincent et al. 2007a).

In studies of the guinea-pig and mouse ileum, 90-100% of nNOS-containing neurons have been reported also to contain VIP (Costa et al., 1992; Qu et al., 2008). This raises the question as to whether high glucose/MG were acting on the same population of nNOS-containing myenteric neurons to cause an increase in VIP together with a decrease in nNOS. Alternatively, high glucose and MG could have been acting on a different subpopulation of nNOS-containing neurons from that at which AGE exerted its effects. It should be noted that the above colocalization studies were performed using colchicine to enhance VIP-immunoreactivity. In a study of myenteric neurons in the rat small intestine, it has been reported that, in the absence of colchicine, the majority of nNOS-containing neurons do not contain VIP. Colchicine treatment

resulted in an increase in VIP-containing neurons together with a decrease in nNOS-containing neurons and an increase in the colocalization of nNOS with VIP. The authors concluded that the level of colocalization observed after colchicine treatment may not reflect the normal condition (Ekblad et al., 1996). In a recent study of the myenteric plexus of a rat model of Parkinson's disease, Colucci et al., (2012) reported a decrease in nNOS-containing neurons and an increase in VIP-containing neurons in the absence of changes in the intrinsic excitatory motor neurons that contain ACh in the distal ileum and proximal colon. This is similar to the pattern observed in the STZ-diabetic rat. Using triple labelling for nNOS, VIP and HuC/D in the absence of colchicine, Colucci et al. demonstrated that the increase in VIP coincided with an increase in the percentage of nNOS-containing neurons that also contain VIP. The authors concluded that there were two subpopulations of nNOS-containing neurons that were affected differently in Parkinson's disease. They proposed that, decreased nNOS expression occurred in a specific population of neurons that selectively expressed nNOS under normal conditions. However, VIP expression was induced in a separate population of nNOS-containing neurons that maintained their expression of nNOS (Colucci et al., 2012). The presence of two populations could explain how the changes in nNOS and VIP expression reported here occurred in response to different diabetic stimuli. However, triple labelling studies are required to confirm if this is the case in STZ-induced diabetes and the *in vitro* model.

In addition to being resistant to oxidative stress and diabetes, calbindin-containing neurons were unaffected by exposure to high glucose, methylglyoxal and AGEs *in vitro*. Although they do not prove a direct link between calbindin and neuroprotection, these findings imply that calbindin seems to confer to neurons a greater resistance to diabetic stimuli. It has been shown that calbindin-positive hippocampal

neurons are better able to buffer acute elevation of intracellular calcium (Mattson et al., 1991). Alexianu et al. showed that absence of calbindin could represent a factor explaining different susceptibility of motor neurons in Amyotrophic Lateral Sclerosis that die from oxidative stress. Motor neurons affected late in the disease process do contain calbindin and/or parvalbumin, but motor neurons that degenerate early do not (Alexianu et al., 1994). In line with this evidence, it was found that calbindin-containing dopaminergic neurons in the midbrain were completely spared after paraquat-induced degeneration and showed no overt signs of lipid peroxidation (McCormack et al., 2006). Also, calbindin-containing neurons from rat cortical cultures exposed to xanthine oxidase were spared, suggesting that calbindin is protective against oxidative stress (Hugon et al., 1996).

Calbindin maintains a significant intracellular role in regulating the excitability of nerve cells. The role of calbindin, as a calcium buffering protein, is to bind calcium ions with high affinity. It is found in high concentrations in neurons and thus it has high buffering capacity (Baimbridge et al., 1992). Calbindin interacts with calcium-dependent processes such as the release of neurotransmitters and influences the activity of calcium channels. It is present in enteric neurons with specific electrophysiological properties (AH neurons) and where various types of calcium channels are present (Naidoo et al., 2010). It has been described that calbindin, as a calcium binding protein, can alter the duration of action potentials; can promote neuronal bursting activity; can allow for a greater contribution of calcium entry to the overall membrane depolarization (Baimbridge et al., 1992). Finally, calbindin can protect the cells against the damaging effects of excessive calcium influx during prolonged periods of high activity slowing down calcium transients and making up a passive system that limits a stimulated rise in intracellular free calcium concentration.

The protective role of calbindin in enteric neurons *in vitro* has not been studied before. The presence of calbindin in myenteric neurons may help to attenuate the degrading consequences of elevated intracellular calcium and to be protective against glucose toxicity. Calcium dyshomeostasis and impaired mitochondrial calcium buffering is a common feature in diabetes (Huang et al., 2002b; Verkhratsky & Fernyhough, 2008;Fernyhough & Calcutt, 2010). The disruption of intracellular calcium metabolism may occur due to impairment of calcium transport and persistent elevated cytosolic calcium concentrations due to mitochondrial injury. Some studies have reported changes in the expression of calcium binding proteins in neurodegenerative disease, but the data are rather inconsistent (Heizmann & Braun, 1992). In this study, the immunoreactivity of calbindin remained in similar values whether exposed to stimuli or not, in contrast to the other neuronal myenteric subpopulations.

2.4.4 Conclusion

As far as we are aware, this is the first study that has reproduced the effects of diabetes in an *in vitro* model in terms of both vulnerability and resistance in discrete subpopulations of myenteric neurons in the same plexus. The results presented here provide evidence that oxidative stress plays an important role in diabetes-induced changes but that the pathway by which oxidative stress occurs differs in different populations of myenteric neurons. The *in vitro* models established in this study could provide a useful tool with which to investigate the mechanisms underlying the development of neuropathy in diabetes that lead to abnormal control of gut motility.

Chapter 3: Study of therapeutic agents for diabetic neuropathy

3.1 Introduction

The management of the gastrointestinal symptoms of diabetic neuropathy mainly relies on various drugs acting on gut motility (Ziegler, 2001; Shakil et al., 2008). For gastroparesis, several specific therapies directed at the presenting symptoms, such as metoclopramide, a 5-HT$_3$ and D2 receptor antagonist; erythromycin, a motilin receptor agonist; acetylcholine release inhibitors and, in some cases, gastric electric stimulation are used. For diarrhea, the relief is directed towards the correction of fluid and electrolyte imbalances and sometimes towards the prescription of antibiotics. For constipation that may alternate with diarrhea the use of laxatives is advised.

In fact, the optimal control of blood glucose levels is the most effective strategy to prevent neuropathy in diabetes including gastroenteropathy. The benefit of maintaining normoglycaemia has been consistently demonstrated. The DCCT multicentre study showed that the prevention of the appearance and the progression of the symptoms of neuropathy can be sustained for many years (The Diabetes Control and Complications Trial Research Group, 1993; Parry, 1999). However, strict glycaemic control can result in regular episodes of hypoglycaemia that may insult the cognitive abilities and cause painful neuropathy. Furthermore, it is not easy, even for the most

determined patient, to keep their blood glucose levels well regulated. For this reason, additional approaches have been investigated that counteract the metabolic consequences of hyperglycaemia that may lead to neurodegeneration. This chapter will focus on agents that act against oxidative stress and/or carbonyl stress.

3.1.1 Pathogenesis oriented treatments: *In vivo* studies & clinical trials

3.1.1.1 α-Lipoic acid

α-Lipoic acid has been characterised as a "universal" anti-oxidant since it can act in both an aqueous and a lipid environment (Packer et al., 1995). Treatment with α-lipoic acid has been investigated in experimental diabetes. STZ-induced diabetic rats, injected intraperitoneally with different doses of α-lipoic acid five times per week, demonstrated improved nerve blood flow, distal nerve conduction velocity and reduced oxidative stress, indicated by GSH levels (Nagamatsu et al., 1995). Another study showed a beneficial action of α-lipoic acid on neurovascular function and nerve conduction velocity in STZ-diabetic rats (Cameron et al., 1998). In a following study (Kishi et al., 1999), the administration of α-lipoic acid intraperitoneally enhanced glucose uptake in a dose dependent manner.

However, Stevens et al. highlighted the selective and complex action of α-lipoic acid. Administration of α-lipoic acid as recommended by Nagamatsu et al. improved selectively sensory nerve conduction velocity but not motor nerve conduction velocity. It restored some energy metabolites [(Na, K)ATPase activity, NAD+: NADH ratios and myoinositol content] and prevented the decrease of endogenous anti-oxidant enzymes activity. On the other hand, it exaggerated aldose reductase pathway metabolites

(Stevens et al., 2000). With parallel dietary and intraperitoneal administration, Coppey et al. found that motor nerve conduction velocity was improved in STZ-diabetic rats but the increase in serum triglyceride and free fatty acids could not be prevented (Coppey et al., 2001). In the study of Yorek et al., combination therapy of α-lipoic acid with an aldose reductase inhibitor, fidalrestat, normalised oxidative stress markers and nerve conduction velocities at lower doses (Yorek et al., 2004). In the case of enteric nerves, α-lipoic acid treatment, on its own, was unable to prevent diabetes-induced changes in VIP- or NA-containing nerves (Shotton et al., 2003). However, in combination with evening primrose oil to supplement γ-linolenic acid, α-lipoic acid did prevent changes in VIP-containing nerves (Shotton et al., 2004).

These positive results in experimental diabetes prompted the initiation of a series of clinical trials of α-lipoic acid in diabetic patients with neuropathy. Ziegler et al. (2004; 2011) have performed meta-analysis of the results of several of these clinical trials. The trials were selected on the basis that they were all randomised, double-masked placebo controlled trials on diabetic patients with symptomatic polyneuropathy. α-lipoic acid was administered intravenously (600 mg per day on weekdays over three weeks) and the total symptom score for neuropathy was assessed daily on weekdays. The results from four trials were analyzed: The alpha-lipoic acid in diabetic neuropathy (ALADIN I and ALADIN III) trials were on outpatients from diabetic centres throughout Germany. The symptomatic diabetic trial (SYDNEY) consisted of in-patients in a Moscow hospital. The neurological assessment of thioctic acid in diabetic neuropathy (NATHAN I) trial investigated outpatients in diabetic centres in the USA, Canada and Europe. The outcomes of the SYDNEY and ALADIN I trials demonstrated significant beneficial effects on neuropathic symptoms compared with placebo. The NATHAN I and ALADIN I also observed some beneficial effects but these trends did

not reach statistical significance. The oral use of α-lipoic acid (600 mg) is now considered helpful in improving sensory neuropathic symptoms, after only 1 week of administration. Clinical trials testing the efficacy of α-lipoic acid on the treatment of autonomic neuropathy including enteropathy (600, 800 mg intravenously and orally), also demonstrate encouraging outcomes and improvement of neuropathic symptoms (Ziegler et al., 1997; Tankova et al., 2004). So far, α-lipoic acid was only compared to placebo. Thus, its efficacy over other commonly prescribed oral treatments has not been yet investigated (Tang et al., 2007). However, it is well tolerated, with moderate adverse events, and this is a strong benefit compared with other treatments.

3.1.1.2 Nicotinamide

Nicotinamide is one of the two principal forms of vitamin B3 and a precursor of NAD+ and NADP+, coenzymes involved in many redox reactions in the cell (Niacinamide.Monograph, 2002). Nicotinamide is not only an essential nutrient for cellular function. It also has a protective ability that prevents NAD+ depletion during DNA repair by inhibiting PARP. Interestingly, nicotinamide has been utilised to prevent experimental and clinical diabetes. Nicotinamide supplementation was protective against the effects of STZ in rats, lowering damage due to lipid peroxidation (Melo et al., 2000) but the European Nicotinamide Diabetes Intervention Trial showed that it was ineffective in the prevention of type 1 diabetes (Gale et al., 2004).

PARP is activated as a downstream effector of oxidant induced DNA damage. Excessive ROS production triggers DNA single strand breakage. By the synthesis of a poly(ADP-ribose) chain on damaged DNA, PARP acts as a signal to initiate DNA repair. Its overactivation initiates an energy consuming cycle: PARP transfers the ADP-

ribose moieties from NAD+ to nuclear proteins leading to the rapid depletion of the intracellular pools of NAD+ and energy failure. However, it is worth emphasizing that in diabetes the levels of ATP and energy substrates are not decreased (Gibson et al., 2006; Kishi et al., 1999). PARP also begins a downstream regulation of various transcription factors including NFκB.

The role of PARP has been studied extensively in diabetic neuropathy. Obrosova et al. reported that PARP activation is an important mechanism in diabetic neuropathy (Obrosova et al., 2004, Obrosova et al., 2005). Inhibitors of PARP can alleviate neuropathy, increase nerve conduction velocity and improve nerve function (Ilnytska et al., 2006; Gibson et al., 2006).

In experimental diabetic neuropathy, nicotinamide, used as a weak PARP inhibitor, reversed impairments in endoneurial blood flow, corrected increased lipid peroxidation in sciatic nerve and attenuated functional and behavioural deficits of diabetic sensory neuropathy (Stevens et al., 2007). In addition, nicotinamide prevented the NAD+ depletion of the diabetic sciatic nerve (Negi et al., 2010).

3.1.1.3 Aminoguanidine

Aminoguanidine or pimagedine has been proposed to act as a carbonyl scavenger that inhibits the formation of AGEs (Thornalley, 2003b). Early studies of aminoguanidine in experimental diabetic neuropathy showed that oral or intravenous administration improves nerve function. Nerve ischemia and conduction velocity deficits of sciatic-tibial and caudal nerves were ameliorated after 24 weeks of aminoguanidine treatment in a dose dependent manner (Kihara et al., 1991). In another

study, the beneficial effect of aminoguanidine on nerve conduction velocity did not depend on the reduction of aldose reductase metabolites (Cameron et al., 1992). Instead, the improvement of nerve conduction velocity occurred through inhibition of AGEs formation, and was accompanied by a partial effect on reduced myelinated fiber size and axonal atrophy in diabetes (Yagihashi et al., 1992; Miyauchi et al., 1996). Treatment with aminoguanidine also partially corrected the enlargement of sural nerve microvessels and the expansion of their vascular and luminal areas (Sugimoto & Yagihashi, 1997). Additionally, other studies reported a partial correction of Na+, K-(ATP)ase activity loss (Wada et al., 1999).

An additional action of aminoguanidine as an NOS inhibitor has also been investigated. It was suggested that the mechanism of treatment of aminoguanidine on peripheral somatic nerves during diabetes involves improved NO action. However, aminoguanidine treatment does not affect NO production in the vasa nervorum of peripheral nerves (Cameron & Cotter, 1996). These findings were also supported by the study of Dewhurst and colleagues (1997). This study showed that inhibiting NOS with NG-nitro-L-arginine methyl ester, reduced the sciatic endoneurial blood flow, but stimulating the synthesis of NO, with L-arginine, enhanced endoneurial blood flow (Dewhurst et al., 1997).

Some studies investigating experimental diabetic neuropathy and other diabetic complications yielded conflicting results of the efficacy of aminoguanidine (Azal et al., 2002; Unlucerci et al., 2001). The study of Birrell and colleagues using primates in chronic aminoguanidine treatment, did not find any improvement on motor nerve conduction velocity, morphometric analysis of nerve fibres or autonomic dysfunction (Birrell et al., 2000). However this study has been criticized of using the very small dose of 10 mg/kg compared with 25 or 50 mg/kg that have been administered in rats

(Cameron et al., 2005). In experimental diabetic autonomic neuropathy, the chronic administration of aminoguanidine did not prevent the frequency or the appearance of neuroaxonal dystrophy in sympathetic ganglia (Schmidt et al., 1996). Similarly, aminoguanidine was unable to prevent diabetes-induced changes in NA-containing nerves within the ileum. However, changes in the intrinsic nNOS- and VIP-containing nerve fibres in the ileum in diabetes were partially prevented by aminoguanidine treatment (Shotton et al., 2007).

Double-blinded, multiple-dose (low and high doses of 50–300 or 100–600 mg/day), placebo-controlled, randomized clinical trials of chronic aminoguanidine treatment in overt diabetic nephropathy (ACTION) were also performed: ACTION I was conducted in patients with type 1 diabetes mellitus and ACTION II in patients with type 2 diabetes mellitus (Freedman et al., 1999;Thornalley, 2003b). Patients with combined high and low aminoguanidine dose showed a non significant alleviation of nephropathy with lower levels of triglycerides, low density lipoproteins (LDL) cholesterol and urinary protein. In ACTION II, the External Safety Monitoring Committee recommended the early termination of the ACTION II trial due to safety concerns and lack of efficacy. Gastrointestinal disturbance, abnormalities in liver function tests, flu-like symptoms, and a rare vasculitis were the reported side effects of the drug.

3.1.1.4 Thiamine

Thiamine belongs to the B1 vitamin complex and is an essential micronutrient absorbed from the diet (Thiamine Monograph, 2003). Once transported into the cell, thiamine is phosphorylated to thiamine pyrophosphate. Thiamine pyrophosphate is a

cofactor of a series of enzymes and fundamental for the intracellular metabolism of glucose. In 1987, it was reported that diabetic patients have low blood thiamine levels (Saito et al., 1987) that is not due to the diet of diabetics (Ba, 2008;Vindedzis et al., 2008), but from impaired metabolism and clearance of thiamine in the diabetic kidney (Thornalley et al., 2007;Rabbani & Thornalley, 2011). Thiamine, and/or its derivative benfotamine, increases the disposal of excess triosephosphates formed in hyperglycaemia thus preventing methylglyoxal-induced carbonyl stress and subsequent formation of AGEs (Berrone et al., 2006). These findings have led to the therapeutic potency of thiamine in diabetes being examined.

Double-blind, randomized, controlled clinical trials of thiamine in diabetic patients with neuropathy have reported benefits with no specific adverse effects. Administration of benfotiamine, a lipophilic derivative of thiamine with better bioavailability (Benfotiamine Monograph, 2006), in a combination therapy with vitamins B6 and B12, improved nerve conduction velocity in the peroneal nerve and induced a trend of improvement of the vibration perception threshold of patients with diabetic polyneuropathy (Stracke et al., 1996). In another clinical trial, thiamine and pyridoxine administration alleviated the pain, numbness and paresthesia symptoms of diabetic peripheral sensory neuropathy (Abbas & Swai, 1997). In a randomized, placebo-controlled, double-blind, two-centered pilot study testing benfotiamine, type 1 and 2 diabetic patients showed improvement on the total neuropathy score, a decrease in pain, a self assessed improvement of their condition, but no effect in the tuning fork test (Haupt et al., 2005). Thiamine was effective also in clinical trials of diabetic nephropathy (Rabbani et al., 2009; Rabbani & Thornalley, 2011).

Although clinical trials of B1 vitamin remain at a preliminary level, evidence from experimental diabetes is in line with the discussed effects in humans.

Benfotiamine suppressed the development of diabetic neuropathy *in vivo* (Stracke et al., 2001). Specifically, motor nerve conduction velocity was improved and was nearly normalized after six months. In addition, AGEs were significantly reduced in peripheral nerve tissue. A high dose of benfotiamine (70 mg/kg) prevented AGEs accumulation in kidney, retina and plasma of STZ-treated rats (Karachalias et al., 2003). Thiamine corrected dyslipidemia normalizing cholesterol and triglycerides (Babaei-Jadidi et al., 2004). Thiamine was protective in ameliorating detrusor contractility and inhibiting the progression of diabetic cystopathy (Yenilmez et al., 2006).

A number of mechanisms have been proposed for the development of neuropathy in diabetes, including carbonyl stress, many of which converge at the level of oxidative stress (Baynes & Thorpe, 1999; Brownlee, 2001; Pop-Busui et al., 2006). In the previous chapter, data using *in vitro* models were presented that provided evidence that exposure of a wholemount myenteric plexus preparation from the ileum of adult rats to oxidative stress did mimic the changes that occur in diabetes *in vivo* but that the stimulus leading to oxidative stress in diabetes may differ depending on the individual nerve population studied. This model also provides a tool with which to examine the ability of potential therapeutic agents to prevent diabetes-induced changes in myenteric neurons and to investigate further the role of oxidative or carbonyl stress.

Therefore, the aims of this study were to examine the effects of several agents on the changes induced in VIP- or nNOS-containing neurons *in vitro.* The effects of α-lipoic acid, an anti-oxidant; nicotinamide, a PARP inhibitor; aminoguanidine, a carbonyl scavenger; and thiamine, an inhibitor of carbonyl stress induced by high glucose, on the responses to oxidative stress, carbonyl stress, high glucose or AGEs were investigated.

3.2 Materials and methods

3.2.1 Culture preparations

Adult male Sprague-Dawley rats (275-350 g) were killed by CO_2 asphyxiation and the ileum was dissected, cleaned, and stored in a dissecting buffer of HBSS containing 10 mM glucose and 1% penicillin-streptomycin. Approximately 4 cm of the gut were put on a 2 ml stripette, scored gently with forceps and the myenteric plexus and the muscle layers were peeled away under a dissecting microscope. The myenteric plexus/muscle preparations were then washed in antibiotic wash solution (HBSS containing 1% penicillin-streptomycin, 2% gentamycin and 2% 5mg ml^{-1} metronidazole). The tissue was cut into segments approximately 1 cm^2, stretched and pinned onto Sylgard (VWR, Buffalo Grove, IL, USA). The samples were cultured in defined culture medium containing 10 mM glucose (M199, supplemented with 1% L-Glutamine, 1% Hepes Buffer, 1% penicillin-streptomycin , 0.35% Pathocyte-4-BSA, 60 ng ml^{-1} progesterone, 0.016 mg ml^{-1} putrescine, 400 ng ml^{-1} l-thyroxine, 38 ng ml^{-1} sodium selenite, 340 ng ml^{-1} triiodothyronine, 100 µg ml^{-1} transferrin).

As described in the previous chapter, for oxidative stress, 1 µM menadione sodium bisulfite was added to the medium, for hyperglycaemia, the medium contained additional glucose to give a final concentration of 30 mM., for carbonyl stress, 10 µM methylglyoxal and for AGEs 250 µg ml^{-1} BSA-AGE (Biovision Research Products, CA, USA) was added. Control preparations were maintained in 10mM glucose in parallel. All preparations were maintained for 24h at 37°C gassed with 95% O_2 and 5% CO_2.

Additional experiments were carried out to examine the ability of different inhibitors to prevent changes caused by the stimuli. The anti-oxidant α-lipoic acid was tested in the concentration of 100 μM. α-lipoic acid was prepared as previously described (Vincent et al., 2005a) and added to media containing high glucose, methylglyoxal or BSA-AGE at the start of the experiment. The carbonyl scavenger aminoguanidine (100 and 500 μM) or two forms of vitamin B, thiamine pyrophosphate (Vitamin B1, 100 μM) or nicotinamide (Vitamin B3, 100 μM) were added in the media containing high glucose, methylglyoxal or menadione at the start of the experiment. The preparations were maintained for 24h at 37 °C gassed with 95% O_2 and 5% CO_2.

The samples were fixed in 4% PFA for 18-24h at 4 °C. Myenteric plexus/muscle preparations were washed and stored in PBS merthiolate (0.05%) at 4 °C before processing. All chemicals mentioned above were obtained from Sigma, Poole, UK unless stated otherwise.

3.2.2 Immunofluorescence procedures: double staining for VIP or nNOS with HuC/D

The myenteric plexus/muscle preparations were placed, longitudinal muscle uppermost, onto microscope slides and processed for immunohistochemical localisation of nNOS and VIP. In order to evaluate the relative frequency of the positive cell bodies, anti-HuC/D was used to label all neuronal cell bodies in the myenteric plexus. The myenteric plexus/muscle preparations were incubated for 1 hour in blocking solution containing 10 % normal horse serum (Gibco-Invitrogen, Paisley, UK) and 0.1% Triton X100 in PBS merthiolate. Primary antisera were diluted in the above blocking solution (rabbit polyclonal anti-nNOS, Santa Cruz, CA, USA, 1:500, rabbit polyclonal anti-VIP,

Immunostar Inc., Hudson, WI, USA, 1:500). The myenteric plexus/muscle preparations were incubated with the primary antisera overnight. After being washed in PBS containing 0.1% X100 Triton, the preparations were incubated in blocking solution containing 10% normal goat serum (Gibco-Invitrogen, Paisley, UK) and 0.1% Triton X100 in PBS merthiolate for 1 hour. Samples were then incubated overnight with mouse monoclonal anti-HuC/D (Molecular Probes Probes, Eugene, OR, USA) diluted 1:200 in the above solution. Finally, the samples were washed, incubated for 1 hour in the dark at room temperature with Alexa 488 Donkey anti-Rabbit (Molecular Probes, Eugene, OR, USA) and Cy3 Goat anti-Mouse (Jackson ImmunoResearch Laboratories, West Grove, PA, USA) diluted 1:100 in PBS Triton, washed, mounted and the coverslips sealed. All procedures were carried out at room temperature.

3.2.3 Analysis and statistics

The samples were processed in parallel and analysed on a Zeiss fluorescence microscope (Carl Zeiss Ltd., Welwyn Garden City, UK). For each sample, a minimum of 200 cell bodies positive for HuC/D was assessed for the presence or absence of nNOS or VIP. The proportion of positive nNOS or VIP cell bodies were expressed as a percentage of the number of HuC/D-immunoreactive myenteric neurons.

The data were analysed with GraphPad Prism 3 software using one way analysis of variance followed by Neumann-Keulls post hoc comparisons, or using an unpaired Student's t test, where $P < 0.05$ was taken to indicate statistical significance.

The samples were also photographed using a Canon EOS Elan II digital camera and micrograph pictures were produced using Photoshop Elements 8.0 software.

3.3 Results

3.3.1 α-lipoic acid

When added to control media, α-lipoic acid did not cause any significant changes in the number of nNOS or VIP immunoreactive neuronal cell bodies. Furthermore, it was established that the solution required to dissolve α-lipoic acid for *in vitro* experiments (Vincent et al. 2005a), had no effect on its own on myenteric neurons. Exposure to 10 μM methylglyoxal for 24h to induce carbonyl stress caused a significant increase in the relative number of VIP-positive neurons ($p<0.01$). Exposure to BSA-AGE caused a decrease of the nNOS-containing neurons ($p<0.05$). Addition of 100 μM α-lipoic acid completely prevented the increase in VIP-containing neurons induced by carbonyl stress and the decrease in nNOS-containing neurons induced by BSA-AGE (fig. 3.1). Representative micrographs are provided in fig. 3.2. Although the data are not presented here, it should be noted that previous studies from this laboratory by H.R. Shotton demonstrated that α-lipoic acid also prevented the increase in VIP-containing neurons induced by high glucose (see Voukali et al., 2011).

α−LIPOIC ACID

A   Effect on methylglyoxal: VIP
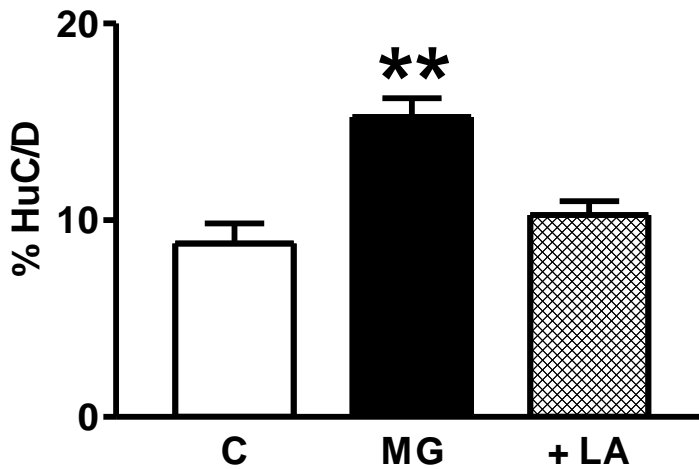
B   Effect on BSA-AGE: nNOS
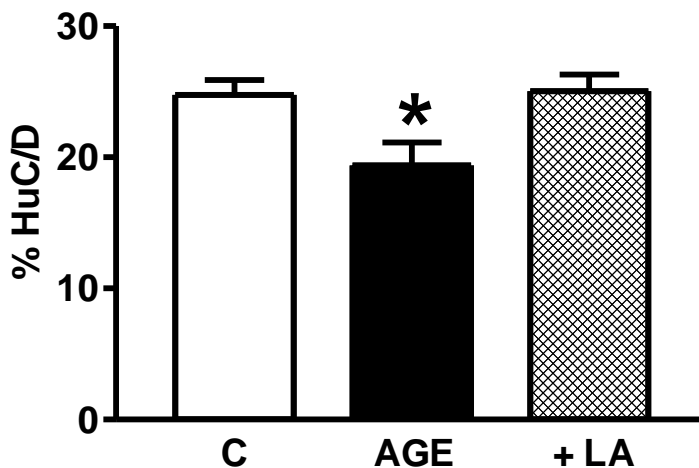
Figure 3.1: Effect of α-lipoic acid (LA) on the action of methylglyoxal (MG) and BSA-AGE (AGE) in myenteric plexus/muscle preparations. Neurons containing VIP or nNOS are expressed as a percentage the number of HuC/D-positive neurons. Clear bars represent data from controls (C), black bars represent data from preparations in the presence of a stimulus (MG or AGE). Hatched bars represent data from preparations incubated with both the stimulus and LA) α-Lipoic acid prevented the increase in VIP-containing neurons induced by methylglyoxal (MG, n = 5; +LA, n = 6; C, n = 6, LA, n=6). (C) α-Lipoic acid prevented the decrease in nNOS-containing neurons induced by BSA-AGE (AGE, n = 5; +LA, n = 6; C, n = 6, LA, n=5).   Data are expressed as the mean ± SEM. (* $p < 0.05$ and ** $p < 0.01$ by ANOVA/ Neumann Keuls post hoc comparisons).
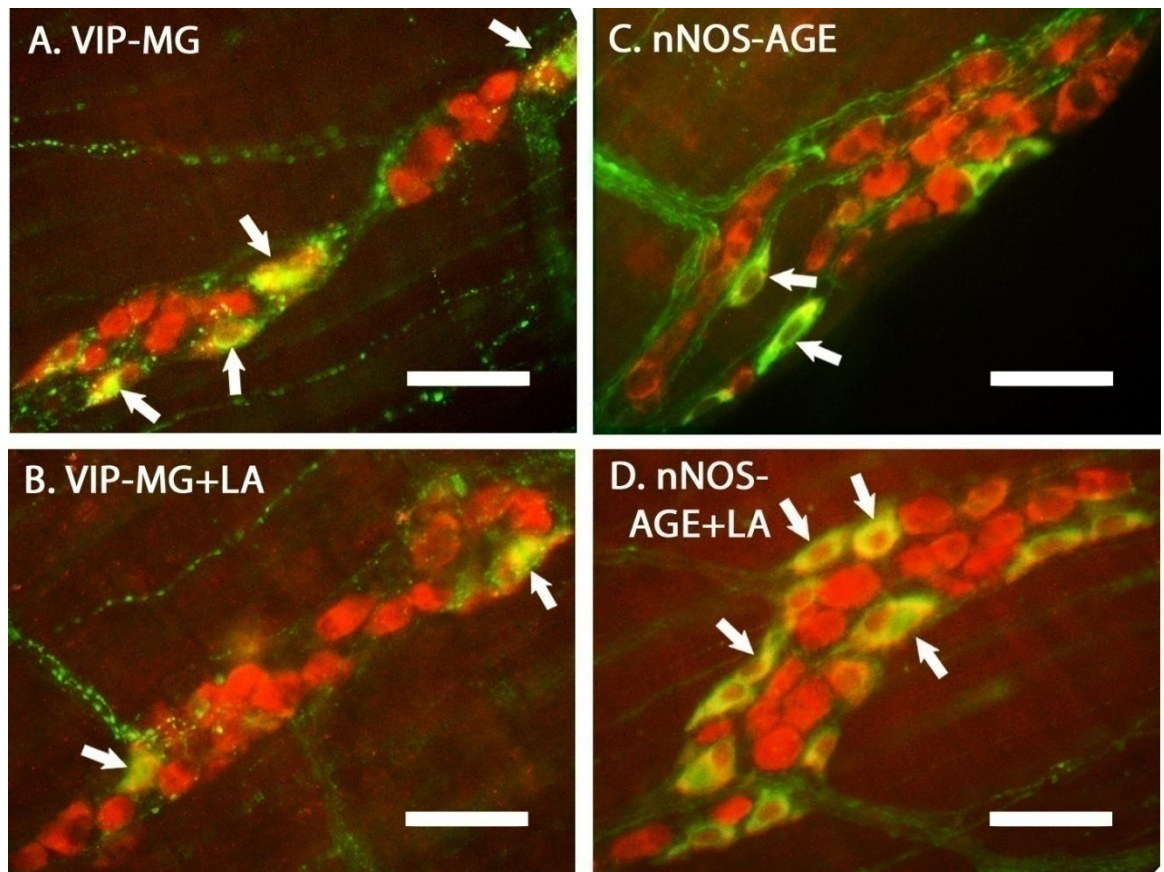
Figure 3.2: Inhibition of changes induced by methylglyoxal (MG) and BSA-AGEs (AGE) by α-lipoic acid (LA) *in vitro* on myenteric neurons. Photomicrographs show the immunoreactivity of VIP (A, B) and nNOS (C, D) double labelled with the neuronal marker HuC/D. A and C depict staining of preparations maintained for 24h *in vitro* after exposure to methylglyoxal or BSA-AGE and B and D depict samples after co-incubation with α-lipoic acid. Green fluorescence indicates VIP or nNOS labelling and red fluorescence HuC/D. The arrows indicate co-localisation with HuC/D (yellow). Note the considerable decrease in VIP staining in B compared with A and the increase in nNOS staining in D compared with C. Scale bars represent 50 μm.

3.3.2 Nicotinamide

Preliminary experiments established that nicotinamide (100 μM) had no significant effect on the expression of VIP or nNOS in control preparations. Exposure to high glucose, methylglyoxal and oxidative stress resulted in a significant increase in the relative number of VIP-containing neurons ($p<0.01$ for all) and oxidative stress caused a significant decrease in the relative number of nNOS-containing neurons ($p< 0.01$). All these changes were prevented by nicotinamide such that VIP and nNOS expression was similar to control preparations (fig. 3.3) Representative micrographs are provided for VIP (fig. 3.4) and nNOS (fig. 3.5).

3.3.3 Aminoguanidine

Preliminary experiments were carried out using aminoguanidine at a concentration of 100 μM according to Thornalley (2003b). However, at this concentration aminoguanidine was not effective as a carbonyl scavenger in preventing changes induced by methylglyoxal and all further experiments used a concentration of 500 μM. At this concentration, aminoguanidine had a significant effect on the expression of VIP and nNOS in preparations maintained under control culture conditions of 10 mM glucose. Exposure to aminoguanidine resulted in a significant increase ($p<0.05$) in the relative number of VIP-containing neurons and a significant decrease ($p<0.01$) in the relative number of nNOS-containing neurons (fig. 3.6). The results from experiments examining the effect of aminoguanidine on changes induced

NICOTINAMIDE

A Effects on high glucose and methylglyoxal

B Effects on oxidative stress
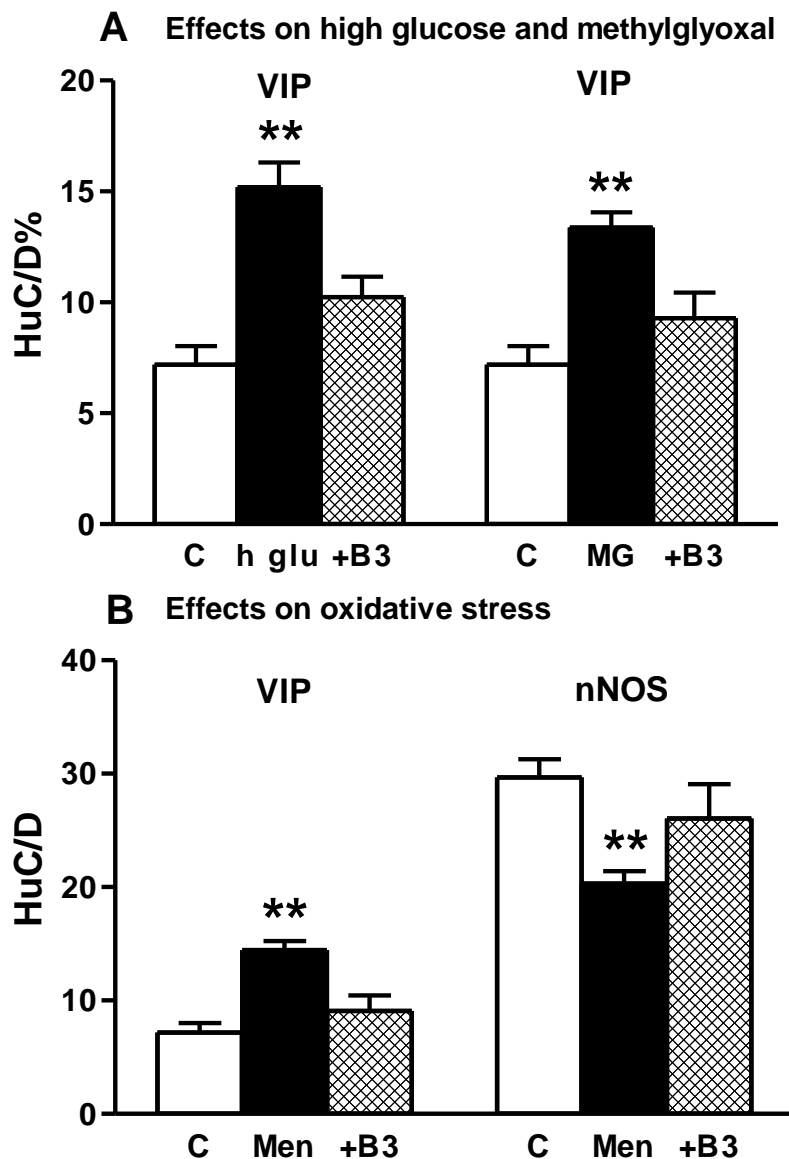
Figure 3.3: Effect of nicotinamide (B3) on the responses to high glucose (h glu), methylglyoxal (MG) and oxidative stress induced by menadione (Men) in myenteric plexus/muscle preparations. Clear bars represent data from controls (C), black bars represent data from preparations in the presence of a stimulus and hatched bars represent data after co-incubation of the stimulus with nicotinamide. (A) Nicotinamide prevented the increase in VIP-containing neurons induced by high glucose (h glu, n = 7; + B3, n = 8; C, n = 9) and methylglyoxal (MG, n = 7; +B3, n = 9; C, n = 9). (B) Nicotinamide prevented the increase in VIP-containing neurons induced by menadione (Men, n = 9; +B3, n = 9; C, n = 9) and the decrease in nNOS-containing neurons induced by menadione (Men, n = 10; +B3, n = 6; C, n = 7). Data are expressed as the mean $\pm$ SEM. (* $p < 0.05$ and ** $p < 0.01$ compared to controls by ANOVA/ Neumann Keuls post hoc comparisons).

VIP
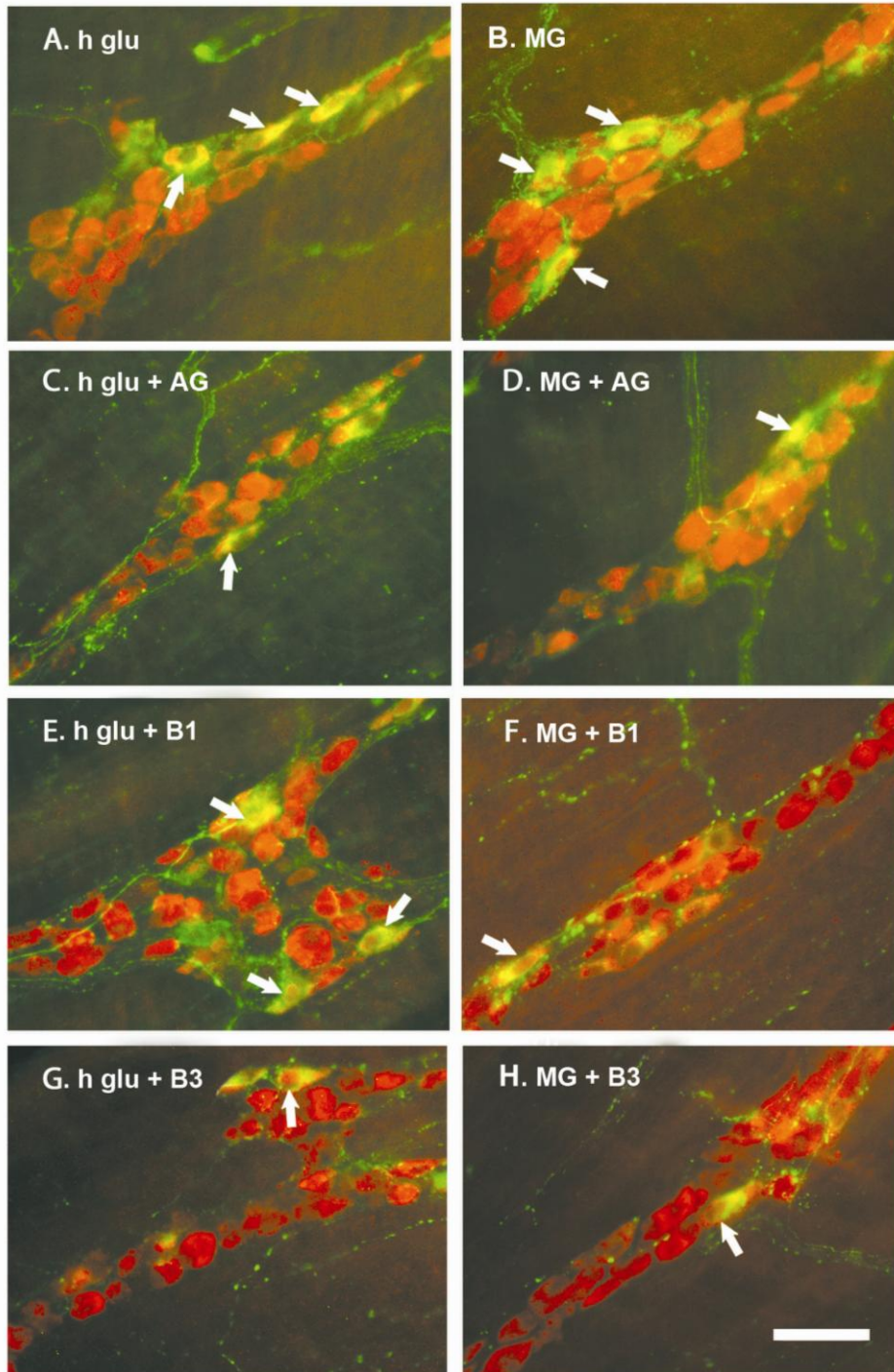
Figure 3.4: Inhibition of changes induced by high glucose (h glu) and methylglyoxal (MG) on VIP-containing myenteric neurons by aminoguanidine (AG), thiamine pyrophosphate (B1) and nicotinamide (B3) *in vitro*. Photomicrographs show the immunoreactivity of VIP double labelled with the neuronal marker HuC/D. Green fluorescence indicates VIP labelling and red fluorescence HuC/D. The arrows indicate co-localisation with HuC/D (yellow). (A) Staining of preparations maintained for 24h *in vitro* after exposure to high glucose. (B) Samples after exposure to methylglyoxal. (C) and (D) show the staining of preparations after co-incubation of high glucose or methylglyoxal with aminoguanidine. Note the decrease of VIP staining correspondingly compared with (A) and (B). (E) and (F) show the staining of preparations after co-incubation of high glucose or methylglyoxal with thiamine pyrophosphate. Note the decrease of VIP staining in (F) compared with (B), but not in (E) compared with (A). (G) and (H) show the staining of preparations after co-incubation of high glucose or methylglyoxal with nicotinamide. Similarly to the effect of aminoguanidine, note the significant decrease of VIP staining correspondingly comparing A and B. Scale bar represents 50 μm.
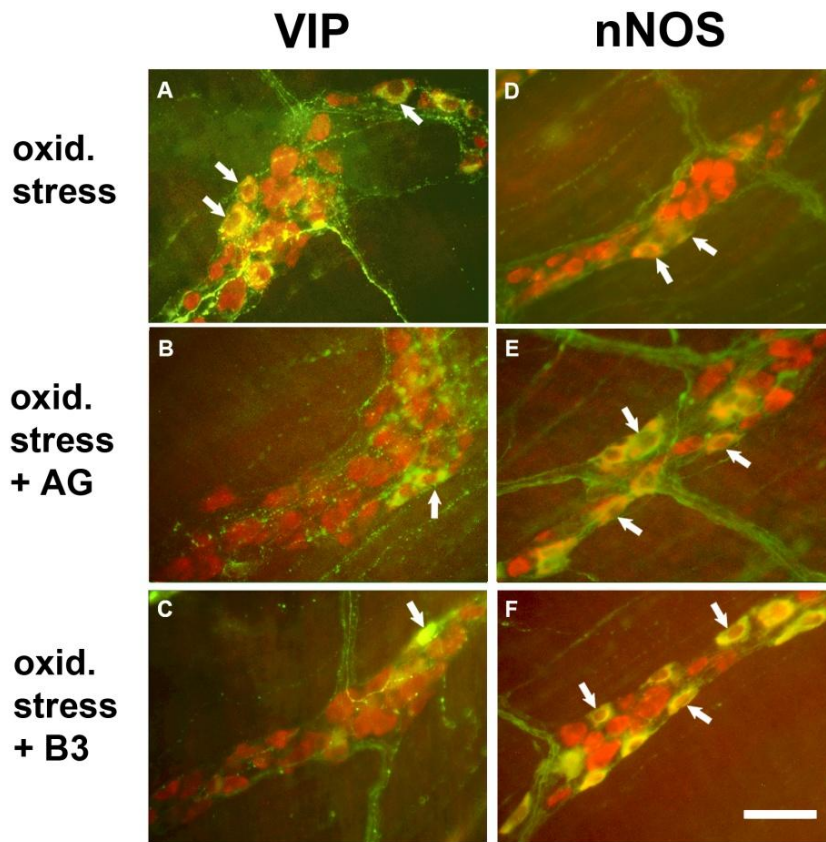
Figure 3.5: Inhibition of changes induced by oxidative stress (oxid. stress) on VIP- and nNOS-containing myenteric neurons by aminoguanidine (AG) and nicotinamide (B3) *in vitro*. Photomicrographs show the immunoreactivity of VIP (A, B, C) and nNOS (D, E, F) double labelled with the neuronal marker HuC/D. Green fluorescence indicates VIP or nNOS labelling and red fluorescence HuC/D. The arrows indicate co-localisation with HuC/D (yellow). (B) and (E) show the staining of preparations after co-incubation with aminoguanidine. Note the considerable decrease in VIP staining in (B) compared with (A) and the increase in nNOS staining in (E) compared with (D). (C) and (F) show the staining of preparations after co-incubation with nicotinamide. Similar to the effect of aminoguanidine, note the significant decrease of VIP staining with nicotinamide (C) compared with (A) and the increase in nNOS staining in (F) with (D). Scale bar represents 50 μm.

Effect of aminoguanidine on controls
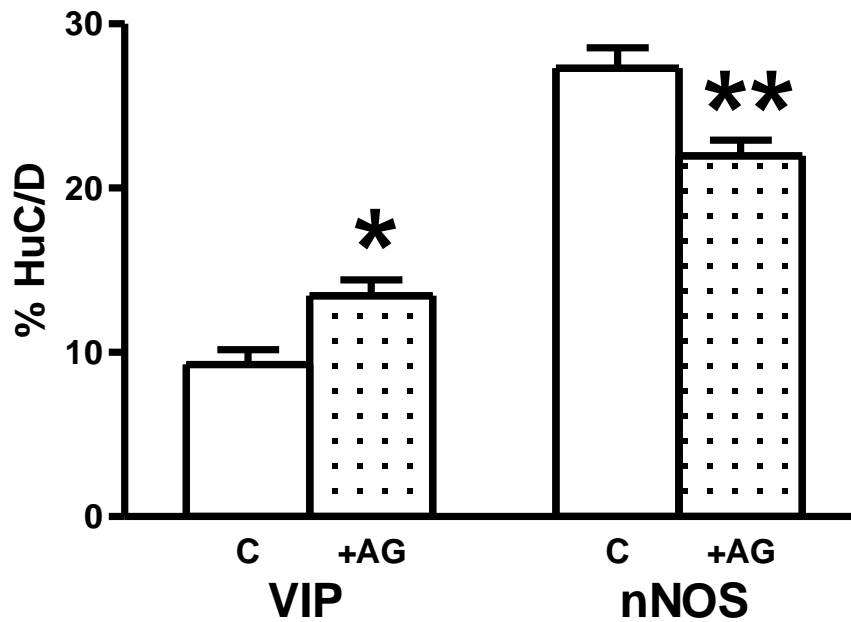
Figure 3.6: Effect of 500 μM aminoguanidine (AG) on VIP- and nNOS-containing neurons in preparations maintained under control conditions of 10 mM glucose. Clear bars represent data from untreated controls (C) and shaded bars represent data after incubation with aminoguanidine (+AG). Aminoguanidine on its own induced increase in VIP-containing neurons (C, n=5, +AG, n=6) and decrease in nNOS-containing neurons (C, n=6, +AG, n=6). Data are expressed as the mean ± SEM. (* $p < 0.05$ and ** $p < 0.01$ by unpaired t-test).

by high glucose, methylglyoxal and oxidative stress in VIP-containing neurons and by oxidative stress in nNOS-containing neurons are given in fig. 3.7. Exposure to high glucose and methylglyoxal caused a significant increase in the relative number of VIP-containing neurons ($p<0.01$ for both) that was prevented by aminoguanidine. Exposure to menadione to induce oxidative stress caused a significant increase in VIP-containing neurons ($p<0.01$) and a significant decrease in nNOS-containing neurons ($p<0.01$). Both changes were prevented by aminoguanidine (fig. 3.7). Representative micrographs are provided for VIP (fig. 3.4) and nNOS (fig. 3.5).

3.3.4 Thiamine pyrophosphate

Preliminary experiments established that 100 μM thiamine pyrophosphate had no effect on the expression of VIP or nNOS in control preparations. Both high glucose and methylglyoxal caused a significant increase in the relative number of VIP-positive neurons, compared to control values ($p<0.01$). The addition of thiamine pyrophosphate did prevent the increase in VIP-containing neurons induced by methylglyoxal but had no effect on the increase induced by exposure to high glucose (fig. 3.8). Oxidative stress induced by menadione caused a significant increase in the relative number of VIP-positive neurons ($p<0.01$) and a significant decrease in nNOS-positive neurons ($p<0.01$). Thiamine pyrophosphate did not prevent the changes induced by oxidative stress in either VIP- or nNOS-containing neurons (fig. 3.8). Representative micrographs are provided in fig. 3.4.

AMINOGUANIDINE

A   Effect on High Glucose and Methylglyoxal

B   Effect on Oxidative Stress
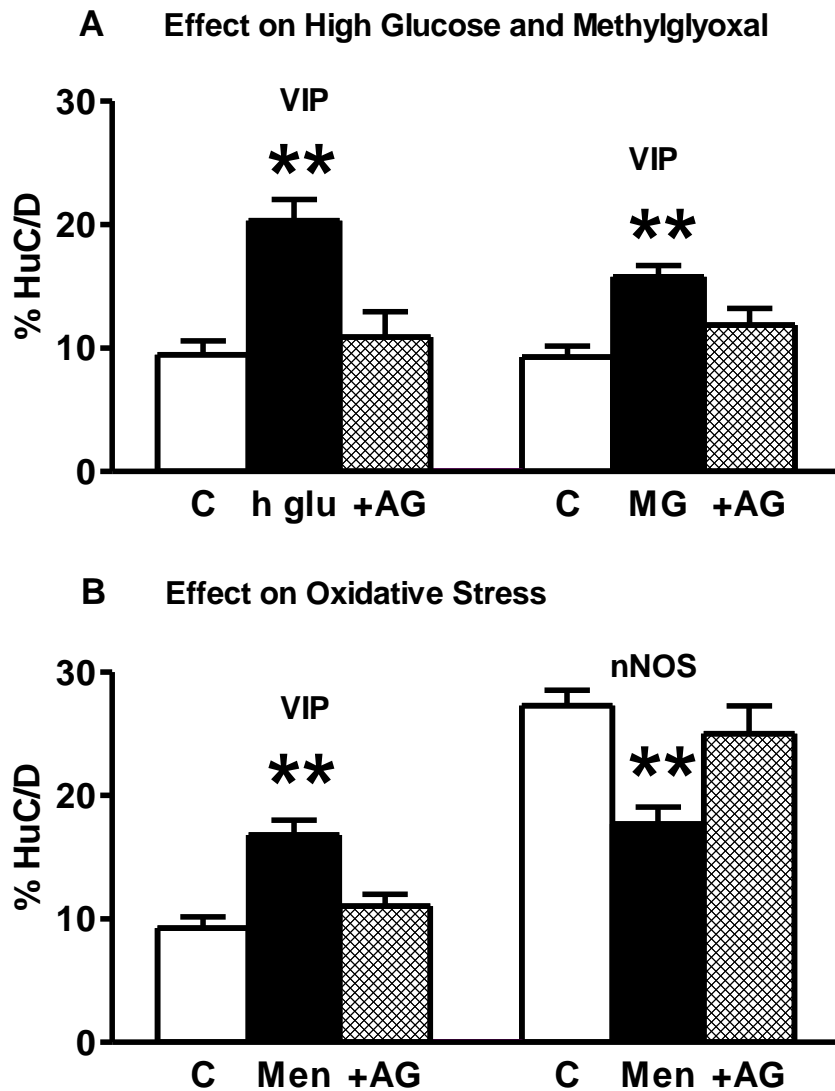
Figure 3.7: Effect of 500 μM aminoguanidine (AG) on the responses to high glucose (h glu), methylglyoxal (MG) and oxidative stress induced by menadione (Men) in myenteric plexus/muscle preparations. Clear bars represent data from controls (C), black bars represent data from preparations in the presence of a stimulus and hatched bars represent data after co-incubation of the stimulus with aminoguanidine. (A) Aminoguanidine prevented the increase in VIP-containing neurons induced by high glucose (h glu, n = 8; + AG, n = 8; C, n = 7) and methylglyoxal (MG, n = 6; +AG, n = 6; C, n = 5. (B) Aminoguanidine prevented the increase in VIP-containing neurons induced by menadione (Men, n = 4; +AG, n = 5; C, n = 5) and the decrease in nNOS-containing neurons induced by menadione (Men, n = 6; +AG, n = 6; C, n = 6). Data are expressed as the mean ± SEM. (* $p < 0.05$ and ** $p < 0.01$ compared to controls by ANOVA/ Neumann Keuls post hoc comparisons).

THIAMINE PYROPHOSPATE

A Effects on high glucose and methylglyoxal

B Effects on oxidative stress
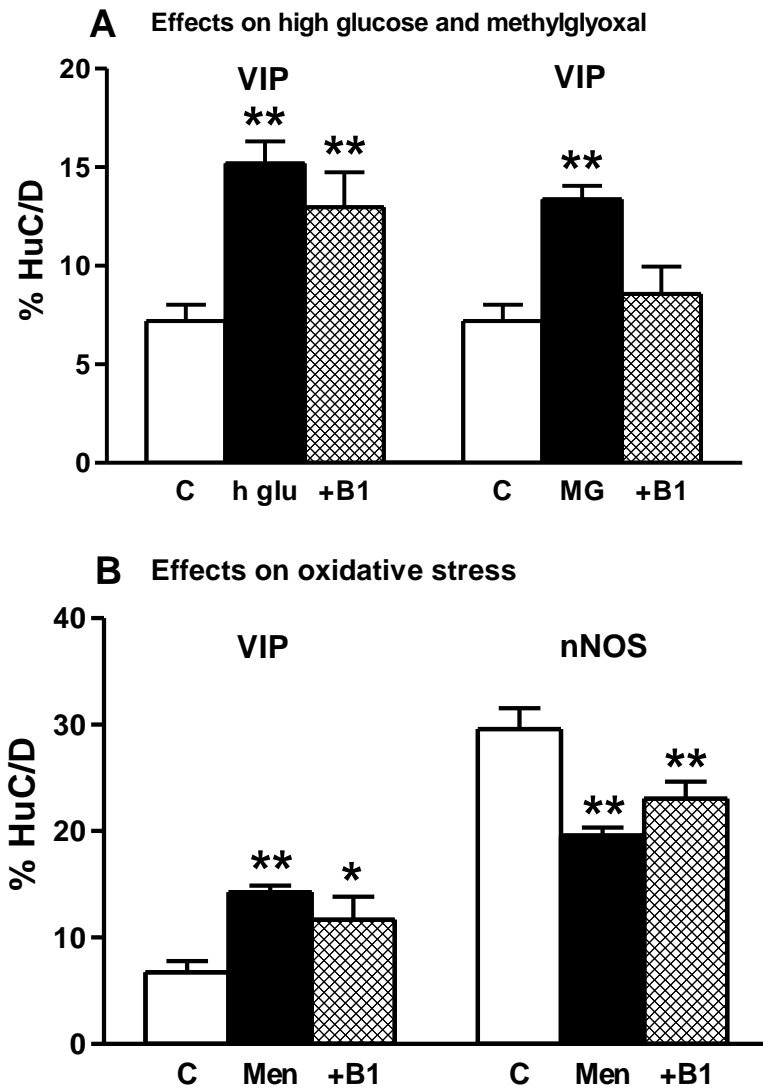
Figure 3.8: Effect of thiamine pyrophosphate (B1) on the responses to high glucose (h glu), methylglyoxal (MG) and oxidative stress induced by menadione (Men) in myenteric plexus/muscle preparations. Clear bars represent data from controls (C), black bars represent data from preparations in the presence of a stimulus and hatched bars represent data after co-incubation of the stimulus with thiamine pyrophosphate. (A) Thiamine pyrophosphate only prevented the increase in VIP-containing neurons induced by methylglyoxal (MG, n = 7; +B1, n = 6; C, n = 9). It did not prevent the effect of high glucose (h glu, n = 7; + B1, n = 6; C, n = 9) (B) thiamine pyrophosphate did not prevent the increase in VIP-containing neurons induced by menadione (Men, n = 9; +B1, n = 7; C, n = 7), or the decrease in nNOS-containing neurons induced by menadione (Men, n = 8; +B1, n = 11; C, n = 8). Data are expressed as the mean ± SEM. (* p < 0.05 and ** p < 0.01 compared to controls by ANOVA/ Neumann Keuls post hoc comparisons).

3.4 Discussion

Four agents were investigated for their ability to prevent the changes induced in myenteric neurons *in vitro* in response to diabetic stimuli described in the previous chapter. All the agents used have been investigated clinically for the treatment of diabetic neuropathy primarily involving the sensory nervous system. The agents differed in their proposed sites of action acting in the prevention of oxidative stress or its consequences or by scavenging carbonyl species or preventing their production. Thus, a comparison of their effects also potentially provides a means with which to assess the relative roles of oxidative stress and carbonyl stress in the effects of acute exposure to high glucose.

3.4.1 Oxidative Stress

3.4.1.1. α-Lipoic acid

In this study, the anti-oxidant, α-lipoic acid, did not influence the changes induced in VIP and nNOS positive neurons by culture *per se*. However, it did prevent the increase in the relative number of VIP-containing neurons on exposure to methylglyoxal and the decrease in the relative number of nNOS-containing neurons on exposure to AGE. Previously, in this laboratory, α-lipoic acid has also been shown to prevent the increase in VIP-containing neurons induced by exposure to high glucose (see Voukali et al., 2011).

The pharmacological properties of α-lipoic acid mainly concern its reductive power and high reactivity with ROS, along with its metal chelating activity. Its mechanism of action is complex as α-lipoic acid is considered a metabolic anti-oxidant in two ways: firstly because of its role in oxidative metabolism and secondly due to its effect on signal transduction and gene regulation, inhibiting NF-κB and Activator Protein 1 activation (Packer et al., 1997). α-Lipoic acid is an essential cofactor of multienzyme complexes controlling key reactions of energy metabolism, as it is involved in oxidative decarboxylation of pyruvate in the formation of acetate (Reed et al., 1951; Loffelhardt et al., 1995). It is located both in aqueous and membrane domains because it is soluble both in water and fats, which is a unique feature among anti-oxidants (Packer et al., 1995). It is synthesised *de novo* or readily absorbed from the diet and enters the cell via a fatty acid carrier. Once inside the cell, it is converted to dihydrolipoic acid (Packer, 1994; Singh & Jialal, 2008;Shay et al., 2009). It interacts with other endogenous anti-oxidants since it is capable of regeneration of vitamins E and C. It has also been shown to induce an increase in intracellular levels of glutathione in a variety of cell types including neuroblastoma cells (Han et al., 1997).

α-Lipoic acid prevented the reduction in nNOS-containing myenteric neurons induced by BSA-AGE in the present study. These findings demonstrate that the mechanism underlying AGE-induced reduction of nNOS in myenteric neurons occurs via oxidative stress. Similarly, activation of RAGE induces oxidative stress in sensory neurons that can be prevented by α-lipoic acid (Vincent et al. 2007a). In endothelial cells, α-lipoic acid reduced AGE-related NF-κB transcription and expression and prevented the depletion of glutathione and ascorbic acid levels (Bierhaus et al., 1997).

α-Lipoic acid also inhibited the increase of VIP induced by high glucose (Voukali et al., 2011). Short term exposure of sensory neurons to high glucose *in vitro*

induced oxidative stress which was similarly inhibited by α-lipoic acid (Vincent et al. 2005a; Vincent et al. 2005b). Moreover, α-lipoic acid reduced lipid peroxidation induced by exposure to high glucose of both sciatic nerve and brain *in vitro* in a dose dependent manner (Nickander et al., 1996). A study on the effect of the carbonyl species, methylglyoxal, in hepatocytes *in vitro* reported that exposure to methylglyoxal results in increased production of ROS and depletion of glutathione and thus provided evidence that the cytotoxic effects of methylglyoxal involve the development of oxidative stress (Shangari & O'Brien, 2004). The results presented here indicate that this is also likely to be the case in the present study on myenteric neurons. Exposure to methylglyoxal caused an increase in VIP-containing neurons that was prevented by the anti-oxidant α-lipoic acid.

3.4.1.2 Nicotinamide

Activation of the nuclear enzyme PARP has been proposed to mediate the cellular damage that occurs as a consequence of oxidative stress. Thus, PARP inhibitors have been investigated for their ability to prevent diabetic neuropathy due to oxidative stress (Obrosova et al. 2004; Stevens et al. 2007). Nicotinamide is a PARP inhibitor and, in the present study, nicotinamide prevented the increase in VIP-containing neurons that occurred on exposure to high glucose and methylglyoxal.

Nicotinamide has been shown to prevent many of the consequences of PARP activation. It prevents the depletion of ATP and NAD that occurs in central neurons following cerebral ischaemia *in vivo* (Yang et al., 2002). *In vitro*, nicotinamide reduced cell injury induced by oxygen-glucose deprivation and reoxygenation of cortical neurons, a model of ischaemia/reperfusion. Markers of cell injury included lactate

dehygrogenase release, increased calcium influx, caspase-3 activation and nuclear condensation (Shen et al., 2004). In STZ-diabetic rats, administration of nicotinamide treatment prevented the reduction of NAD levels and the increased immunoreactivity for poly (ADP-ribose) induced in the sciatic nerve by diabetes (Negi et al., 2010). In the sciatic nerve, activation of PARP occurs in the nuclei of endothelial cells and Schwann cells (Obrosova et al., 2004). Exposure of human Schwann cells to high glucose *in vitro* causes increase in the levels of poly (ADP-ribosyl)ated proteins without changing the levels of PARP itself, an effect that can be prevented by nicotinamide (Stevens et al., 2007). In functional studies, nicotinamide treatment has been shown to prevent or reverse sensory and motor nerve deficits in STZ-diabetic rats (Negi et al., 2010). To date, the effect of nicotinamide on autonomic neuropathy in diabetes has not been reported. However, another PARP inhibitor, 3-aminobenzamide, has been shown to partially correct impaired relaxation responses in the gastric fundus from diabetic rats, largely due to an improvement in nitrergic transmission (Gibson et al., 2006).

In the present study, nicotinamide prevented the increase in the relative number of VIP-containing neurons induced by exposure to high glucose and methylglyoxal, but there is evidence that nicotinamide can also act as an anti-oxidant. It prevents the increased production of ROS induced in cortical neurons by hypoxia/reoxygenation (Shen et al., 2004). Nicotinamide also prevents lipid peroxidation in the sciatic nerve of STZ-diabetic rats and the increased levels of 4-hydroxynonenal adducts (marker for oxidative stress) in Schwann cells exposed to high glucose (Stevens et al., 2007). Using cultures of embryonic rat DRG neurons nicotinamide markedly inhibited the increased levels of apoptosis induced by both high glucose and hydrogen peroxide-mediated oxidative stress (Vincent et al., 2005b). Therefore, in the present study, the effect of nicotinamide on changes induced in myenteric neurons by oxidative stress on exposure

to menadione was also investigated. The effect of nicotinamide was examined at the same concentration (100 μM) that prevented the increase in VIP-containing neurons induced by high glucose and methylglyoxal and was the same as the concentration of α-lipoic acid investigated here. At this concentration, nicotinamide prevented both the increase in VIP-containing neurons and the decrease in nNOS-containing neurons resulting from menadione-induced oxidative stress. In the study of embryonic DRG neurons *in vitro*, much higher concentrations of nicotinamide (10-25 mM) were required to prevent apoptosis induced by high glucose and only moderate inhibition of superoxide production was achieved at lower concentrations (0.5-1 mM). Thus the authors concluded that the primary mechanism by which nicotinamide prevents neuronal cell death is via the inhibition of PARP (Vincent et al., 2005b). In the present study, neuronal cell death was not a feature of the response to high glucose or methylglyoxal (see Chapter 2). From the results presented here, it appears more likely that the prevention of the effects of high glucose and methylglyoxal on adult VIP-containing myenteric neurons by nicotinamide is by its ability to act as an anti-oxidant and that the changes observed in the myenteric plexus preparation may not occur via the activation of PARP.

3.4.2 Carbonyl Stress

3.4.2.1 Aminoguanidine

Aminoguanidine was studied in an attempt to distinguish between the relative contributions of oxidative stress and carbonyl stress to the increase in VIP expression induced by high glucose. In an *in vitro* study using primary cultures of endothelial cells, the effects of exposure to methylglyoxal and high glucose concentrations were

investigated (Dhar et al., 2010). Incubation with high glucose and methylglyoxal resulted in increased levels of methylglyoxal within endothelial cells. Both methylglyoxal and high glucose had similar effects on endothelial cells, reducing the production of NO, the levels of glutathione and increasing the activity of the NADPH oxidase. All these changes were attenuated by the carbonyl scavenger aminoguanidine. The authors proposed that methylglyoxal could act as the mediator between hyperglycaemia and endothelial dysfunction (Dhar et al., 2010).

Initially, in the present study, the effect of aminoguanidine was examined at the same concentration (100 μM) as was used for α-lipoic acid and nicotinamide. However, preliminary experiments revealed that, at this concentration, aminoguanidine was not effective in preventing the response to the carbonyl species methylglyoxal. Therefore a higher concentration of 500 μM that was effective against methylglyoxal was used thereafter. Unlike α-lipoic acid and nicotinamide, aminoguanidine had a significant effect on the expression of both VIP and nNOS in myenteric neurons maintained under control conditions of 10 mM glucose producing an increase in the relative number of VIP-containing neurons and a decrease in the number of nNOS-containing neurons. However, aminoguanidine had an opposite effect on preparations exposed to diabetic stimuli, lowering VIP expression and, in the case of oxidative stress, raising nNOS expression to levels observed in untreated control culture preparations. Thus, in the presence of diabetic stimuli, aminoguanidine was protective and prevented the effects of both high glucose and methylglyoxal. The mechanism by which aminoguanidine alters the expression of VIP and nNOS in control culture preparations is not known but a similar differential effect of aminoguanidine on nNOS-containing nerve fibres in control and STZ-diabetic rats has been reported. Aminoguanidine caused a significant increase

in the thickness of nNOS-containing nerve fibres in control rats but prevented the increase in fibre thickness caused by diabetes (Shotton et al., 2007).

Aminoguanidine is a nucleophilic hydrazine compound, available as hydrochloride salt. The hydrazine group of aminoguanidine is the most reactive group with α-oxoaldehydes. The derivative of this interaction is a triazine product (Thornalley et al., 2000; Abdel-Rahman & Bolton, 2002; Thornalley, 2003b). The primary action of aminoguanidine is the inhibition of the formation of AGEs by scavenging dicarbonyls and reducing their concentrations in the cell (Brownlee et al., 1986). Other potential therapeutic actions of aminoguanidine are the inhibition of competitive enzymes such as inducible nitric oxide synthase, histaminase and semicarbazide-sensitive amine oxidase, a minor source of methylglyoxal (Thornalley, 2003b). In higher concentrations than those able to react with α-oxoaldehydes, aminoguanidine reacts with pyruvate and glucose with a potent pro-oxidant effect (>60 mM) (Suji & Sivakami, 2006). It has also been reported to be an aldose reductase inhibitor and chelator of metal ions (Cameron et al., 1992; Price et al., 2001). Finally, aminoguanidine can also act as an anti-oxidant, preventing the formation of ROS and lipid peroxidation in retinal Müller cells exposed to hydrogen peroxide (Giardino et al., 1998).

In the present study, aminoguanidine prevented the changes in both VIP- and nNOS-containing neurons induced by oxidative stress indicating that it is also able to act as an anti-oxidant in myenteric plexus preparations. Thus, aminoguanidine was not sufficiently specific as a carbonyl scavenger to differentiate the contribution of carbonyl stress and oxidative stress to the responses to high glucose.

3.4.2.2 Thiamine

Thiamine pyrophosphate, the phosphorylated active form of thiamine was added to myenteric neurons to evaluate its potential in inhibiting the effects induced by diabetic stimuli. Unlike all the other agents studied here, thiamine did not act as an anti-oxidant since it did not prevent the increased expression of VIP or the decreased expression of nNOS in myenteric plexus preparations exposed to menadione. However, thiamine did prevent the increase in VIP-containing neurons induced by methylglyoxal. Thiamine has been reported to prevent lipid peroxidation of liver microsomes and the free radical oxidation of oleic acid in a cell free system thus a direct anti-oxidant action of thiamine was proposed (Lukienko et al., 2000). The thiamine derivative, benfotiamine, prevented oxidative stress due to a variety of stimuli in kidney cell lines and a direct anti-oxidant action of benfotiamine was observed in a cell-free assay. However, thiamine was unable to act as an anti-oxidant in either system (Schmid et al., 2008). Thus, there is little evidence for thiamine being able to act as an anti-oxidant in intact cells. It has been suggested that the presence of the pyrophosphate group on thiamine limits its anti-oxidant capacity (Suji & Sivakami, 2007). Thiamine has been reported to prevent hepatocyte cell death induced by carbonyl stress but not oxidative stress (Mehta et al., 2008). This is similar to the pattern observed here where thiamine prevented the response of VIP-containing neurons to methylglyoxal but not to menadione.

In the present study, thiamine did not prevent the response of VIP-containing neurons to high glucose while preventing the response to methylglyoxal. This is unlike studies of endothelial cells where thiamine or benfotiamine have been shown to protect against the effects of high glucose. The effects of high glucose on endothelial cells such

as impaired cell replication and migration, aldose reductase aberrant expression and apoptosis were countered when thiamine or benfotiamine were incubated together with high glucose (La et al., 1996;Ascher et al., 2001;Berrone et al., 2006;Beltramo et al., 2009). Benfotiamine also prevented the activation of three major pathways involved in hyperglycaemia-induced vascular damage: the hexosamine pathway, the intracellular AGE formation pathway and the diacylglycerol-PKC pathway in both endothelial cells exposed to high glucose *in vitro* and the retina from STZ-diabetic rats (Hammes et al., 2003).

It has been proposed that thiamine or benfotiamine prevents hyperglycaemic damage by increasing the activity of transketolase. Increased transketolase activity has been demonstrated in the renal glomeruli and retina of diabetic rats (Babaei-Jadidi et al., 2003), and in human red blood cells bovine aortic endothelial cells exposed to high glucose (Thornalley et al., 2001;Hammes et al., 2003). Transketolase is the rate limiting enzyme of the non oxidative branch of the pentose phosphate pathway, dependent on substrate and product concentration and on NADP+/NADPH ratio. Thiamine pyrophosphate acts as a coenzyme for transketolase and its activity in erythrocytes is often used as a marker for a deficit in thiamine. Transketolase, containing a tightly bound thiamine pyrophosphate as its prosthetic group, is able to shift excess fructose-6-phosphate and glyceraldehyde- 3-phosphate (triosephosphates) from glycolysis into the pentose-phosphate shunt, thus preventing an accumulation of triosephosphates. This has the effect of preventing the formation of methylglyoxal and intracellular AGEs (Thornalley et al., 2001). As fas as we are aware, transketolase activity has not been measured in neurons. Whether differences between the endogenous levels of transketolase activity in endothelial cells and neurons accounts for the finding thiamine or benfotiamine prevents the effect of high glucose in endothelial cells but not in

myenteric neurons remains to be determined. However, the results presented here do not provide any evidence that the response of VIP-containing neurons to high glucose involves carbonyl stress.

The activation of transketolase by thiamine and subsequent prevention of the intracellular production of methylglyoxal could not be the mechanism for the prevention of the effect of carbonyl stress demonstrated here since carbonyl stress was induced by the exogenous application of methylglyoxal. Some years ago, it was reported that thiamine deficiency in rats results in a marked decrease in glyoxalase activity in the liver but it was not established whether this was due to a decrease in protein expression or a lack of its cofactor glutathione (Salem, 1954). More recently, it has been shown that the susceptibility of hepatocytes to glyoxal is dependent on cell thiamine content. Thiamine-deficient cells were unable dispose of glyoxal. In addition, glyoxal caused a depletion of glutathione in control hepatocytes that could be prevented by thiamine (Shangari et al., 2007). It is possible that in these myenteric plexus preparations, thiamine was preventing the effect of carbonyl stress by preserving the activity of glyoxalase and disposal of methylglyoxal.

3.4.5 Conclusion

In conclusion, oxidative stress appears to be produced by all the diabetic stimuli since agents that were able to act as anti-oxidants also inhibited the effects of high glucose, methylglyoxal and AGEs. Aminoguanidine did not act exclusively as a carbonyl scavenger and could not be used to investigate the role of carbonyl stress in the

effect of high glucose. Thiamine was the only agent examined that did not act as an anti-oxidant and it prevented the effect of the carbonyl species, methylglyoxal but not the effect of high glucose. Therefore, the effect of high glucose on VIP-containing neurons did not appear to involve the production of carbonyl stress. This study was confined to the investigation of acute effects. It does not exclude the possibility that long term exposure to high glucose does lead to the production of carbonyl species and AGEs that subsequently affect myenteric neurons *in vivo*.

Chapter 4: Effect of Acute High Glucose on Different Populations of Living Sympathetic Neurons

4.1 Introduction

4.1.1 The Pyridine Nucleotides – NAD and NADP

4.1.1.1 Biological roles of NAD and NADP

The pyridine nucleotides NAD and the phosphorylated form NADP can both exist in oxidised (NAD+ or NADP+) or reduced (NADH or NADPH) states. NADP+ structurally differs from NAD+ only by the additional 2' phosphate on the adenosine ribose moiety. NAD+ and NADH or NADP+ and NADPH accept or donate a hydride in numerous reactions involving hydride transfer enzymes or oxidoreductases where the oxidized and reduced forms of pyridine nucleotides are interconverted dynamically. The NAD+/NADH couple is used in substrate oxidation. In contrast, the NADP+/NADPH couple is used in substrate reduction due to its more reduced state (Houtkooper et al., 2010). Pyridine nucleotides are water soluble and usually free to diffuse away after reaction.

Pyridine nucleotides can act as coenzymes in a wide range of intracellular reactions. In the case of NAD, it has long been recognized that it has a major role in energy metabolism. It acts as an electron acceptor in glycolysis and, as NADH, is the major electron source for the electron transport chain in oxidative phosphorylation (Skala et al., 2007b; Ying, 2008). NAD$^+$ also plays a role in regulatory and signalling pathways. These include: ADP-ribosylation reactions; gene transcription via its action on the Sir2 family of histone deacetylases; and acting as a precursor to the calcium mobilizing molecule cyclic ADP-ribose. In addition, depletion of NAD$^+$ following activation of PARP-1 mediates cell death (Pollak et al., 2007; Ying, 2008). Apart from its role in reductive synthesis, NADPH plays a key role in cellular anti-oxidant defence. For example, NADPH is required for the recycling of the major intracellular anti-oxidant, glutathione, from GSSG by glutathione reductase (Wu et al., 2004;Pollak et al., 2007;Ying, 2008). However, NADPH is also a substrate for NADPH oxidase. This enzyme was initially studied in phagocytes where the activation of NADPH oxidase is a major generator of superoxides used in host defence. Since then NADPH oxidases have been identified in various tissues and cell types and activation has been implicated in a range of pathological conditions (Ying, 2008;Kakehi & Yabe-Nishimura, 2008).

4.1.1.2 Cellular concentrations and redox ratio

Estimates of total cellular pyridine nucleotide are commonly in the submillimolar range. The relative concentrations of these coenzymes differ in different cell compartments and this has a direct effect on metabolic pathways within those compartments (Krebs, 1967; Pollak et al., 2007). Intracellular levels of NAD (NAD+ plus NADH) are significantly higher than NADP (NADP+ plus NADPH) (Pollak et al.,

126

2007; Ying, 2008). The majority of NAD is mitochondrial whereas the majority of NADP is cytosolic. Under physiological conditions, NAD+ is far more abundant than NADH and in contrast, the levels of NADPH are much higher than those of NADP+. Thus, total NADPH cellular levels are about 2-3 times higher than those of NADH. However, this may vary with cell type. Cells with high metabolic demand, such as neurons and heart cells have many more mitochondria containing NAD and NADPH levels are lower in cerebral and cardiac tissues than the liver (Wakita et al., 1995; Kann & Kovacs, 2007; Pollak et al., 2007; Ido, 2007; Ying, 2008).

The cell has the capacity to regulate the ratios NAD+/NADH and NADP+/NADPH, the balance of which determines the cellular redox state, thus influencing cell function (Krebs, 1967). If any component of these couples increases, it does so at the expense of the other component of the system. Almost all metabolic pathways rely on pyridine nucleotides (energy metabolism and biosynthesis, antioxidation, calcium regulation, cell death and gene expression). Therefore, information on the value of the redox ratio is important, because it reflects the metabolic behaviour of oxidizable and reducible substrates.

Normally, the cytosolic ratio of free NADP+/NADPH is about 0.02 whereas the ratio of free NAD+/NADH is about 700, this is due to the majority of NADH being protein bound. Thus, in the cytosol, any oxidative reactions involving NAD will proceed by the conversion of NAD+ to NADH whereas the reducing capacity of the cytosol relies almost completely on the NADPH pool. In mitochondria where NAD dominates, the relationship shifts markedly towards the reduced form such that the NAD+/NADH ratio is about 7-8 (Ido, 2007;Pollak et al., 2007).

Mitochondrial and cytosolic redox ratios will be the complicated end result of all the pathways in which pyridine nucleotides act as coenzymes, for instance the

glycolytic pathway; the mitochondrial pyruvate transporter and pyruvate dehydrogenase complex; the citric acid cycle; the respiratory chain where NADH is one of the major electron donors; and antioxidation systems where NADPH is a key component (Houtkooper et al., 2010). The resultant ratios can then influence cell metabolism. For example, in the cytosol, redox ratio determines the rate of glycolysis (Wahlberg et al., 2000). In mitochondria, it determines the magnitude of the free energy changes of oxido-reductions like the transfer of the electrons from NADH to flavoproteins in the electron transport chain (Krebs, 1967).

The ratios of NAD+/NADH and NADP+/NADPH can also modulate the opening of mitochondrial transition pores controlling the transport of small molecules across the mitochondrial membranes. NAD(P)+/NAD(P)H in the subcellular compartments are in direct contact and, in order to maintain ratios homeostasis, redox shuttles allow the transfer of the reducing equivalents across membranes which in general are impermeable toward the various nucleotides (Pollak et al., 2007).

4.1.1.3 Pyridine nucleotides in diabetes

High intracellular glucose levels have been proposed to lead to alterations in the levels of NADH and NADPH and thus to a change in the redox balance of the cell. In the cytosol, the polyol pathway is activated by high glucose. The first step in this pathway is the conversion of glucose to sorbitol by aldose reductase during which NADPH is converted to NADP+. Sorbitol is then converted to fructose by sorbitol dehydrogenase via the reduction of NAD+ to NADH. The oxidation of glucose by glycolysis also occurs in the cytoplasm resulting in production of NADH and pyruvate. Following transport of pyruvate into mitochondria, further NADH is produced by the

TCA cycle providing electrons for the electron transport chain and oxidative phosphorylation (Wahlberg et al., 2000; Brownlee, 2001; Ido, 2007). Together these pathways will lead to an increase in NADH and a decrease in NADPH.

Therefore, altered glucose catabolism leads to the reduction of the ratios of NAD+/NADH and NADPH/NADP+ in the cytosol and mitochondria, and this is described as "the reduction stress hypothesis" or pseudohypoxia. The fluctuations of free NADH and NADPH levels may lead to fundamental biochemical changes in metabolism and play a significant role in the development of diabetic complications. (Wahlberg et al., 2000). Imbalance of NADP+/ NADPH can also affect antioxidation pathways, such as GSH recycling from GSSG, inhibition of the reactivation of catalase and inhibition of the regeneration of thioredoxin (Ido et al., 1997; Ido, 2007).

It is generally accepted that mitochondria are the major source of ROS in cells. However, more recently it has been proposed that ROS produced by a non-mitochondrial enzyme-NADPH oxidase, are responsible for neuronal cell death in excitotoxicity (Brennan et al., 2009). Activation of NADPH oxidase has been implicated in oxidative stress in diabetes and the development of diabetic complications predominantly affecting the vasculature and kidney (Nitti et al., 2007; Kakehi & Yabe-Nishimura, 2008;Sedeek et al., 2012).

4.1.2 The intrinsic fluorescence of NAD(P)H and multiphoton microscopy imaging

A particular NAD(P)+/NAD(P)H ratio, localised in one particular subcellular compartment may be calculated from the concentrations of certain oxidized or reduced substrates participated in a dehydrogenase reaction. Thus, NAD+/NADH and NADP+/NADPH are reflected by several sets of metabolites (for example lactate and pyruvate, β-hydroxybutyrate and acetoacetate). The concentration of these metabolites has been used to indicate the NAD redox state in mitochondria and the cytosol (Krebs, 1967; Tischler et al., 1977; Houtkooper et al., 2010). The problem with the metabolite indicator methods is that it is difficult to calculate the overall reduced forms of pyridine nucleotides because these methods do not differentiate free nucleotides from those that bind to proteins.

This methodological difficulty is now overcome by advanced technologies of imaging and microscopy. Multiphoton microscopy and FLIM enable more exact and dynamic estimates of the intracellular distribution of pyridine nucleotides. By these techniques, the researchers are now able to image intracellular pyridine nucleotides and distinguish between protein-bound and free nucleotides in living cells, based on the fluorescence properties of the reduced pyridine nucleotides.

Changes in the oxidation-reduction levels can be continuously recorded through the fluorescence yield of the reduced forms of pyridine nucleotides since the oxidized forms do not fluoresce (Chance & Thorell, 1959). Imaging of intrinsic fluorescence has been a useful tool to study the NADH:NAD+ ratio and cellular energy metabolism (Chance et al., 1962). NADPH fluorescence is weaker than that of NADH and is constant with respect to metabolic perturbations (Kumar et al., 2007). However, it is common to refer NAD(P)H in fluorescence studies because the spectra of NADH and

NADPH are indistinguishable. NAD(P)H are poor fluorophores compared with artificial probes (Piston & Knobel, 1999). Nevertheless, NAD(P)H is present in submillimolar amounts in the cell so it is possible to measure the native fluorescence using microscopy particularly in highly metabolic cells.

Initially, methods for imaging NAD(P)H in high resolution involved one-photon excitation (confocal microscopy) at near UV wavelengths. Absorption of a single photon delivers sufficient energy for the fluorophore molecule to reach the excited state, from which it returns to the ground state by emitting a photon of fluorescence (Lichtman & Conchello, 2005). Normally, native NAD(P)H fluorescence is excited with light of about 360 nm and emits at about 550 nm wavelength. With confocal laser scanning microscopy, the microscope uses a laser beam to supply the energy for excitation, uniformly focused within a small spot on the specimen, and a photomultiplier tube then detects the fluorescent light emitted from the sample (Gadella et al., 2012). With this technique, the excitation of fluorescent species is achieved above and below the plane of focus, resulting in blurring of the image. To overcome this, confocal microscopes utilise a pinhole to exclude out-of-focus background fluorescence from detection and increase the spatial resolution from within thick samples (Fine et al., 1988;Piston et al., 2012).

Fluorescence laser scanning microscopy offers the possibility of working with living specimens. However, applications of one-photon microscopy have been limited due to photobleaching of the intrinsic fluorophores, photodamage to biological samples and significant light scattering. The high intensity UV radiation is particularly damaging to living cells and tissues (Piston & Knobel, 1999). In addition, although fluorescence is excited throughout the specimen, only a signal originating in the focal plane passes through the confocal pinhole, allowing background data to be collected. Thus, the entire

specimen can be bleached even when only a single plane is imaged (Denk et al., 1990; Piston et al., 2012).

These difficulties are overcome by using two photon (or multiphoton) microscopy with near-infrared excitation. According to the physical principle that the absorption depends on the square of the excitation intensity, it is possible for multiple photons to add their energy to bring the molecule to the excited state (Zipfel et al., 2003; Lichtman & Conchello, 2005). With two photon excitation, the fluorescence arises from the simultaneous absorption of two photons of about twice the wavelength required for single photon excitation. Thus, NAD(P)H that normally absorbs UV of about 360 nm, can also be excited by two photons of near-infrared light of ~750 nm if both reach the fluorophore at the same time. The resulting emission is the same as emission generated in one-photon excitation with the same high level of resolution.

In addition to reduced photobleaching and photodamage (resulting in increased viability of the biological samples), two photon microscopy provides intrinsic 3-D resolution due to the capability of deep imaging (up to 500 μm) and minor light scattering (Zipfel et al., 2003;Cicchi & Pavone, 2011). The probability of two photons being scattered simultaneously to the same specimen location is close to zero. Since out-of-focus fluorescence is never generated, two photon microscopy provides optical sectioning without the introduction of a pinhole in the detection path. All of the signal is collected by a large area detector and contributes to the final image (nondescanned acquisition mode) (Rubart, 2004;Piston et al., 2012).

Two photon NAD(P)H fluorescence has become the preferred method to image living cells and tissue providing spatiotemporal information at subcellular resolution. Since the probes are active participants in cellular processes, NAD(P)H imaging yields the optical dissection of dynamic metabolism. So far, NAD(P)H multiphoton imaging

has been applied to a range of cell types (Patterson et al., 2000;Shuttleworth et al., 2003;Rocheleau et al., 2004;Kasischke et al., 2004).

4.1.3 Fluorescence Lifetime Imaging Microscopy (FLIM)

In combination with multiphoton fluorescence microscopy, FLIM allows the protein bound and free NAD(P)H native fluorescence to be distinguished in living cells. Instead of the measurement of the fluorescence intensity, FLIM is based on the measurement of the fluorescence lifetime. The fluorescent lifetime is one of the inherent characteristics of a fluorophore, along with brightness and wavelength. Its value derives from the measurement of the average time the fluorophore spends in the excited state, before returning to the ground state, or otherwise, the decay rate of the fluorescence emission after the excitation radiation has ceased (Tadrous, 2000; Sud et al., 2006). Lacowicz et al. firstly showed that free NAD(P)H and bound NAD(P)H in malate dehydrogenase had different fluorescence lifetimes in solution and were able to map the spatially-dependent decay times on 3-D projection in which the height represents the local decay time (Lakowicz et al., 1992b). NAD(P)H have typical fluorescence lifetimes in the range of hundreds of picoseconds when free, to a few nanoseconds when protein-bound.

The advantage of FLIM is that fluorescence lifetime is independent of fluorophore concentration, photobleaching, absorption and scattering, but it is determined by the local microenvironment of the fluorophore. Oxygen, pH, ions such as Ca^{2+}, energy transfer and molecular associations may all influence its value. Therefore, the measurement of the fluorescence lifetime of a fluorophore can be used to probe the

local chemical composition of the cell or tissue (Lacowicz et al., 1992a; Lacowicz et al., 1992b;Bastiaens & Squire, 1999;Tadrous, 2000;Cicchi & Pavone, 2011). Each pixel from an image obtained by means of FLIM maps such measurements and provides a contrast based on the local biophysical and biochemical properties of the sample. Accordingly, pixel values in a FLIM image calculated for NAD(P)H lifetimes, besides the imaging of free vs. protein bound NAD(P)H in cells recovered from (sub)nanosecond fluorescence lifetimes, also reflect the chemical variation in the intracellular milieu.

The multiphoton FLIM instrumentation setup employs the multiphoton microscope system with the laser mode-locked titanium sapphire pumped by an Argon Ion Laser as light source, nondescanned detectors connected with the data acquisition computer with Time Correlated Single Photon Counting (TCSPC) card (French et al., 1998;Van Munster & Gadella, 2005;Niesner et al., 2008b). TCSPC is a precise technique applied with the time domain method for FLIM and requires fast electronics. With the time domain method, the fluorescence lifetime is determined by the measurement of the fluorescence decay when the fluorescence intensity drops to about 37% of its initial value, after the sample has been excited by a pulse of laser scanning imaging systems with picosecond and femtosecond pulsed sources (pulsed diode laser and Ti:Sapphire) (Bastiaens & Squire, 1999;Tadrous, 2000;Cicchi & Pavone, 2011).

The TCSPC method measures the distribution in time of the exponential of the fluorescence emission of the molecules (Cicchi & Pavone, 2011). Multidimensional TCSPC recording process builds up a 4-D photon distribution over the times of the photons in the excitation pulse period, the wavelengths of the photons and the co-ordinates of the scan area and can be used for double exponential decays such as NAD(P)H free and NAD(P)H protein bound fluorescence lifetimes (Becker et al.,

2007b). TCSPC is the preferred technique for measuring fluorescence lifetime of tissue endogenous molecules because it is sensitive to the low signal fluorescence (Cicchi & Pavone, 2011).

4.1.4 Selective vulnerability of the prevertebral CG/SMG sympathetic neurons in diabetes

In clinical and experimental diabetes, the sympathetic ganglia do not all respond in the same way to diabetes. The prevertebral CG/SMG complex that innervates the stomach, gall bladder and small intestine, selectively develops neuroaxonal dystrophy as a morphologic response to metabolic alterations caused by diabetes and aging (Schmidt et al., 1993; Schmidt, 1996; Schmidt et al., 1997; Schmidt, 2002). Neuroaxonal dystrophy is characterised by the presence of abnormal neurites and synaptic constituents and impaired neuroaxonal regenerating capability without neuronal loss (Schmidt et al., 1993;Schmidt, 1996;Schmidt et al., 1997;Schmidt, 2002).

In contrast, the paravertebral SCG or prevertebral IMG are resistant to diabetes. SCG innervate the face and the neck and are located behind the bifurcations of the superior cervical arteries. Extensive literature provides evidence that SCG are not affected by human and experimental diabetes whereas the CG/SMG are (Schmidt, 2002). Also, the IMG that innervates the distal colon is relatively spared. NA accumulates in the CG/SMG but not the IMG in the STZ-diabetic rats and this is accompanied by a decrease in the level of NA in the ileum but not in the distal colon (Belai et al. 1991;Shotton et al., 2007). Thus, pathologic lesions affecting the

sympathetic innervation of the alimentary tract primarily affect the sympathetic neurons innervating the small intestine.

The activity and the mRNA levels of TH increase in the CG/SMG of diabetic STZ rats (Schmidt & Cogswell, 1989) and TH and NA immunoreactivity levels are reduced in the diabetic STZ rat ileum (Shotton et al., 2007), suggesting neurodegeneration of the nerve fibres. Increased activity of TH in CG/SMG was accompanied with increased endogenous NGF, but not with changes in its receptors (Schmidt et al., 2000). The increase in this case was considered to be indicative of a harmful role of the neurotrophic factor. Also, the ability of CG/SMG nerve fibres to regenerate is diminished in several diabetic animal models (Yagihashi & Sima, 1985;Schmidt et al., 2003;Schmidt et al., 2004).

In vitro studies comparing CG/SMG and SCG provide evidence that vulnerability in diabetes may reflect properties of the neurons themselves, since CG/SMG are particularly susceptible to oxidative stress and glucose toxicity. CG/SMG showed a slower neurite regenerative capacity than SCG neurons *in vitro* after exposure to high glucose for 24 h (Semra et al., 2004). Oxidative stress selectively caused increased TH immunoreactivity in CG/SMG but not in SCG, a pattern that was also observed in diabetes *in vivo* (Semra et al., 2006). Application of NGF *in vitro* prevented the decreased cell viability induced by hyperglycaemic stress in SCG but not in CG/SMG (Semra et al., 2009).

It is important to note that neuronal cell death is not a feature in sympathetic ganglia in STZ-diabetes (Schmidt, 2001). Using dissociated sympathetic neurons from embryonic SCG, high glucose has been shown to cause inhibition of neurite outgrowth and growth cones and apoptosis (Russell & Feldman, 1999). However, studies from this laboratory have demonstrated that neonatal SCG neurons are more susceptible to high

glucose than adult SCG neurons and that less cell death occurs in explants than dissociated neurons on exposure to high glucose (Semra et al., 2006;Semra et al., 2009). NAD(P)H metabolism has not been investigated in sympathetic neurons. However, NAD(P)H lifetimes are known to change on activation of hippocampal neurons (Chia et al., 2008). NADPH oxidase activation has been demonstrated in CG neurons in hypertensive rats (Cao et al., 2009). In addition, the mitochondrial enzyme, NADH oxidase has been reported to be activated in embryonic DRG neurons on exposure to high glucose (Vincent et al., 2005a).

The overall aim of this chapter was to investigate NAD(P)H metabolism in living SCG and CG/SMG explants from adult rats after exposure to hyperglycaemic stress *in vitro* using two photon microscopy and FLIM. Specifically, in living SCG and CG/SMG neurons, we aimed to compare the effects of high glucose on native NAD(P)H fluorescence, to determine the lifetimes of free and bound NAD(P)H using FLIM and to compare the effects of exposure to high glucose on NAD(P)H lifetimes between the ganglia.

4.2 Materials and methods

4.2.1 Tissue preparation

Adult male Sprague–Dawley rats (275-350 g) were killed by CO_2 asphyxiation complying with UK Home Office legislation. The SCG and the CG/SMG ganglia complexes were dissected out, desheathed and washed in antibiotic solution (HBSS containing 1% penicillin-streptomycin, 2% gentamycin and 2% 5mg ml^{-1} metronidazole). Each ganglion was cut into 2-3 segments and pinned onto glass petridishes with a Sylgard covered base (VWR, Buffalo Grove, IL, USA). The samples were cultured in defined culture medium without Phenol Red, containing 10 mM glucose (M199, supplemented with 1% L-Glutamine, 1% Hepes Buffer, 1% penicillin-streptomycin, 0.35% Pathocyte-4-BSA, 60 ng ml^{-1} progesterone, 0.016 mg ml^{-1} putrescine, 400 ng ml^{-1} l-thyroxine, 38 ng ml^{-1} sodium selenite, 340 ng ml^{-1} triiodothyronine, 100 µg ml^{-1} transferrin) in the absence of NGF and serum. The presence of Phenol Red in the culture medium has been found to absorb approximately 30% of the emitted fluorescence signal thus significantly reducing sensitivity (Becker et al., 2007a). Ganglia were allowed to equilibrate for 24 h under control conditions (10 mM glucose) before acute exposure to 30 mM glucose concentration (30 min and 120 min). Additional experiments included CG/SMG and SCG neurons maintained for 24h in media containing 10mM and 30mM glucose.

4.2.2 Imaging

Multiphoton imaging of ganglia was performed in the dark on a Leica SP2 multiphoton microscope (Leica, Milton Keynes, UK) with a Spectra-Physics (Didcot, Oxon) Millennia 8 W pump laser driving a mode-locked Tsunami Ti:Sapphire laser. The pulse width was 100fs at 80MHz repetition rate with the laser power set to deliver 30-70 mW of average power to the specimen at 750 nm.

Detection of the signal was via the non-de-scanned detectors by a photon-counting photomultiplier tube (H7422P-40; Hamamatsu Photonics K.K., Hamamatsu, Japan).

The microscope utilized a Gibraltar motorized xy- stage and was housed inside a Ludin chamber which maintained the temperature at $37^{o}C$ with a delivery of 5% CO_2 to the specimen. The specimen was kept stable in a sylgard-coated petridish, and viewed using a 63x (0.9 NA) ceramic dipping objective. In order to overcome problems of relative movement of microscope and tissue associated with temperature changes, it was necessary to heat the Ludin chamber to 37°C for at least 30 min prior to imaging and to allow the specimen to equilibrate for at least 30 min before imaging began.

To compare the emitted fluorescence intensity between controls and treated cells, images from 4D data sets were saved using the Leica SP2 Multiphoton confocal LCS (Leica Microsystems Ltd, Milton Keynes, UK) software package. Image resolution was set to 1024×1024 pixels at 8-bit gray depth. All images were obtained under identical experimental conditions. Preliminary experiments were carried out to determine if exposure of the neurons to FLIM analysis had an effect on native fluorescence intensity.

Time domain FLIM images were captured using a BH SPC-830 multichannel single-photon counting board (Becker & Hickl GmbH, Berlin, Germany). NAD(P)H

fluorescence was filtered through a 550 nm short-pass filter (Chroma Technologies, Rockingham, VT). Additional short pass and Instrument Response cut off filters were used to reject reflected or scattered excitation light at 750 nm. Images were acquired by summation of 30, 4-second scans to ensure enough photon counts were collected at the laser power used for further data/statistical analysis.

Fluorescence decay curves in image pixels were processed using SPC Image software (version 2.9.4, Becker & Hickl). The software was able to calculate the basic fluorescence lifetimes on a pixel-by-pixel basis and account for the instrument response function. For every pixel in the image, the four nearest-neighbor pixels relative to each central pixel were binned together to increase photon counts for improved decay fits. All NAD(P)H lifetime calculations were fitted to two-components (T1 and T2), as determined by obtaining the lowest χ^2 value; this gives an indication of how accurate the fit is and should be as close to 1 as possible. Typical signal levels after binning were roughly 1,000 photons per pixel. The software minimizes the χ^2 value between the data and the model function during the fit process (Becker, 2008). The result is a set of parameters such as lifetimes of individual species and their relative amplitudes for each individual pixel of the image. In this study the selected fit parameters were T1 and T2 (free NAD(P)H and bound NAD(P)H fluorescence lifetimes, respectively), *a1%* (percentage or amplitude of the T1 lifetime) and χ^2 (accuracy of fit for a 2-component system).

4.2.3 Analysis and statistics

Estimation of the fluorescence intensity was processed using Image J (ver. 1.43u). For each image, all the fluorescent neurons were delineated and the fluorescence intensity was measured in each neuron. The average fluorescence intensity (from a minimum of 8 neurons) was calculated for each explant and this value was used for statistical analysis. Images from the same field in each explant were acquired following exposure to high glucose and fluorescence intensity measured as above and the effect of glucose was assessed using a paired student's t-test. Separate explants, maintained in 10 mM or 30 mM glucose, were used for the study of the effect of 24 h exposure to high glucose. The analysis of native fluorescence intensity was as described above except that an unpaired student's t-test was used for statistical analysis.

In preliminary experiments on SCG explants, the SPC image acquired by FLIM was analyzed in two ways. Firstly, the fluorescence lifetimes T1 and T2 were calculated for the entire field (neurons and neuropil) and the lifetime ranges were colour coded to examine the distribution of lifetimes throughout the explant. In the same image T1 and T2 were also calculated for individual delineated neurons in order to exclude the contribution from the neuropil and the average was taken from a minimum of 10 neurons. In all subsequent experiments, T1, T2, $a1\%$ and χ^2 were calculated in delineated neurons and an average was taken from a minimum of 10 neurons per explant under control conditions (10 mM glucose) and after exposure to 30 mM glucose for 30, 120 mins and 24 h. Two-way ANOVA followed by Bonferroni post hoc tests (GraphPad Prism 3 software) were used to analyze the effects of the ganglionic source of the sympathetic neurons (CG/SMG or SCG) and of high glucose. A level of probability of $p < 0.05$ was taken to indicate statistical significance. Micrograph pictures were produced using Photoshop Elements 8 software.

4.3 Results

Using two photon excitation at 750 nm, the native NAD(P)H fluorescence at ~550nm emission was readily observed without photobleaching the specimen. Examples are given in figs. 4.1 and 4.2 with green pseudocolour mapping representing native NAD(P)H fluorescence. Only the neuronal soma could be discerned and the neuronal nuclei were negative. Within the cytoplasm the fluorescence appeared punctate.

4.3.1 NAD(P)H fluorescence intensity in CG/SMG and SCG after acute and 24 h exposure to high glucose

Preliminary experiments were carried out on SCG explants maintained under control conditions to examine the effect of exposure to FLIM on native NAD(P)H fluorescence and the results are given in fig. 4.3. NAD(P)H intensity was measured before exposure to FLIM and then in the same neurons following either one (at t0) or two successive exposures to FLIM (t0 and t12). NAD(P)H fluorescence intensity was significantly increased within 24mins following two exposures to FLIM and within 50mins following one exposure. As a consequence all subsequent analyses on the effect of high glucose on native NAD(P)H fluorescence were only performed on fields within the explants that had not been exposed to FLIM.

The acute effect of high glucose was assessed by measuring native NAD(P)H fluorescence in the same neurons before and after exposure to 30mM glucose for 30 and 120 mins and the results are given in fig. 4.1. The values within each explant have been

given individually to illustrate the effect on the paired samples. In all CG/SMG explants, exposure to high glucose resulted in an increase in native NAD(P)H fluorescence and there was a statistically significant ($p < 0.001$) increase in the mean values at after both 30 and 120 mins. In contrast, no consistent effect was observed in SCG explants after 30 mins and there was no significant difference between the means. There was a trend for an increase in fluorescence intensity in the SCG after 120 mins. However, only 3 SCG explants were available for analysis 120 mins after administration of high glucose that had not been exposed to FLIM.

NAD(P)H fluorescence intensity was also measured in explants exposed to 30mM glucose for 24h and compared with explants maintained under control conditions (10mM glucose) for 24h and the results are given in fig. 4.2. The increase in NAD(P)H fluorescence observed in CG/SMG neurons after 30 mins was not maintained such that there was no significant difference between the two groups after 24 h. SCG neurons were unaffected by exposure to high glucose for 24 h.
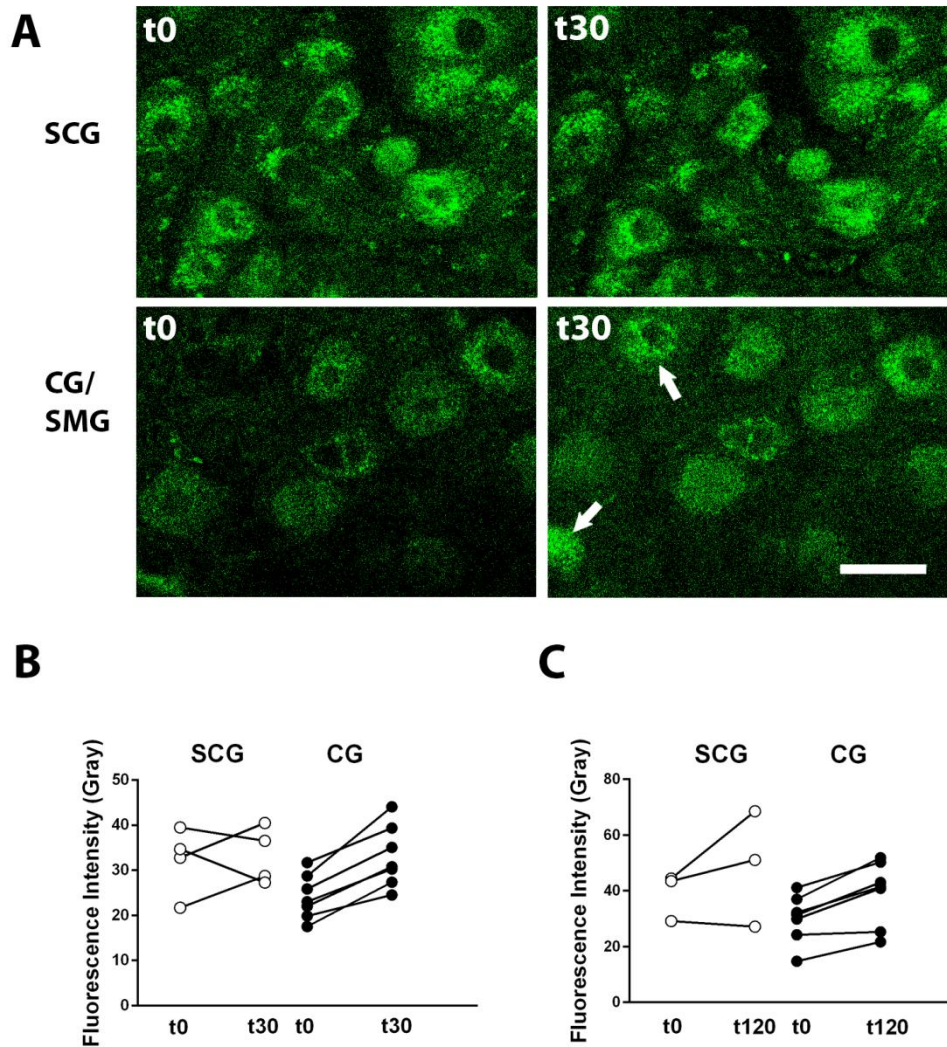
Figure 4.1: Effect of incubation with 30 mM glucose for 30 minutes on native NAD(P)H fluorescence in living CG/SMG (CG) and SCG neurons.

(A) Photomicrographs of native NAD(P)H fluorescence of SCG and CG/SMG neurons incubated with control glucose (t0, 10mM) and 30 minutes after incubation with high glucose (t30, 30 mM). No difference was observed in SCG neurons, however, fluorescence increased in CG/SMG neurons after exposure to 30mM glucose. Arrows indicate neurons that become visible after exposure to high glucose. Calibration bar represents 30 μm.

(B and C) Quantitation of fluorescence intensity (Gray values). Fluorescence intensity was measured in the same SCG and CG/SMG neurons before and after exposure to 30mM glucose for 30 and 120 mins respectively. The average value for each SCG explant is represented by open circles (n = 3-4) and for each CG/SMG explant by closed circles (n = 7). Note the significant increase in fluorescence intensity in CG/SMG neurons ($p < 0.001$, paired t-test) while fluorescence intensity in SCG neurons was not affected.
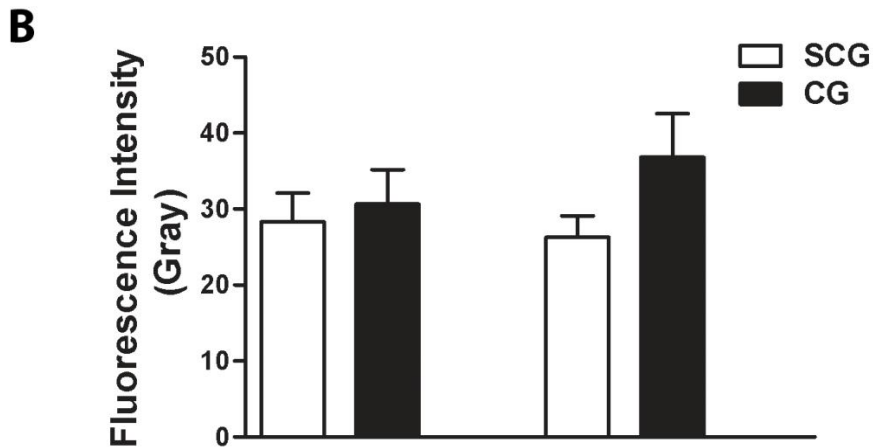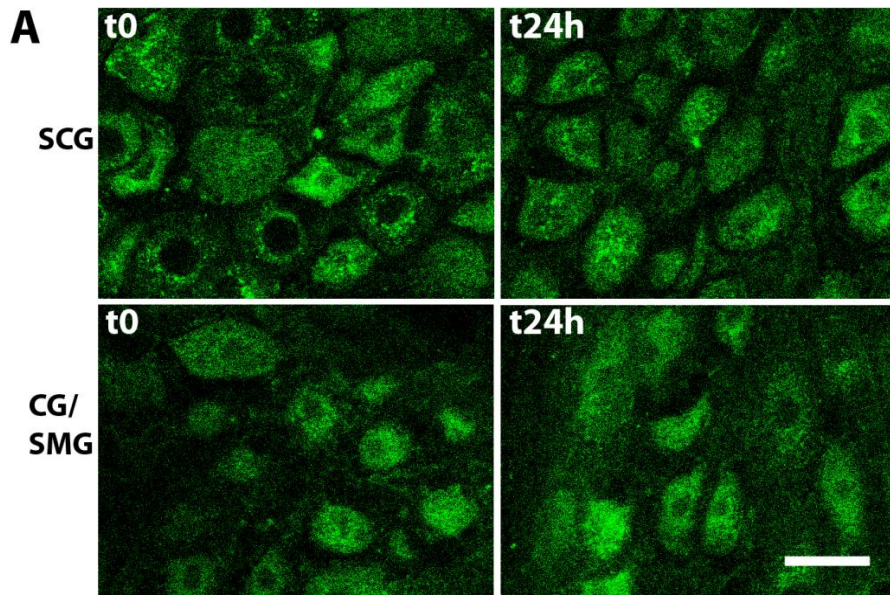
Figure 4.2: Effect of incubation with 30 mM for 24 hrs on native NAD(P)H fluorescence in living CG/SMG (CG) and SCG neurons.
(A) Photomicrographs of native NAD(P)H fluorescence of SCG and CG/SMG neurons incubated with control glucose (t0, 10 mM) and after overnight incubation with high glucose (t24h, 30 mM). No difference was observed in either SCG or CG/SMG neurons after exposure to 30 mM glucose for 24 h. Calibration bar represents 30 μm.
(B) Quantitation of fluorescence intensity (Gray values). Intensity was measured in control neurons (t0, clear bars) in SCG (n = 6) and CG/SMG (n = 7) explants. Different explants were assessed after 24 h incubation with 30 mM glucose (t24h, black bars, SCG n = 6; CG n = 5) Data are presented as the mean ± SEM. No significant differences were observed in either SCG or CG/SMG neurons (unpaired t-test).

FLIM repetitive photoexcitation
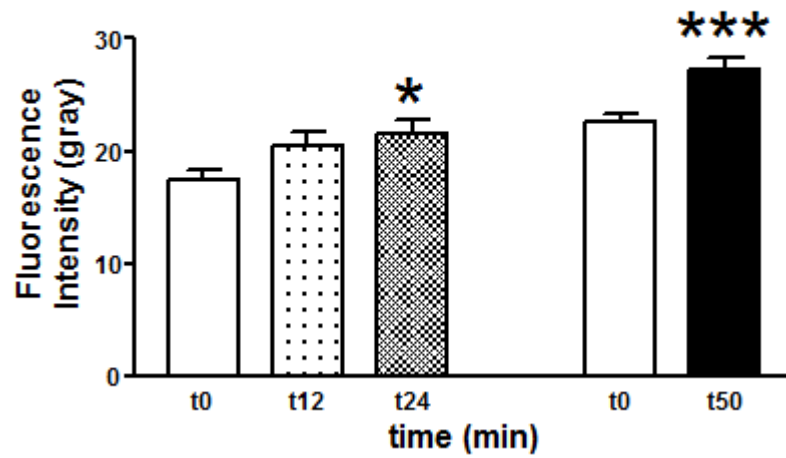
Figure 4.3: Effect of repetitive FLIM photoexcitation on native NAD(P)H fluorescence intensity. Data for two individual experiments on SCG explants are represented and given as the mean ± SEM. In the first experiment, intensity was measured before (t0, clear bar, n = 13 neurons) and 12 mins (t12, gray bar, n = 15) and 24 mins (t24, hatched bar, n = 15) after exposure to FLIM. In the second experiment, intensity was measured before (t0, clear bar, n = 24) and 50 mins after exposure to FLIM (t50, black bar, n = 24). Note that in both cases, exposure to FLIM resulted in a significant increase in fluorescence intensity for NAD(P)H over time. * $p < 0.05$, *** $p < 0.001$.
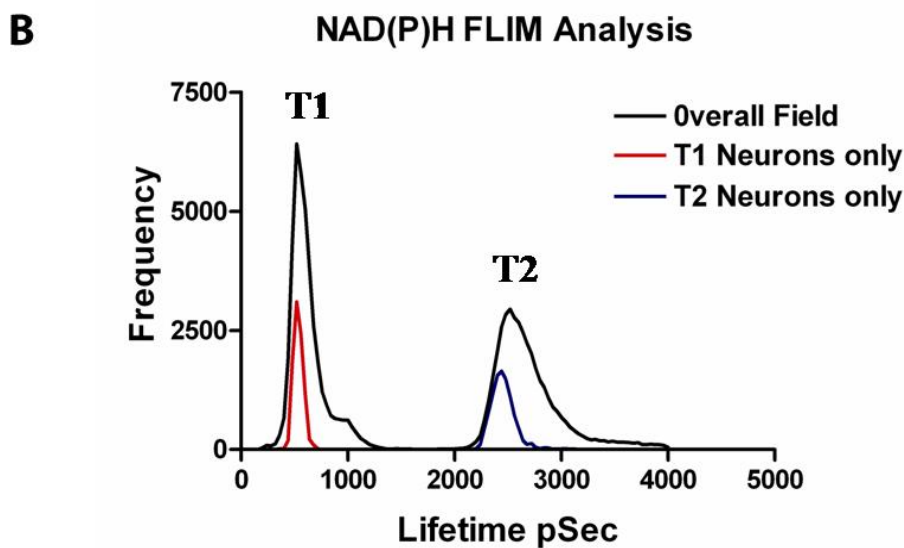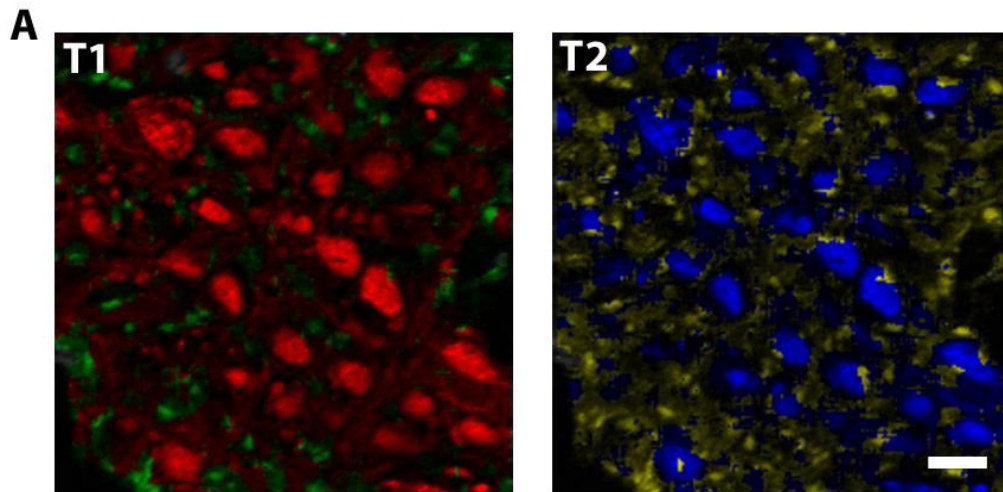
Figure 4.4: NAD(P)H fluorescence lifetime analysis of an SCG explant.
The explant was scanned from 0 to 4000 psecs and revealed two species, T1
representing free NAD(P)H and T2 representing bound NAD(P)H.
(A) The whole field was analyzed without discrimination of the neurons from the
neuropil and colour coding was used to visualize different lifetime ranges. T1: red
represents 200-650 psecs and green 650-1300 psecs. T2: blue represents 2000-2700
psecs and yellow 2700-4000 psecs. Note that for both T1 and T2 the lower lifetime
range was localized exclusively in neurons and the higher range was localized in the
neuropil. Calibration bar respresents 50 μm.
(B) Lifetime analysis was performed on the entire field and exclusively on the neurons
within the same field and the data are represented graphically. Note that when the entire
field including both neurons and neuropil was analyzed the peaks for both T1 and T2
were broader and skewed indicating the presence of more than one component for each
species. In contrast, when neurons were analyzed separately the peaks for T1 and T2
were narrow and symmetrical.

4.3.2 FLIM analysis

Preliminary experiments using SCG explants demonstrated that when the field was analysed as a whole, without discrimination of the neurons from the neuropil, two main components, free NAD(P)H (T1) and bound NAD(P)H (T2) were revealed. However, the peaks were not symmetrical indicating that each component might not be homogeneous over the entire field (fig. 4.4B). This was confirmed when using colour coding. It was demonstrated that both T1 and T2 lifetimes in neuronal cell bodies tended to be shorter than those in the neuropil (fig 4.4A). It should be noted that in order to obtain sufficient photons in the neuropil for analysis, it was necessary to increase the bin width (15) which reduced the resolution such that the distribution of free and bound NAD(P)H no longer appeared punctate. When T1 and T2 were analysed selectively in delineated neurons from the same field, the peaks were sharp and symmetrical (fig. 4.4B) indicating that components with slightly longer lifetimes from the neuropil had been excluded. As a consequence all subsequent analysis was performed on delineated neuronal cell bodies alone.

4.3.3 FLIM analysis of the effects of glucose and ganglionic source

FLIM analysis was performed for the following parameters: T1 [free NAD(P)H], T2 [bound NAD(P)H], a1 (the percentage of the total photons within the T1 component), and χ^2 values. The results for CG/SMG and SCG neurons under control conditions and following exposure to high glucose for 30 min and 24 h have been given in fig. 4.5. The values for χ^2 were close to 1 for all the groups indicated that the

NAD(P)H fluorescence did conform to a two component system. There were no significant differences between the ganglia and exposure to high glucose had no effect. The majority of NAD(P)H was in the unbound form since the average *a1* was 70%. There was no significant difference in this percentage between the different ganglia or on exposure to high glucose. The fluorescence lifetime of free NAD(P)H (T1) tended to be higher in CG/SMG neurons than SCG neurons. Two way ANOVA revealed that there was a significant effect of the ganglionic source on T1 ($p < 0.01$). Comparisons between individual groups demonstrated that following exposure to high glucose for 30 mins, the difference in T1 between CG/SMG and SCG neurons was significant ($p < 0.05$). However, glucose did not significantly affect T1 in neurons from either ganglion. The values for T2 were similar in all groups with no significant effect of ganglionic source or high glucose.
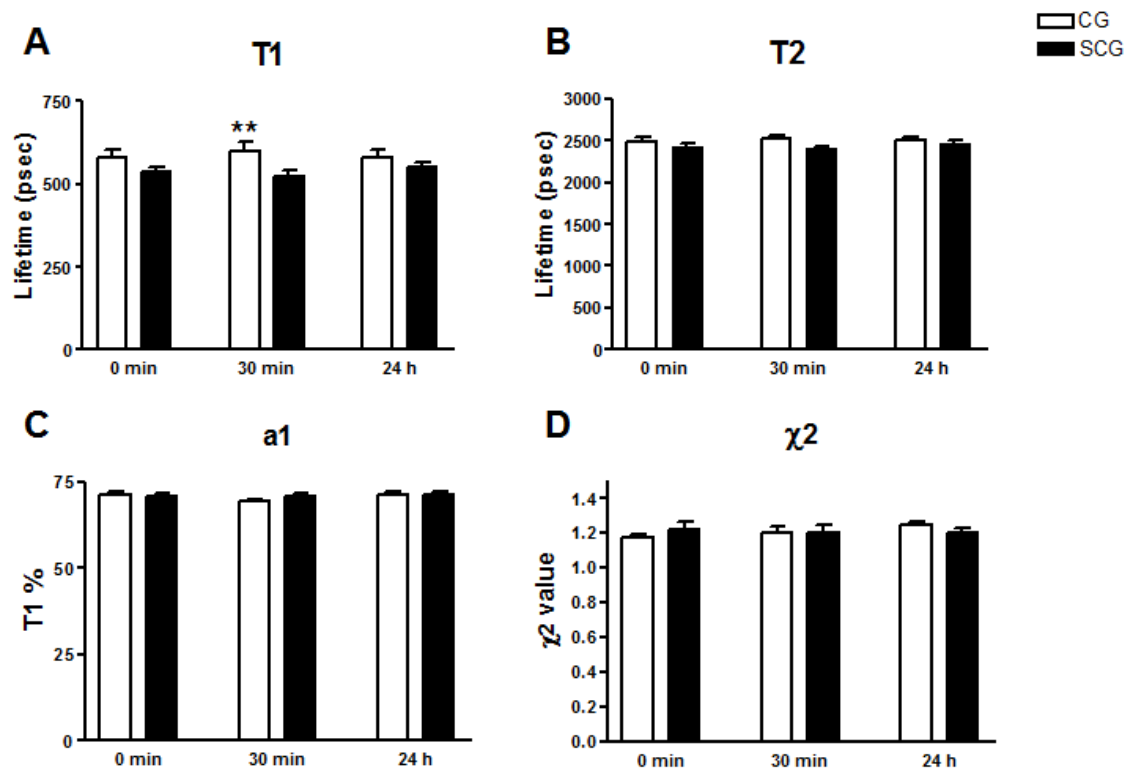
Figure 4.5: Comparison of the effect of high glucose on fluorescence lifetime analysis of NAD(P)H in SCG and CG/SMG (CG) neurons. Analysis was performed before (t0) and 30 min (t30) and 24 h (t24h) after exposure to 30 mM glucose. Data are given as the mean ± SEM and were analyzed using two-way ANOVA with high glucose and ganglionic source as factors. Clear bars represent SCG neurons (n = 6 for all time points). Black bars represent CG/SMG neurons (t0 and t30, n = 7; t24h, n = 5).
A. T1: Fluorescence lifetime of free NAD(P)H. Exposure to high glucose did not have any effect on T1 in either SCG or CG/SMG. T1 tended to be lower in the CG/SMG than SCG and this was statistically significant after 30 min exposure to high glucose. B. T2: Fluorescence lifetime of bound NAD(P)H. T2 was not affected by exposure to high glucose or ganglion. C. a1: Percentage of the total number of photons due to T1. The proportion of photons detected due to free NAD(P)H was not affected by either exposure to high glucose or ganglion. D. χ^2: Assessment of the two component analysis. Neither exposure to high glucose nor ganglion influenced χ^2.

4.4 Discussion

In this study we investigated the pyridine nucleotide metabolism after acute and 24 h exposure to high glucose *in vitro* using two photon excitation of NAD(P)H native fluorescence and FLIM analysis of the free and bound components of NAD(P)H. The results from this study show that adult CG/SMG and SCG neurons from normal rats survive after exposure to hyperglycemic insult. However, changes in NAD(P)H metabolism were detectable after exposure to high glucose for 30 min that were not maintained with longer exposure for 24 h. These acute effects occurred selectively in CG/SMG and not in SCG neuronal cell bodies.

The non-invasive technique of fluorescence microscopy offers the possibility to detect four species of autofluorescence in a cell. Besides NAD(P)H, flavoproteins, catecholamines and indoleamines are autofluorescent. The parameters used for the two photon microscopy (excitation 750 nm, emission 550 nm) were similar to those used for imaging NAD(P)H in rat brain slices (Chia et al., 2008). Serotonin and tryptophan fluoresce in the near UV range (340 nm). Furthermore, serotonin, dopamine, norepinephrine and tryptophan do not fluoresce at excitation wavelengths above 580 nm (Balaji et al., 2004;Botchway et al., 2008). Flavins do fluoresce in the 550 nm region. However, flavins require an excitation wavelength of at least 890 nm and, at an excitation wavelength of 750 nm, fluorescence has been reported to be due to NAD(P)H (Huang et al., 2002a;Skala et al., 2007b). In addition, the fluorescence lifetimes corresponded to those reported for NAD(P)H rather than flavins (Skala et al., 2007b). Thus, the fluorescence quantified here represents NAD(P)H rather than other potential autofluorescent species within the cell.

Only the neuronal cell bodies could be visualized with native NAD(P)H fluorescence which probably reflects the high density of mitochondria in neurons (Kann & Kovacs, 2007). In cardiac myocytes, the contribution of cytosolic NAD(P)H to native fluorescence has been reported to be negligible compared with that of mitochondria. On its own, fluorescence does not distinguish between NADH and NADPH. However, changes in fluorescence in cardiac myocytes in response to cyanide and a mitochondrial uncoupler indicated that it was primarily due to NADH rather than NADPH (Eng et al., 1989). After synaptic activation, mitochondrial NADH transients dominate NAD(P)H autofluorescence signals in CNS neurons (Shuttleworth et al., 2003;Brennan et al., 2006;Brennan et al., 2007;Shuttleworth, 2010). Thus, it is likely that the fluorescence measured here reflects mitochondrial NADH but similar experiments are required to establish unequivocally that this is the case for sympathetic neurons.

4.4.1 Effect of exposure to high glucose on NAD(P)H metabolism

It was originally intended to measure NAD(P)H fluorescence and fluorescence lifetimes in the same neurons. However, FLIM requires more prolonged excitation than that required for native fluorescence alone with potential cellular effects. Preliminary experiments demonstrated that exposure to FLIM caused an increase in NAD(P)H fluorescence. Therefore, NAD(P)H fluorescence intensity was only measured in neurons that had not been exposed to FLIM.

Exposure to high glucose for 30 min caused a significant increase in NAD(P)H fluorescence intensity in CG/SMG neurons. A transient decrease in NAD(P)H fluorescence was observed in adult DRG neurons 10 min after exposure to 50 mM

glucose (Huang et al., 2003). However, this was measured using one photon confocal microscopy and it cannot be excluded that this was harmful to the cells. Our results are in line with a study by Evans and colleagues who reported similar increased fluorescence in response to high glucose *in vitro* in adipocytes and fibroblasts and attributed this to mitochondrial NADH (Evans et al., 2005). Vincent et al. (2005a) reported that mitochondrial NADH oxidase activity increased in embryonic DRG neurons within 1 h after exposure to high glucose and suggested that this was due to increased production of NADH by the TCA cycle and overloading of the electron transport chain. The results presented here provide evidence that NADH levels do increase rapidly in neurons in response to high glucose. Interestingly, no change in fluorescence intensity was observed in SCG neurons on exposure to high glucose for 30 min.

In the 1960s Chance and colleagues, pioneers in the measurement of the fluorescence of reduced pyridine nucleotides, established that the increased fluorescence due to the reduced form of pyridine nucleotides was indicative of cell metabolism (Chance & Baltscheffsky, 1958;Chance & Thorell, 1959;Chance & Hollunger, 1960). Initially it was held that increased autofluorescence indicated changes in the binding of mitochondrial NADH (Chance & Baltscheffsky, 1958). Later, Jobsis at al. argued that changes in the intensity of NADH fluorescence can be interpreted as changes in intracellular NADH concentrations. They performed parallel studies using fluorometric and biochemical methods and reported that under circumstances, such as hypoxia, where NADH levels increase and NAD+ levels decrease, fluorescence does indeed rise (Jobsis et al., 1971). The results presented here indicate that high glucose may cause an increase in the NADH/NAD+ ratio in CG/SMG neurons, a condition that has been characterized as pseudohypoxia and proposed to contribute to the development of

diabetic complications (Wahlberg et al., 2000; Ido, 2007). The effect of high glucose on NAD(P)H fluorescence in CG/SMG neurons was temporary since there was not a significant difference in fluorescence intensity in CG/SMG neurons following 24 h exposure to high glucose. It is possible that fluctuations in glucose concentrations would have had a greater effect than constant exposure. Intermittent exposure to high glucose has been shown to be more harmful to endothelial cells *in vitro* than constant high glucose levels (Risso et al., 2001).

Brownlee and colleagues have proposed a unifying mechanism and the link between the pathways responsible for oxidative stress and hyperglycemic damage in endothelial cells. Hyperglycemia-induced accelerated glycolysis and increased flux through the TCA cycle is the source of the increased ROS in the mitochondria of endothelial cells. Hyperglycemia causes overproduction of electron donors like NADH by the TCA cycle, the proton gradient is increased, the electrochemical potential difference across the inner mitochondrial membrane rises above the limit and superoxide production is markedly increased (Du et al., 2001;Brownlee, 2001). However this mechanism may not apply to neurons. Studies of adult DRG neurons have demonstrated mitochondrial membrane depolarization rather than hyperpolarization in diabetic rats and no evidence for the production of ROS in mitochondria (Akude et al., 2011). It remains to be determined how long term diabetes *in vivo* affects NAD(P)H metabolism in sympathetic neurons.

4.4.2 Mitochondrial and cytosolic NAD(P)H and NAD(P)H oxidase

4.4.2.1 FLIM analysis

The FLIM analysis was carried out on the basis that the native fluorescence consisted of two components, free (T1) and bound NAD(P)H (T2). However, fluorescence lifetimes are sensitive to environment and may vary in different cell types and in different cellular compartments. Two major peaks were observed when the overall field (neurons plus neuropil) was analyzed. The peaks were not symmetrical indicating that each peak probably contained more than one species. When FLIM data was analyzed exclusively in neuronal cell bodies in the same field, the peaks sharpened. Colour coding of lifetime ranges revealed that both T1 and T2 lifetimes were shorter in the neurons than the neuropil. A study by Chia et al. also demonstrated that the fluorescence lifetimes were different in the neuropil and neuronal cell bodies (Chia et al., 2008). Since χ^2 values were close to 1 throughout the rest of the study where only neurons were analyzed, this indicates that the data conformed closely to a two component system. This is unlike a study of cardiac myocytes where a third component was observed (Blinova et al., 2005). In control SCG and CG/SMG neurons, the lifetime of free NAD(P)H, (T1) was in the range 520-600 ps and of bound NAD(P)H, (T2) 2000-3000 ps. This is similar to the ranges reported for NAD(P)H fluorescence lifetimes (T1 300-600 ps; T2, 2000-3000 ps) in a range of cell types (Bird et al., 2005;Skala et al., 2007a;Niesner et al., 2008a). The majority of the NAD(P)H fluorescence was in the free form as the average *a1%* was approximately 70% in both ganglia, and, by substraction, 30% was in the bound form. This is very similar to values reported for epithelial cells (Skala et al., 2007b). It should be noted that this does not mean that the majority of the native fluorescence intensity was due to free NAD(P)H.

155

Fluorescence molecules with long lifetimes contribute almost 80% to fluorescence intensity images due to their greater quantum yield (Blinova et al., 2008;Chia et al., 2008). A diminution of the amplitude of the bound form (*a2*) reflects a very low metabolic activity (Niesner et al., 2008a).

4.4.2.2 FLIM Analysis of the effect of High Glucose

A study of embryonic DRG neurons reported that the increase in mitochondrial NADH oxidase activity within 1h of high glucose exposure was followed rapidly by caspase activation and apoptosis (Vincent et al., 2005a) and embryonic SCG neurons also undergo apoptosis in response to high glucose (Russell & Feldman, 1999). Apoptosis has been reported to cause a significant increase in average NAD(P)H fluorescence lifetimes (Wang et al., 2008). Since fluorescence lifetimes were not significantly altered after 24 h exposure to high glucose, there was no evidence in this study that exposure to high glucose initiated neuronal cell death in adult sympathetic ganglia. This probably reflects greater susceptibility of embryonic neurons to apoptosis since there is also no evidence for apoptosis being induced in adult DRG neurons by high glucose (Huang et al., 2003).

Similarly there was no evidence for the activation of NADPH oxidase by high glucose in this study. Activation of NADPH oxidase requires the translocation of regulatory subunits to the cellular membrane. Activated NADPH oxidase has been demonstrated in CG neurons from hypertensive but not control rats by increased immunostaining in the plasma membrane (Cao et al., 2007). However, no shift in the distribution of NAD(P)H fluorescence was observed during FLIM analysis after exposure of sympathetic neurons to high glucose. In addition, activation of

polymorphonuclear cells involves translocation and activation of NADPH oxidase resulting in the production of superoxides for host defence. FLIM analysis of activated cells revealed the development of a new fluorescence lifetime species with the longer lifetime of 3700 ps with NADPH oxidase activation but no new fluorescence lifetime species were detected in sympathetic neurons here. Since *a1%* values were similar in SCG and CG/SMG neurons with and without exposure to high glucose, the increase in fluorescence intensity observed in CG/SMG neurons 30 min after exposure to high glucose was not due to a change in the distribution of NAD(P)H between the free and bound forms. T2 values were also similar in all neurons studied. However there were subtle differences between neurons from the two ganglia. Two way ANOVA with ganglionic source and exposure to glucose as factors revealed that the ganglionic source did have a significant effect. T1 values tended to be higher in CG/SMG neurons than SCG neurons and this was significant following exposure to high glucose for 30 min, the time at which NAD(P)H fluorescence intensity was significantly increased selectively in CG/SMG neurons. This may reflect an initial change in the environment of free NADH in CG/SMG neurons with high glucose.

CG/SMG are particularly vulnerable in human and experimental diabetes (Schmidt et al., 1993). The differences in CG/SMG and SCG in response to diabetes have been attributed to their differences in their blood-ganglion-barrier (Chau & Lu, 1995), levels of anti-oxidant defence and responses to NGF (Semra et al., 2004;Semra et al., 2006;Semra et al., 2009). There are also metabolic differences between prevertebral and paravertebral sympathetic ganglia. CG/SMG display more tonic activity than paravertebral neurons (Szurszewski, 1981), demonstrate higher metabolic activity (Carroll et al., 2004) and have different expression of genes coding glycolytic and mitochondrial based enzymes (Carroll et al., 2004).

4.4.3 Conclusion

In conclusion, this is the first study using time domain fluorescence and FLIM to explore the changes induced by high extracellular glucose in living neurons *in vitro*. Temporary effects of glucose in NADH/NAD+ redox ratio were observed selectively in CG/SMG neuronal cell bodies. However, the CG/SMG neurons were able to recover and return to the control state after 24 h high glucose stimulation. These results suggest that acute exposure to high glucose causes subtle abnormalities in redox ratio from which the CG/SMG neurons are able to adapt and such changes do not cause cell death. Longer term studies both *in vitro* and *in vivo* are required to determine the stage at which CG/SMG neurons are no longer able to adapt to high glucose and if this is reflected by altered NAD(P)H metabolism.

Chapter 5: Discussion, Conclusions and Future Study

In vitro models of diabetes provide a useful tool for studying pathological mechanisms in greater detail than *in vivo,* since they enable the cellular environment to be strictly controlled. *In vitro* models are also valuable for the preclinical screening of therapeutic agents prior to studies in animal models *in vivo* and subsequently clinical trials. In a simplified system, it is possible to accomplish the mapping of biochemical pathways induced by toxic compounds mimicking the diabetic environment. Investigating isolated parts of a living organism permits the manipulation of experimental parameters and the prediction of drug efficacy and toxicity in early stage drug testing. In diabetic neuropathy, *in vitro* models also allow potential mechanisms to be studied in isolation from vascular abnormalities that may occur in parallel as part of the disease processes. The identification of changes *in vitro* may also provide information for the design of functional studies to elucidate how neuropathy leads to motility disorders in diabetes. These reasons, in conjunction with ethical and financial considerations, have raised the necessity of developing *in vitro* methods for investigating diabetic neuropathy.

A variety of *in vitro* models of diabetic neuropathy have already provided significant information about the pathogenesis of diabetic neuropathy and the possibilities for treatment. The most common model used to date has been cultures of

embryonic sensory neurons from non-diabetic rodents treated with high glucose. These have demonstrated defective neurite outgrowth, mitochondrial degeneration and apoptosis, caused by high glucose-induced oxidative stress. In diabetic gastroenteropathy, *in vitro* studies have mainly used cell lines. In these studies, proapoptotic factors, oxidative stress and apoptosis were also the consequences of high glucose insult (Russell et al., 1999;Russell et al., 2002;Vincent et al., 2004b;Vincent et al., 2005a;Vincent et al., 2007b). All these findings have concluded that normal neurons are extremely sensitive, cannot adapt and die due to the toxicity induced by high glucose. However, these findings do not correlate well with what occurs in the *in vivo* state, since there is little evidence for the death of sympathetic and sensory neurons in experimental or human diabetes (Schmidt et al., 1993;Schmidt et al., 2001;Zherebitskaya et al., 2009;Chowdhury et al., 2012).

5.1 Cell death as an experimental endpoint

A loss of myenteric neurons has been reported in STZ-induced diabetic rats (Izbeki et al., 2009;De Mello et al., 2009). Such reductions were based on finding significant decreases in HuC/D neuronal density per unit area. Studies using other neuronal markers have also used this method of assessment. However, it is well recognized that there is marked distension and hypertrophy of the gastrointestinal tract in experimental diabetes (Schmidt, 2002). Thus, any increase in the area of the gut wall in diabetes would result in a decrease in neuronal density when expressed per unit area, even if there were no change in neuronal number. Studies from this laboratory have demonstrated that this is a significant factor since no loss of myenteric neurons was

160

observed in STZ-diabetic rats when this was assessed on the basis of the average number of HuC/D neurons per myenteric ganglion which is independent of area (Voukali et al. 2011).

Enhanced cleaved caspase-3 staining has been reported in human colonic enteric neurons in diabetes (Chandrasekharan et al., 2011). In sensory neurons, enhanced caspase-3 staining in diabetes is not always accompanied by TUNEL staining or neuronal loss (Guo et al. 2004). After 4-8 weeks diabetes in the rat, caspase 3-staining was increased in nodose ganglion, dorsal root ganglion and myenteric ganglia. However, in all cases the percentage of neurons expressing caspase-3 was significantly higher than the percentage expressing TUNEL. Furthermore, only 1.1 % of the myenteric neurons were TUNEL-positive in experimental diabetes indicating that apoptosis was not occurring in the vast majority of the neurons. Although apoptotic factors are present, counter regulatory elements appear to prevent apoptosis (Cheng & Zochodne, 2003;Guo et al., 2004;Kamiya et al., 2005).

When it was first reported that high glucose causes apoptosis in DRG and SCG neurons it was proposed that neuronal cell death was responsible for the loss of axons that occurs in diabetic neuropathy (Russell et al., 1999; Russell & Feldman, 1999). However, in the light of subsequent studies, the current view of the pathological process has reverted back to the traditional concept that diabetic neuropathy is a dying back type of axonopathy resulting in neuroaxonal dystrophy in the absence of neuronal cell death (Zherebitskaya et al., 2009). It has been proposed that neurons have two distinct self-destruct programs in response to insult. The first involves neuronal cell death via apoptosis. The second occurs exclusively in the axons and is more common in polyneuropathies such as occur in diabetes where axonal degeneration occurs progressively from the distal end. The importance of this distinction is that with dying

back axonopathy the neuron can retain the ability to regrow its axon should conditions improve (Raff et al., 2002). This is of key significance to the prospect of treating diabetic neuropathy once it has developed. It is concluded that diabetes does not cause a significant decrease in the number of HuC/D-positive neurons per myenteric ganglion and neuronal cell death is not a prominent feature of sensory, sympathetic and enteric neurons in diabetes *in vivo* (Schmidt et al., 1993;Schmidt et al., 1997;Schmidt, 2001, Zochodne et al., 2001;Voukali et al., 2011). This calls into question whether cell death is a valid endpoint with which to assess the mechanisms underlying diabetic neuropathy in *in vitro* models.

5.2 Establishment of the *in vitro* model for studying the effects of diabetes on myenteric neurons

Several factors were taken into consideration here when developing an *in vitro* model for studying diabetic enteropathy. The first was that the neurons should be fully mature. Studies of both DRG and sympathetic neurons have demonstrated that neurons that are not fully developed are more likely to respond to high glucose by undergoing apoptosis than adult neurons (Zherebitskaya et al., 2009;Semra et al., 2009). Secondly, the neurons should be subjected to as little disruption as possible since apoptosis of adult rat SCG neurons in response to high glucose occurs to a greater extent in cultures consisting of dissociated neurons than in ganglionic explants (Semra et al., 2004;Semra et al., 2009). Thirdly, the endpoints used for assessing responses should be the same as

those that are known to occur in animal models of diabetes *in vivo* and should take into account that not all neurons are affected in the same way in diabetes.

Some enteric neuronal subpopulations exhibit degeneration (Belai et al., 1988), some undergo change in neurotransmitter content without degeneration (Belai et al., 1988) while some are unaffected (Belai et al., 1985). Myenteric neurons in the ileum are more affected than those in the large intestine (Belai et al., 1991). In addition, intrinsic motor inhibitory neurons appear to be more affected than excitatory motor neurons (Chandrasekharan & Srinivasan, 2007). Therefore, wholemount preparations of the myenteric plexus from the ileum of the adult rat were used for the *in vitro* model. For the purposes of this study, three subpopulations of myenteric neurons containing VIP, nNOS or calbindin were selected for investigation since it had been shown that they respond differently following 12 wks STZ-diabetes (Shotton et al., 2006; Voukali et al., 2011). Therefore the endpoints used to determine whether the *in vitro* model did reflect the *in vivo* pattern were an increase in the expression of VIP, a decrease in the expression of nNOS and no change in the expression of calbindin. The only previous study to date that had investigated the response of wholemount myenteric plexus preparations to potential diabetic stimuli (Korenaga et al. 2006) examined the effect of BSA-AGE exposure for 24 h and only studied nNOS-containing neurons, reporting a decrease in expression. We extended this approach, not only by studying additional populations of myenteric neurons but also by investigating additional stimuli that may mimic the diabetic environment. A concentration of 30 mM glucose was used to examine the effect of high glucose *per se* since this is a level known to occur in poorly controlled diabetes. The possibility that reactive carbonyl species formed as a consequence of increased glucose levels induced diabetic-like changes was examined using methylglyoxal. In addition, menadione was used to investigate the effect of

oxidative stress since this has been proposed to be a key element in sensory neuropathy (Figueroa-Romero et al., 2008). In all cases it was established that the concentrations of diabetic stimuli used did not cause a loss of HuC/D myenteric neurons in our culture system.

Using this model, an interesting pattern was observed. Only oxidative stress could replicate completely the changes that occur *in vivo*. High glucose and carbonyl stress only affected VIP expression and AGE only affected nNOS expression. VIP and nNOS have been reported to be colocalized in the same myenteric neurons following colchicine treatment. However, a study of myenteric neurons in Parkinson's disease demonstrated similar changes in VIP and nNOS expression as those demonstrated here using triple immunolabelling and in the absence of colchicine. Following analysis of neurons that contained nNOS or VIP on their own or both nNOS and VIP, the authors concluded that nNOS expression was decreased in a subpopulation of nNOS-containing neurons that was separate from the subpopulation of nNOS-containing neurons in which VIP expression was induced (Colucci et al., 2012). If a similar situation applies in diabetic neuropathy, the results presented here indicate that individual subpopulations may be more or less susceptible to specific pathways implicated in the development of neuropathy but that oxidative stress is the common element. Myenteric neurons that contained calbindin were consistently resistant to all the stimuli. These results imply that calbindin has a neuroprotective role and its presence in a neuron could reflect an intrinsic advantage to buffer elevated intracellular waves of calcium (Mattson et al., 1991;Iacopino et al., 1992;McCormack et al., 2006).

Why VIP expression but not nNOS expression should be affected by high glucose and carbonyl stress is not known. However, the selective effect of AGE on nNOS may reflect the selective expression of RAGE in a subpopulation of nNOS-

containing neurons in which VIP expression is not induced. RAGE expression has been demonstrated in myenteric ganglia where it is colocalized with neurons but not enteric glia (Korenaga et al., 2006). However, it has not been established whether RAGE is present in all myenteric neurons or in specific subpopulations. Similarly, susceptibility to methylglyoxal could be related to the levels of glyoxalase I, the enzyme that detoxifies reactive carbonyl species, in individual subpopulations of neurons. A study of DRG has demonstrated that glyoxalase I is selectively expressed in small, nociceptive DRG neurons and that activity is reduced in STZ-diabetes (Jack et al., 2011). Whether there is heterogeneous expression of glyoxalase I in myenteric neurons has not been investigated.

It is important to acknowledge that culture *per se* did have an effect on myenteric neurons. The expression of both nNOS and VIP was increased in preparations maintained for 24 h under control culture conditions relative to preparations that had not been subjected to culture. In the case of VIP, this has been reported previously and it has been suggested that VIP may be protective (Lin et al., 2003). However, the results presented here indicate that it is not likely that the same pathways that caused the changes under control culture conditions were the same as those that occurred in response to the diabetic stimuli. In the case of nNOS, AGE and oxidative stress caused a decrease rather than an increase in nNOS expression. In addition, the anti-oxidant α-lipoic acid, prevented the altered expression of nNOSand VIP in response to high glucose, carbonyl stress or AGE but had no effect on nNOS or VIP expression in control culture preparations.

5.3 Prevention of induced changes and oxidative stress as the unifying factor

Having identified the changes that occur in myenteric neurons *in vitro* to different diabetic stimuli, this established a model with which to examine further the mechanisms involved and to screen potential therapeutic agents. Four agents were selected for investigation here based on the fact that they had already been investigated for the treatment of diabetic sensory neuropathy and that they differed in their proposed sites of action. The effects of α-lipoic acid, an anti-oxidant (Packer, 1995); nicotinamide, a PARP inhibitor (Stevens et al., 2007); aminoguanidine, a carbonyl scavenger (Thornalley 2003b); and thiamine, an inhibitor of carbonyl stress (Mehta et al., 2008) on VIP- and nNOS- containing myenteric neurons on the responses to oxidative stress, carbonyl stress, high glucose or AGEs were examined.

In sensory nerves, several pathologic mechanisms have been proposed to account for neuropathy such as defects in neural blood flow and metabolic deficits (Cameron et al., 2001; Zochodne, 2007) and these are not mutually exclusive. However, it has been proposed that such deficits join to form the common link of oxidative stress which is responsible for the development and progression of sensory neuropathy (see Figueroa-Romera et al., 2008). Whether this is also the case with autonomic neurons has not been investigated before. Having demonstrated that oxidative stress mimicked the effects of diabetes on myenteric neurons, the effects of α-lipoic acid on the changes induced by individual diabetic stimuli were investigated. The data presented here confirmed that all these stimuli appeared to be acting via the production of oxidative stress since the anti-oxidant prevented the changes in VIP- and nNOS containing nerves whatever the stimuli used.

Oxidative stress has been implicated in a wide range of diseases affecting the nervous system including neurodegeneration disorders such as Alzheimer's disease, Parkinson's disease, Motor Neuron disease, Huntington's disease (Valko et al., 2007). While cell necrosis or apoptosis usually follow oxidative stress in the CNS, this is not necessarily the case in the peripheral nervous system. In diabetic sensory neuropathy, there is evidence that the production of ROS occurs selectively in the axon providing a mechanism whereby oxidative stress could cause axonal degeneration without initiating apoptosis (Leinninger et al., 2006;Zherebitskaya et al., 2009).

Additional experiments were performed with aminoguanidine and nicotinamide to examine the contribution that the production of carbonyl species or the activation of PARP made to the effect of high glucose on VIP-containing neurons. Unfortunately, both agents were shown to have anti-oxidant properties as they prevented the response of both VIP- and nNOS-containing neurons to oxidative stress induced by menadione. More specific carbonyl scavengers or PARP inhibitors will be required to differentiate the roles of these individual pathways. However, these results did demonstrate the advantages of studying the effects of drugs on *in vitro* models of diabetes, using individual diabetic stimuli, and using oxidative stress induced by menadione in parallel. In contrast, thiamine did not prevent changes induced by oxidative stress but did prevent increased VIP-expression induced by carbonyl stress. Since thiamine was unable to prevent the response of VIP-containing nerves to high glucose this provided evidence that the effect of high glucose does not occur via the production of reactive carbonyl species.

Taken together these studies on wholemount preparations of the myenteric plexus have demonstrated its potential use in the investigation both of individual stimuli that mimic the diabetic environment and of potential therapeutic agents. It should be

noted that the model used here only investigated the prevention of diabetes-induced changes. For effective therapy, it is also important to establish whether agents can also reverse changes once they are induced.

5.4 Energy metabolism and intrinsic heterogeneity of sympathetic neurons

It is well recognized that diabetes does not affect all sympathetic neurons. In both humans and animal models, CG/SMG neurons undergo axonal dystrophy while SCG neurons are spared (Schmidt, 2002). In addition, in STZ-diabetic rats, the nerves supplying the ileum from the CG/SMG undergo degeneration while the nerves supplying the distal colon from the inferior mesenteric ganglion are unaffected (Belai et al., 1991). The understanding of the causes of such heterogeneity could shed light on the mechanisms underlying diabetic gastroenteropathy. While changes in the target of innervation has been suggested to contribute (Schmidt, 2002), inherent characteristics such as the axon length, the neuronal activity and the level of anti-oxidant defence may also be significant factors.

Spencer & Schaumburg noted the importance of axon diameter & length in determining the hierarchy of fiber vulnerability (Spencer & Schaumburg, 1977a, Spencer & Schaumburg, 1977b). In diabetic sensory neuropathy, there is general consensus that longer fibres are more vulnerable to degeneration. DRG neurons isolated from the lumbar L4-L6 segments of spinal cord are more susceptible than DRG from higher spinal cord levels (C3-L3) and this was correlated with the axonal length (Huang et al., 2002b). However, sympathetic axons supplying the ileum are dystrophic in diabetes but equally long sympathetic axons supplying the mesenteric vessels of the

ileum do not develop dystrophy. Therefore, axon length is not the only factor that determines the susceptibility of different sympathetic nerves in diabetes (Schmidt, 2002).

There is considerable heterogeneity in the intrinsic morphological and physiological properties between SCG and CG/SMG neurons. The activities of the anti-oxidant enzymes glutathione peroxidase and superoxide dismutase have been shown to be lower in CG/SMG than in SCG under normal conditions (Semra et al., 2004). In addition, the blood-ganglion barrier is less effective in the CG/SMG (Chau & Lu, 1995). Both of these properties could contribute to the greater susceptibility of CG/SMG neurons to hyperglycaemia and subsequent oxidative stress. Some differences are related to the different functional roles of CG/SMG and SCG neurons within the ANS. It has been reported that SCG neurons may have fundamentally different calcium dynamics because they display a differential expression of a significant range of ion channels (Jobling & Gibbins, 1999). The dendritic field in SCG neurons is small and simple in whereas the dendritic field of CG/SMG neurons is large and complex (Jobling & Gibbins, 1999). CG/SMG and SCG also have different neuronal firing properties that reflect the nature of their synaptic inputs and the pattern of activity induced in their targets. Half of CG/SMG neurons have tonic activity, meaning that they fire continuously in response to a maintained depolarising stimulus. In contrast, all SCG neurons have phasic activity meaning that they respond with transient bursts of action potentials after one suprathreshold synaptic input from spinal cord (Wang & McKinnon, 1995). These distinct properties may be reflected with different degrees of metabolic activity.

Preliminary evidence has been obtained from this laboratory that susceptibility to diabetes may be related to metabolic activity. Cytochrome oxidase activity was

measured histochemically together with the intensity of TH-immunofluorescence in the same neurons from CG/SMG and SCG from STZ-diabetic rats. Cytochrome oxidase activity was shown to be higher in CG/SMG neurons under normal conditions but was unaffected by diabetes. However, the intensity of TH-immunofluorescence was correlated positively with cytochrome oxidase activity in CG/SMG neurons. This indicates that the accumulation of TH, a characteristic of diabetic neuropathy was more likely to occur in the CG/SMG neurons with higher metabolic activity. No such correlation was observed in SCG neurons and TH-immunoreactivity was unchanged in diabetes (Shotton, 2008). Diabetes has also been shown to selectively induce significant changes in the expression of genes involved in the structure and function of synapses, mitochondria and oxidative stress in CG/SMG (Carroll et al., 2004). Metabolic activity has not been measured in intrinsic inhibitory motor neurons in the GI tract but it has been reported that they discharge continuously and action potentials and contractions in the muscle occur only when the inhibitory neurons are switched off by input from interneurons (Wood et al., 1999; Hansen et al., 2003b).

Sustained hyperglycaemia brings about fundamental metabolic changes in cells. As early as 1979, when Cavanagh described the "dying back" process of degeneration of multifocal neuropathies, it was held that the principle pathway that is seriously disturbed by a metabolic insult like the hyperglycemia is the TCA cycle. Lack of energy follows and this is critical to the initiation of pathological changes (Cavanagh, 1979). Current theory suggests that the polyol pathway, accelerated glycolysis and increased flux by the TCA cycle leads to the inhibition of Complex 1 activity in mitochondria and decreased production of ATP. In addition, such metabolic changes lead to changes in the balance between the oxidized and reduced forms of the pyridine dinucleotides, NAD

and NADP potentially altering the redox status of the cell (Ido et al., 1997; Brownlee, 2001; Ido, 2007;Hinder et al., 2012).

Recent technological advances now allow NAD(P)H metabolism to be examined in living cells using two photon microscopy with FLIM. To date, this experimental approach has not been used to investigate sympathetic neurons. Therefore, the last part of this thesis involved the investigation of the effect of high glucose *in vitro* on NAD(P)H levels and fluorescence lifetimes in living sympathetic neurons. Both SCG and CG/SMG neurons were studied to provide a comparison between a neuronal population that is susceptible to diabetic neuropathy with one that is unaffected. As discussed for the model of myenteric neurons, the system investigated used adult neurons in ganglion explants to avoid the increased vulnerability of immature neurons and minimize disruption. Exposure to high glucose caused a selective increase in NAD(P)H fluorescence in CG/SMG within 30 min. However, this effect was not maintained and no differences in NAD(P)H fluorescence intensity were observed in either ganglia after exposure to high glucose for 24 h. FLIM analysis of NAD(P)H fluorescence in neuronal soma did not reveal any significant changes on exposure to high glucose in either ganglia. However, there was a subtle difference between the ganglia. The fluorescence lifetime (T1) for the unbound form of NAD(P)H tended to be higher in the CG/SMG than the SCG and this was significant 30 mins after exposure to high glucose, the stage when NAD(P)H levels were increased in the CG/SMG. These results demonstrate that it is feasible to study NAD(P)H metabolism in living sympathetic neurons using two photon microscopy with FLIM but provided no evidence for the activation of NAD(P)H oxidase or mitochondrial dysfunction leading to oxidative stress and apoptosis that has been reported in embryonic SCG or DRG neurons in response to high glucose (Russell & Feldman, 1999;Vincent et al., 2005a).

This is in line with a study of adult DRG neurons *in vitro* where exposure to high glucose had no effect on mitochondrial membrane potential (Huang et al., 2003). It should be noted that these findings do not exclude the possibility that NAD(P)H metabolism is altered in diabetes *in vivo* or that changes occur in the axons rather than the neuronal cell soma. Altered mitochondrial membrane potential (measured *in vitro*) has been reported in DRG isolated from STZ-diabetic rats and high glucose causes oxidative stress selectively in neurites growing *in vitro* from DRG isolated from diabetic but not control rats (Huang et al., 2003;Zherebitskaya et al., 2009). In the present study, it was observed that NAD(P)H fluorescence lifetimes differed depending on whether the NAD(P)H was present in the cell soma or the neuropil and measurements were only made on the cell soma.

5.5 Conclusions

One of the demands of an appropriate *in vitro* model is that it should closely mimic the *in vivo* setting. A major contribution of this thesis was the development of an *in vitro* model that mimics the response of myenteric neurons to diabetes *in vivo* replicating the pattern of changes that occur in terms of susceptibility and resistance of individual populations of myenteric neurons. It provided a tool to elucidate mechanisms of pathogenesis by examining diabetic stimuli that mimic hyperglycemia, carbonyl stress, AGEs and oxidative stress. It provided evidence that oxidative stress is a common factor unifying various pathways through which the peptide/enzyme changes occur in myenteric plexus *in vivo*. However, the pathways leading to oxidative stress do

not appear to be the same for all subpopulations of myenteric neurons. A population of nNOS-containing neurons that do not express VIP may be particularly vulnerable to pathways involving AGE resulting in decreased nNOS expression. In contrast, high glucose and carbonyl stress may induce increased expression of VIP in a separate population of neurons that also contain nNOS. It was also demonstrated that this model can be used to screen potential therapeutic agents for their ability to prevent changes induced by the different diabetic stimuli. From these experiments it was possible to show that an agent with anti-oxidant properties was able to prevent induced changes whatever the stimulus. In addition, the study of thiamine which inhibited the effect of carbonyl stress but not oxidative stress provided evidence that the effect of high glucose on VIP-containing neurons did not occur via the production of carbonyl species.

Finally, the dynamics of the changes that short term exposure to high glucose elicits in living normal adult sympathetic neurons were studied for the first time. This was made possible by multiphoton FLIM using the NAD(P)H autofluorescence intensity and lifetimes as a marker of altered metabolism. Although no evidence was found for sustained effects of glucose on mitochondrial function, this study has established the feasibility of using this approach for investigating NAD(P)H metabolism following chronic exposure to high glucose and for comparing the effects in different sympathetic ganglia or between the cell soma and axons.

5.6 Future work

The observations of the studies in this thesis suggest a number of areas that merit future investigation. In the case of the *in vitro* model of myenteric plexus adherent to muscularis externa it would be possible to examine whether the accumulation of VIP on exposure to high glucose is due to a failure of release as has been demonstrated in STZ-diabetes *in vivo* (Belai et al., 1987). Colocalization studies of RAGE or glyoxalase I in specific subpopulations of myenteric neurons could determine whether their presence or absence may contribute to selective vulnerability to AGEs or carbonyl stress. Additional stimuli could be investigated for their ability to mimic the diabetic environment. For example, it has been previously reported that oxidised LDLs can directly affect adult sensory neurons in culture and induce neuropathy in mice (Vincent et al., 2009). It would be interesting to investigate whether dyslipidemia can also affect myenteric or sympathetic neurons. This would be of particular significance to type 2 diabetes since it has been demonstrated dyslipidemia is a risk factor for diabetic neuropathy and may explain why strict glucose control is not sufficient for the prevention of diabetic complications in type 2 diabetic patients (Vincent et al., 2009). Additional agents could be screened for their ability to prevent diabetes-induced changes prior to *in vivo* studies and to provide further information on the mechanisms involved in such changes. For example, pyridoxamine (vitamin B6) has been shown to react with intermediates involved in the formation of both glyoxidation and lipoxidation endproducts (Onorato et al., 2000). The role of the polyol pathway in diabetes-induced changes could be examined with the use of aldose reductase and sorbitol dehydrogenase inhibitors. Furthermore, the model could readily be adapted to investigate whether

therapeutic agents are able to reverse diabetes-induced changes by adding them to the culture medium after the preparations have been exposed to diabetic stimuli.

Finally, the new technologies of multiphoton FLIM generally offer a wide range of new opportunities for cell biology. In this thesis, the characterisation of short-term changes in the cell bodies of living sympathetic neurons after exposure to high glucose was only the beginning. The same protocol could be used to investigate SCG and CG/SMG explants from STZ-diabetic rats to examine the effects of chronic exposure to hyperglycaemia on NAD(P)H metabolism. Analysis could be done in conjunction with the use of fluorescent markers for mitochondria, calcium and ROS. Explants could be adapted to include the nerve trunks exiting from the ganglia. This would enable a comparison to be made of the effect of high glucose (or other diabetic stimuli) on the neuronal cell soma and the axons. In the present study the presence of axons in individual ganglionic explants was not sufficiently consistent to allow reliable quantitation. Finally, this approach could be used to investigate a recent controversy that has arisen concerning the precise source of ROS in diabetes. Most of the studies to date have assumed that ROS are produced by excessive flux through the electron transport chain (see Hinder et al., 2012 for review). However, a recent study involving proteomic analysis of mitochondria and assessing mitochondrial function has proposed that this is not the case, since respiration was reduced in DRG from diabetic rats despite the fact that ROS were evident in their axons. It was suggested that NADPH oxidase could provide an alternative source of ROS in the axon (Akude et al., 2011). NADPH oxidase is present in both sympathetic and sensory axons (Cao et al., 2009). FLIM analysis could be used to determine if additional fluorescent species involving NAD(P)H are present in the axon on exposure to high glucose.

Appendix 1

Details of the contents of solutions used in chapters 2 & 3

<u>M199 serum free medium 100 ml</u>

10 ml 10x medium 199 (Sigma, Poole, UK)

1 ml 20 mM glutamine (Sigma, Poole, UK)

1 ml penicillin-streptomycin solution (containing 10'000u penicillin and 10mg/ml

streptomycin, from Sigma, Poole, UK)

1 ml 20mM Hepes buffer (Sigma, Poole, UK)

1.5 ml 7.5% Sodium Hydrogen Carbonate solution (VWR, Lutterworth, UK)

1 ml N1 supplement [1]

1 ml 1M glucose[2]

Plus one of the following experimental stimuli and/or treatments: -

- 10 ml of 1 mM D L-6,8- Thioctic acid (α-lipoic acid, from Sigma, Poole, UK) [3]

- 2.5 ml of 10 mg/ml AGE-conjugated BSA (Biovision, Mountain View, CA) to

  give a final concentration of 250 μg/ml of AGE-BSA[4]

- 10 μl of 1 mM menadione sodium bisulfite (Sigma, Poole, UK) to give 1μM

  concentration of menadione for oxidative stress experiment.

- 5 μl, 50 μl, 250 μl, 500 μl, 2,500 μl of methylglyoxal solution (1.17g/ml, Sigma,

  Poole, UK) to give 1 μM, 10 μM, 50 μM, 100 μM, 500 μM concentrations

  respectively of methylglyoxal for carbonyl stress experiment.

- 100 μl or 500 μl of 1 mM aminoguanidine (Sigma, Poole, UK) to give 100 μM or

  500 μM concentrations respectively of aminoguanidine.

- 100 μl of 1 mM thiamine pyrophosphate (Sigma, Poole, UK) to give a 100 μM final concentration of thiamine pyrophosphate.

- 100 μl of 1 mM nicotinamide (Sigma, Poole, UK) to give a 100 μM final concentration of nicotinamide.

And made up to 100 ml with sterile distilled water.

[1] N1 Supplement 50 ml

Putrescine 2 ml (40 mg/ml)

Tri-iodothryonine 170 μl (10mg/ml)

L-Thyroxine 5 ml (400 mg/ml)

Progesterone 300 μl (1 mg/ml in ETOH)

Bovine Serum Albumin Pathocyte 4 (Miles Laboratories, Inc., Elkhart, Ind) 17.5 ml

Sodium Selenite 3.75 ml (0.5 mg/ml)

[2] for 10 mM glucose solution.

For 30 mM: 3 ml 1M glucose (VWR, Lutterworth, Leistershire, UK)

[3] α-lipoic acid was initially dissolved at 0.5 M in dimethylsulfoxide (DMSO), then diluted to 1 mM in M199 medium. In order to counteract the possible pro-oxidant effect of dissolving reagent preincubated for 30 minutes in the dark at 37°C with 1000u/ml of lyophilised catalase (Sigma, Poole, UK), after Vincent et al. (Vincent et al, 2005a).

Control experiments for α-lipoic acid study included in addition to the standard control and experimental groups: incubation with DMSO with and without BSA-AGE, methylglyoxal.

[4]In AGE experiments, BSA (without conjugated AGE) was added to control media to give a concentration of 250 μg/ml, equivalent to the concentration of AGE-BSA in experimental media (over and above the BSA already in the media as standard).

Dissecting Buffer 100 ml

10 ml 10x HBSS (Sigma, Poole, UK)

1 ml penicillin-streptomycin solution (as above)

1 ml 1M glucose (Sigma, Poole, UK)

1 ml 7.5% Sodium hydrogen Carbonate (VWR, Leicester, UK)

Antibiotic wash 100 ml

10 ml 10x HBSS (as above)

1 ml penicillin-streptomycin solution (as above)

0.5ml of 10mg/ml gentamicin solution (Sigma, Poole, UK)

0.5 ml of 5mg/ml metrodiazole (Sigma, Poole, UK)

1 ml of 7.5% Sodium hydrogen Carbonate (as above)

Appendix 2

Publication arising from this thesis

- Voukali, E.;Shotton, H R;Lincoln, J., 2011, Selective responses of myenteric neurons to oxidative stress diabetic stimuli, *Neurogastroenterol. Motil.,* 23, (10) 964-e411.

References

Abbas, Z.G. & Swai, A.B. 1997. Evaluation of the efficacy of thiamine and pyridoxine in the treatment of symptomatic diabetic peripheral neuropathy. *East Afr.Med.J.*, 74, (12) 803-808.

Abdel-Rahman, E. & Bolton, W.K. 2002. Pimagedine: a novel therapy for diabetic nephropathy. *Expert.Opin.Investig.Drugs*, 11, (4) 565-574.

Abordo, E.A., Minhas, H.S., & Thornalley, P.J. 1999. Accumulation of alpha-oxoaldehydes during oxidative stress: a role in cytotoxicity. *Biochem. Pharmacol.*, 58, (4) 641-648.

Adeghate, E., Ponery, A.S., Sharma, A.K., El-Sharkawy, T., & Donath, T. 2001. Diabetes mellitus is associated with a decrease in vasoactive intestinal polypeptide content of gastrointestinal tract of rat. *Arch.Physiol. Biochem.*, 109, (3) 246-251.

Adeghate, E., al-Ramadi, B., Saleh, A.M., Vijayarasathy, C., Ponery, A.S., Arafat, K., Howarth, F.C., & El-Sharkawy, T. 2003. Increase in neuronal nitric oxide synthase content of the gastroduodenal tract of diabetic rats. *Cell Mol.Life Sci.*, 60, (6) 1172-1179.

Ahmed, N. & Thornalley, P.J. 2007. Advanced glycation endproducts: what is their relevance to diabetic complications? *Diabetes Obes.Metab.*, 9, (3) 233-245.

Akude, E., Zherebitskaya, E., Chowdhury, S.K., Smith, D.R., Dobrowsky, R.T., & Fernyhough, P. 2011. Diminished superoxide generation is associated with respiratory chain dysfunction and changes in the mitochondrial proteome of sensory neurons from diabetic rats. *Diabetes*, 60, (1) 288-297.

Alexianu, M.E., Ho, B.K., Mohamed, A.H., La, B., V, Smith, R.G., & Appel, S.H. 1994. The role of calcium-binding proteins in selective motoneuron vulnerability in amyotrophic lateral sclerosis. *Ann.Neurol.*, 36, (6) 846-858.

Anitha, M., Gondha, C., Sutliff, R., Parsadanian, A., Mwangi, S., Sitaraman, S.V., & Srinivasan, S. 2006. GDNF rescues hyperglycemia-induced diabetic enteric neuropathy through activation of the PI3K/Akt pathway. *J.Clin.Invest.*, 116, (2) 344-356.

Apfel, S.C. 2002. Nerve growth factor for the treatment of diabetic neuropathy: what went wrong, what went right, and what does the future hold? *Int.Rev.Neurobiol.*, 50, 393-413.

Arciszewski, M.B. & Ekblad, E. 2005. Effects of vasoactive intestinal peptide and galanin on survival of cultured porcine myenteric neurons. *Regul.Pept.*, 125, (1-3) 185-192.

Ascher, E., Gade, P.V., Hingorani, A., Puthukkeril, S., Kallakuri, S., Scheinman, M., & Jacob, T. 2001. Thiamine reverses hyperglycemia-induced dysfunction in cultured endothelial cells. *Surgery*, 130, (5) 851-858.

Azal, O., Yonem, A., Guler, S., Cakir, B., Baydar, A., Corakci, A., & Kutlu, M. 2002. Effects of aminoguanidine and tolrestat on the development of ocular and renal structural changes in experimental diabetic rats. *Diabetes Obes.Metab.*, 4, (1) 75-79.

Ba, A. 2008. Metabolic and structural role of thiamine in nervous tissues. *Cell Mol.Neurobiol.*, 28, (7) 923-931.

Babaei-Jadidi, R., Karachalias, N., Ahmed, N., Battah, S., & Thornalley, P.J. 2003. Prevention of incipient diabetic nephropathy by high-dose thiamine and benfotiamine. *Diabetes*, 52, (8) 2110-2120.

Babaei-Jadidi, R., Karachalias, N., Kupich, C., Ahmed, N., & Thornalley, P.J. 2004. High-dose thiamine therapy counters dyslipidaemia in streptozotocin-induced diabetic rats. *Diabetologia*, 47, (12) 2235-2246.

Baimbridge, K.G., Celio, M.R., & Rogers, J.H. 1992. Calcium-binding proteins in the nervous system. *Trends Neurosci.*, 15, (8) 303-308.

Balaji, J., Reddy, C.S., Kaushalya, S.K., & Maiti, S. 2004. Microfluorometric detection of catecholamines with multiphoton-excited fluorescence. *Appl.Opt.*, 43, (12) 2412-2417.

Bansal, V., Kalita, J., & Misra, U.K. 2006. Diabetic neuropathy. *Postgrad.Med.J.*, 82, (964) 95-100.

Bastiaens, P.I. & Squire, A. 1999. Fluorescence lifetime imaging microscopy: spatial resolution of biochemical processes in the cell. *Trends Cell Biol.*, 9, (2) 48-52.

Baynes, J.W. & Thorpe, S.R. 1999. Role of oxidative stress in diabetic complications: a new perspective on an old paradigm. *Diabetes*, 48, (1) 1-9.

Becker, D.L., Webb, K.F., Thrasivoulou, C., Lin, C.C., Nadershahi, R., Tsakiri, N., & Cook, J.E. 2007a. Multiphoton imaging of chick retinal development in relation to gap junctional communication. *J.Physiol.*, 585, (Pt 3) 711-719.

Becker, W., Bergmann, A., & Biskup, C. 2007b. Multispectral fluorescence lifetime imaging by TCSPC. *Microsc.Res.Tech.*, 70, (5) 403-409.

Becker, W. 2008. SPCImage 2.9.4. Data Analysis Software for Fluorescence Lifetime Imaging Microscopy. http://www.becker-hickl.de/literature.htm. (info@becker-hickl.com) Ref Type: Internet Communication

Belai, A., Lincoln, J., Milner, P., Crowe, R., Loesch, A., & Burnstock, G. 1985. Enteric nerves in diabetic rats: increase in vasoactive intestinal polypeptide but not substance P. *Gastroenterology*, 89, (5) 967-976.

Belai, A., Lincoln, J., & Burnstock, G. 1987. Lack of release of vasoactive intestinal polypeptide and calcitonin gene-related peptide during electrical stimulation of enteric nerves in streptozotocin-diabetic rats. *Gastroenterology*, 93, (5) 1034-1040.

Belai, A., Lincoln, J., Milner, P., & Burnstock, G. 1988. Progressive changes in adrenergic, serotonergic, and peptidergic nerves in proximal colon of streptozotocin-diabetic rats. *Gastroenterology*, 95, (5) 1234-1241.

Belai, A., Lincoln, J., Milner, P., & Burnstock, G. 1991. Differential effect of streptozotocin-induced diabetes on the innervation of the ileum and distal colon. *Gastroenterology*, 100, (4) 1024-1032.

Belai, A., Facer, P., Bishop, A., Polak, J.M., & Burnstock, G. 1993. Effect of streptozotocin-diabetes on the level of VIP mRNA in myenteric neurones. *Neuroreport*, 4, (3) 291-294.

Belai, A., Calcutt, N.A., Carrington, A.L., Diemel, L.T., Tomlinson, D.R., & Burnstock, G. 1996. Enteric neuropeptides in streptozotocin-diabetic rats; effects of insulin and aldose reductase inhibition. *J.Auton.Nerv.Syst.*, 58, (3) 163-169.

Belai, A., Boulos, P.B., Robson, T., & Burnstock, G. 1997 . Neurochemical coding in the small intestine of patients with Crohn's disease. *Gut*, 40, (6) 767-774.

Beltramo, E., Berrone, E., Tarallo, S., & Porta, M. 2009. Different apoptotic responses of human and bovine pericytes to fluctuating glucose levels and protective role of thiamine. *Diabetes Metab. Res.Rev.*, 25, (6) 566-576.

Benfotiamine.Monograph 2006. Benfotiamine. Monograph. *Altern.Med.Rev.*, 11, (3) 238-242.

Berrone, E., Beltramo, E., Solimine, C., Ape, A.U., & Porta, M. 2006. Regulation of intracellular glucose and polyol pathway by thiamine and benfotiamine in vascular cells cultured in high glucose. *J.Biol.Chem.*, 281, (14) 9307-9313.

Betteridge, D.J. 2000. What is oxidative stress? *Metabolism*, 49, (2 Suppl 1) 3-8.

Bierhaus, A., Chevion, S., Chevion, M., Hofmann, M., Quehenberger, P., Illmer, T., Luther, T., Berentshtein, E., Tritschler, H., Muller, M., Wahl, P., Ziegler, R., &

Nawroth, P.P. 1997. Advanced glycation end product-induced activation of NF-kappaB is suppressed by alpha-lipoic acid in cultured endothelial cells. *Diabetes*, 46, (9) 1481-1490.

Bird, D.K., Yan, L., Vrotsos, K.M., Eliceiri, K.W., Vaughan, E.M., Keely, P.J., White, J.G., & Ramanujam, N. 2005. Metabolic mapping of MCF10A human breast cells via multiphoton fluorescence lifetime imaging of the coenzyme NADH. *Cancer Res.*, 65, (19) 8766-8773.

Birrell, A.M., Heffernan, S.J., Ansselin, A.D., McLennan, S., Church, D.K., Gillin, A.G., & Yue, D.K. 2000. Functional and structural abnormalities in the nerves of type I diabetic baboons: aminoguanidine treatment does not improve nerve function. *Diabetologia*, 43, (1) 110-116.

Blinova, K., Carroll, S., Bose, S., Smirnov, A.V., Harvey, J.J., Knutson, J.R., & Balaban, R.S. 2005. Distribution of mitochondrial NADH fluorescence lifetimes: steady-state kinetics of matrix NADH interactions. *Biochemistry*, 44, (7) 2585-2594.

Blinova, K. 2008. Mitochondrial NADH fluorescence is enhanced by complex I binding. *Biochemistry*, 47, (36) 9636-9645.

Bolognani, F. & Perrone-Bizzozero, N.I. 2008. RNA-protein interactions and control of mRNA stability in neurons. *J.Neurosci.Res.*, 86, (3) 481-489.

Botchway, S.W., Parker, A.W., Bisby, R.H., & Crisostomo, A.G. 2008. Real-time cellular uptake of serotonin using fluorescence lifetime imaging with two-photon excitation. *Microsc.Res.Tech.*, 71, (4) 267-273.

Boulton, A.J., Gries, F.A., & Jervell, J.A. 1998. Guidelines for the diagnosis and outpatient management of diabetic peripheral neuropathy. *Diabet.Med.*, 15, (6) 508-514.

Boulton, A.J., Vinik, A.I., Arezzo, J.C., Bril, V., Feldman, E.L., Freeman, R., Malik, R.A., Maser, R.E., Sosenko, J.M., & Ziegler, D. 2005. Diabetic neuropathies: a statement by the American Diabetes Association. *Diabetes Care*, 28, (4) 956-962.

Brennan, A.M., Connor, J.A., & Shuttleworth, C.W. 2006. NAD(P)H fluorescence transients after synaptic activity in brain slices: predominant role of mitochondrial function. *J.Cereb.Blood Flow Metab.*, 26, (11) 1389-1406.

Brennan, A.M., Connor, J.A., & Shuttleworth, C.W. 2007. Modulation of the amplitude of NAD(P)H fluorescence transients after synaptic stimulation. *J.Neurosci.Res.*, 85, (15) 3233-3243.

Brennan, A.M., Suh, S.W., Won, S.J., Narasimhan, P., Kauppinen, T.M., Lee, H., Edling, Y., Chan, P.H., & Swanson, R.A. 2009. NADPH oxidase is the primary source of superoxide induced by NMDA receptor activation. *Nat.Neurosci.*, 12, (7) 857-863.

Briere, J.J., Schlemmer, D., Chretien, D., & Rustin, P. 2004. Quinone analogues regulate mitochondrial substrate competitive oxidation. *Biochem. Biophys. Res. Commun.*, 316, (4) 1138-1142.

Britland,S.T., Young,R.J., Sharma,A.K., Lee,D., Ah-See,A.K., Clarke,B.F. 1990. Vagus nerve morphology in diabetic gastropathy. *Diabet. Med*. 7, (9), 780-787.

Brownlee, M., Vlassara, H., Kooney, A., Ulrich, P., & Cerami, A. 1986. Aminoguanidine prevents diabetes-induced arterial wall protein cross-linking. *Science*, 232, (4758) 1629-1632.

Brownlee, M. 2001. Biochemistry and molecular cell biology of diabetic complications. *Nature*, 414, (6865) 813-820.

Buchan, A.M. & Baimbridge, K.G. 1988. Distribution and co-localization of calbindin D28k with VIP and neuropeptide Y but not somatostatin, galanin and substance P in the enteric nervous system of the rat. *Peptides*, 9, (2) 333-338.

Burnstock, G. 1976. Do some nerve cells release more than one transmitter? *Neuroscience*, 1, (4) 239-248.

Burnstock, G. 2004. Cotransmission. *Curr.Opin.Pharmacol.*, 4, (1) 47-52.

Buttow, N.C., Miranda Neto, M.H., & Bazotte, R.B. 1997. Morphological and quantitative study of the myenteric plexus of the duodenum of streptozotocin-induced diabetic rats. *Arq Gastroenterol.*, 34, (1) 34-42.

Bytzer, P., Talley, N.J., Leemon, M., Young, L.J., Jones, M.P., & Horowitz, M. 2001. Prevalence of gastrointestinal symptoms associated with diabetes mellitus: a population-based survey of 15,000 adults. *Arch.Intern.Med.*, 161, (16) 1989-1996.

Cameron, N.E., Cotter, M.A., Dines, K., & Love, A. 1992. Effects of aminoguanidine on peripheral nerve function and polyol pathway metabolites in streptozotocin-diabetic rats. *Diabetologia*, 35, (10) 946-950.

Cameron, N.E. & Cotter, M.A. 1996. Rapid reversal by aminoguanidine of the neurovascular effects of diabetes in rats: modulation by nitric oxide synthase inhibition. *Metabolism*, 45, (9) 1147-1152.

Cameron, N.E., Cotter, M.A., Horrobin, D.H., & Tritschler, H.J. 1998. Effects of alpha-lipoic acid on neurovascular function in diabetic rats: interaction with essential fatty acids. *Diabetologia*, 41, (4) 390-399.

Cameron, N.E., Eaton, S.E., Cotter, M.A., & Tesfaye, S. 2001. Vascular factors and metabolic interactions in the pathogenesis of diabetic neuropathy. *Diabetologia*, 44, (11) 1973-1988.

Cameron, N.E., Gibson, T.M., Nangle, M.R., & Cotter, M.A. 2005. Inhibitors of advanced glycation end product formation and neurovascular dysfunction in experimental diabetes. *Ann.N.Y.Acad.Sci.*, 1043, 784-792.

Camilleri, M. & Malagelada, J.R. 1984. Abnormal intestinal motility in diabetics with the gastroparesis syndrome. *Eur.J.Clin.Invest*, 14, (6) 420-427.

Camilleri, M. 1996. Gastrointestinal problems in diabetes. *Endocrinol.Metab Clin.North Am.*, 25, (2) 361-378.

Campbell, P.L. & Smith, A.D. 2000. Biochemistry Illustrated, 4 ed. London, Churchill Livingstone, pp 120-130.

Cao, X., Demel, S.L., Quinn, M.T., Galligan, J.J., & Kreulen, D. 2009. Localization of NADPH oxidase in sympathetic and sensory ganglion neurons and perivascular nerve fibers. *Auton.Neurosci.*, 151, (2) 90-97.

Carroll, S.L., Byer, S.J., Dorsey, D.A., Watson, M.A., & Schmidt, R.E. 2004. Ganglion-specific patterns of diabetes-modulated gene expression are established in prevertebral and paravertebral sympathetic ganglia prior to the development of neuroaxonal dystrophy. *J.Neuropathol.Exp.Neurol.*, 63, (11) 1144-1154.

Cavanagh, J.B. 1979. The 'dying back' process. A common denominator in many naturally occurring and toxic neuropathies. *Arch.Pathol.Lab Med.*, 103, (13) 659-664.

Cellek, S., Foxwell, N.A., & Moncada, S. 2003. Two phases of nitrergic neuropathy in streptozotocin-induced diabetic rats. *Diabetes*, 52, (9) 2353-2362.

Cellek, S., Qu, W., Schmidt, A.M., & Moncada, S. 2004. Synergistic action of advanced glycation end products and endogenous nitric oxide leads to neuronal apoptosis in vitro: a new insight into selective nitrergic neuropathy in diabetes. *Diabetologia*, 47, (2) 331-339.

Chance, B. & Baltscheffsky, H. 1958. Respiratory enzymes in oxidative phosphorylation. VII. Binding of intramitochondrial reduced pyridine nucleotide. *J.Biol.Chem.*, 233, (3) 736-739.

Chance, B. & Thorell, B. 1959. Localization and kinetics of reduced pyridine nucleotide in living cells by microfluorometry. *J.Biol.Chem.*, 234, 3044-3050.

Chance, B. & Hollunger, G. 1960. Energy-linked reduction of mitochondrial pyridine nucleotide. *Nature*, 185, 666-672.

Chance, B., Cohen, P., Jobsis, F., & Schoener, B. 1962. Intracellular oxidation-reduction states in vivo. *Science*, 137, (3529) 499-508.

Chandrasekharan, B. & Srinivasan, S. 2007. Diabetes and the enteric nervous system. *Neurogastroenterol.Motil.*, 19, (12) 951-960.

Chandrasekharan, B., Anitha, M., Blatt, R., Shahnavaz, N., Kooby, D., Staley, C., Mwangi, S., Jones, D.P., Sitaraman, S.V., & Srinivasan, S. 2011. Colonic motor dysfunction in human diabetes is associated with enteric neuronal loss and increased oxidative stress. *Neurogastroenterol.Motil.*, 23, (2), 131-8, e26.

Chau, Y.P. & Lu, K.S. 1995. Investigation of the blood-ganglion barrier properties in rat sympathetic ganglia by using lanthanum ion and horseradish peroxidase as tracers. *Acta Anat.(Basel)*, 153, (2) 135-144.

Chen, H., Charlat, O., Tartaglia, L.A., Woolf, E.A., Weng, X., Ellis, S.J., Lakey, N.D., Culpepper, J., Moore, K.J., Breitbart, R.E., Duyk, G.M., Tepper, R.I., & Morgenstern, J.P. 1996. Evidence that the diabetes gene encodes the leptin receptor: identification of a mutation in the leptin receptor gene in db/db mice. *Cell*, 84, (3) 491-495.

Cheng, C. & Zochodne, D.W. 2003. Sensory neurons with activated caspase-3 survive long-term experimental diabetes. *Diabetes*, 52, (9) 2363-2371.

Chia, T.H., Williamson, A., Spencer, D.D., & Levene, M.J. 2008. Multiphoton fluorescence lifetime imaging of intrinsic fluorescence in human and rat brain tissue reveals spatially distinct NADH binding. *Opt.Express*, 16, (6) 4237-4249.

Chiou, T.J., Chu, S.T., & Tzeng, W.F. 2003. Protection of cells from menadione-induced apoptosis by inhibition of lipid peroxidation. *Toxicology*, 191, (2-3) 77-88.

Chowdhury, S.K., Smith, D.R., & Fernyhough, P. 2012. The role of aberrant mitochondrial bioenergetics in diabetic neuropathy. *Neurobiol.Dis.*(Epub ahead of print).

Cicchi, R. & Pavone, F.S. 2011. Non-linear fluorescence lifetime imaging of biological tissues. *Anal.Bioanal.Chem.*, 400, (9) 2687-2697.

Colucci, M., Cervio, M., Faniglione, M., De Angelis, S., Pajoro, M., Levandis, G., Tassorelli, C., Blandini, F., Feletti, F., De Giorgio, R., Dellabianca, A., Tonini, S., Tonini, M. 2012. Intestinal dysmotility and enteric neurochemical changes in a Parkinson's disease rat model. *Auton Neurosci*, 169(2) 77-86.

Costa, M., Furness, J.B., Pompolo, S., Brookes, S.J.H., Bornstein, J.C., Bredt, D.S., Snyder, S.H.1992. Projections and chemical coding of neurons with immunoreactivity for nitric oxide synthase in the guinea-pig small intestine. *Neurosci Lett*, 148:121–125.

Coppey, L.J., Gellett, J.S., Davidson, E.P., Dunlap, J.A., Lund, D.D., & Yorek, M.A. 2001. Effect of antioxidant treatment of streptozotocin-induced diabetic rats on endoneurial blood flow, motor nerve conduction velocity, and vascular reactivity of epineurial arterioles of the sciatic nerve. *Diabetes*, 50, (8) 1927-1937.

De Mello, S.T., De Miranda Neto, M.H., Zanoni, J.N., & Furlan, M.M. 2009. Effects of insulin treatment on HuC/HuD, NADH diaphorase, and nNOS-positive myenteric neurons of the duodenum of adult rats with acute diabetes. *Dig.Dis.Sci.*, 54, (4) 731-737.

DeAngelis, K., Irigoyen, M.C., & Morris, M. 2009. Diabetes and cardiovascular autonomic dysfunction: application of animal models. *Auton.Neurosci.*, 145, (1-2) 3-10.

Decktor, D.L., Weems, W.A. 1981. A study of renal-efferent neurones and their neural connexions within cat renal ganglia using intracellular electrodes. *J Physiol*, 321, 611-626.

Denes, V. & Gabriel, R. 2004. Calbindin-immunopositive cells are cholinergic interneurons in the myenteric plexus of rabbit ileum. *Cell Tissue Res.*, 318, (2) 465-472.

Denk, W., Strickler, J.H., & Webb, W.W. 1990. Two-photon laser scanning fluorescence microscopy. *Science*, 248, (4951) 73-76.

Dewhurst, M., Omawari, N., & Tomlinson, D.R. 1997. Aminoguanidine--effects on endoneurial vasoactive nitric oxide and on motor nerve conduction velocity in control and streptozotocin-diabetic rats. *Br.J.Pharmacol.*, 120, (4) 593-598.

Dhar, A., Dhar, I., Desai, K.M., & Wu, L. 2010. Methylglyoxal scavengers attenuate endothelial dysfunction induced by methylglyoxal and high concentrations of glucose. Br.J.Pharmacol., 161, (8) 1843-1856.

Domoto, T., Gonda, T., Oki, M., & Yanaihara, N. 1984. Coexistence of substance P- and methionine5-enkephalin-like immunoreactivity in nerve cells of the myenteric ganglia in the cat ileum. *Neurosci.Lett.*, 47, (1) 9-13.

Du, X.L., Edelstein, D., Dimmeler, S., Ju, Q., Sui, C., & Brownlee, M. 2001. Hyperglycemia inhibits endothelial nitric oxide synthase activity by posttranslational modification at the Akt site. *J.Clin.Invest*, 108, (9) 1341-1348.

Duran-Jimenez, B., Dobler, D., Moffatt, S., Rabbani, N., Streuli, C.H., Thornalley, P.J., Tomlinson, D.R., & Gardiner, N.J. 2009. Advanced glycation end products in extracellular matrix proteins contribute to the failure of sensory nerve regeneration in diabetes. *Diabetes*, 58, (12) 2893-2903.

Eichberg, J. 2002. Protein kinase C changes in diabetes: is the concept relevant to neuropathy? *Int.Rev.Neurobiol.*, 50, 61-82.

Ekblad, E., Mulder, H., & Sundler, F. 1996. Vasoactive intestinal peptide expression in enteric neurons is upregulated by both colchicine and axotomy. *Regul.Pept.*, 63, (2-3) 113-121.

Ekblad, E., Sjuve, R., Arner, A., & Sundler, F. 1998. Enteric neuronal plasticity and a reduced number of interstitial cells of Cajal in hypertrophic rat ileum. *Gut*, 42, (6) 836-844.

El-Salhy, M. 1998. Neuroendocrine peptides of the gastrointestinal tract of an animal model of human type 2 diabetes mellitus. *Acta Diabetol.*, 35, (4) 194-198.

El-Salhy, M. 2001. Gastrointestinal transit in nonobese diabetic mouse: an animal model of human diabetes type 1. *J.Diabetes Complications*, 15, (5) 277-284.

Eng, J., Lynch, R.M., & Balaban, R.S. 1989. Nicotinamide adenine dinucleotide fluorescence spectroscopy and imaging of isolated cardiac myocytes. *Biophys.J.*, 55, (4) 621-630.

Evans, N.D., Gnudi, L., Rolinski, O.J., Birch, D.J., & Pickup, J.C. 2005. Glucose-dependent changes in NAD(P)H-related fluorescence lifetime of adipocytes and fibroblasts in vitro: potential for non-invasive glucose sensing in diabetes mellitus. *J.Photochem.Photobiol.B*, 80, (2) 122-129.

Feigenbaum, K. 2006. Update on gastroparesis. *Gastroenterol.Nurs.*, 29, (3) 239-244.

Feldman, M. & Schiller, L.R. 1983. Disorders of gastrointestinal motility associated with diabetes mellitus. *Ann.Intern.Med.*, 98, (3) 378-384.

Feldman, E.L. 2003. Oxidative stress and diabetic neuropathy: a new understanding of an old problem. *J.Clin.Invest*, 111, (4) 431-433.

Fernyhough, P. & Calcutt, N.A. 2010. Abnormal calcium homeostasis in peripheral neuropathies. *Cell Calcium*, 47, (2) 130-139.

Figueroa-Romero, C., Sadidi, M., & Feldman, E.L. 2008. Mechanisms of disease: the oxidative stress theory of diabetic neuropathy. *Rev.Endocr.Metab Disord.*, 9, (4) 301-314.

Fine, A., Amos, W.B., Durbin, R.M., & McNaughton, P.A. 1988. Confocal microscopy: applications in neurobiology. *Trends Neurosci.*, 11, (8) 346-351.

Freedman, B.I., Wuerth, J.P., Cartwright, K., Bain, R.P., Dippe, S., Hershon, K., Mooradian, A.D., & Spinowitz, B.S. 1999. Design and baseline characteristics for the aminoguanidine Clinical Trial in Overt Type 2 Diabetic Nephropathy (ACTION II). *Control Clin.Trials*, 20, (5) 493-510.

French, T., So, P.T., Dong, C.Y., Berland, K.M., & Gratton, E. 1998. Fluorescence lifetime imaging techniques for microscopy. *Methods Cell Biol.*, 56, 277-304.

Furness, J.B. 2000. Types of neurons in the enteric nervous system. *J.Auton.Nerv.Syst.*, 81, (1-3) 87-96.

Furness, J.B. 2005. The Enteric Nervous System, 2006 ed. Oxford, UK, Willey-Blackwell, pp 3-21.

Gadella, B.M., van Haeften, T., van Bavel, K., and Valentijn, J.A. 2012. Multi-photon excitation microscopy for advanced biomedical imaging. www.vetcite.org/publish/articles/000040/print.html Ref Type: Internet Communication

Gale, E.A., Bingley, P.J., Emmett, C.L., & Collier, T. 2004. European Nicotinamide Diabetes Intervention Trial (ENDIT): a randomised controlled trial of intervention before the onset of type 1 diabetes. *Lancet*, 363, (9413) 925-931.

Gebhart, G.F. 2000. Visceral pain-peripheral sensitisation. *Gut*, 47 Suppl 4, iv54-iv55.

Gerasimenko, J.V., Gerasimenko, O.V., Palejwala, A., Tepikin, A.V., Petersen, O.H., & Watson, A.J. 2002. Menadione-induced apoptosis: roles of cytosolic Ca(2+) elevations and the mitochondrial permeability transition pore. *J.Cell Sci.*, 115, (Pt 3) 485-497.

Giardino, I., Fard, A.K., Hatchell, D.L., & Brownlee, M. 1998. Aminoguanidine inhibits reactive oxygen species formation, lipid peroxidation, and oxidant-induced apoptosis. *Diabetes*, 47, (7) 1114-1120.

Gibson, T.M., Cotter, M.A., & Cameron, N.E. 2006. Effects of poly(ADP-ribose) polymerase inhibition on dysfunction of non-adrenergic non-cholinergic neurotransmission in gastric fundus in diabetic rats. *Nitric.Oxide.*, 15, (4) 344-350.

Goyal, R.K. & Hirano, I. 1996. The enteric nervous system. *N.Engl.J.Med.*, 334, (17) 1106-1115.

Greene, D.A., Stevens, M.J., & Feldman, E.L. 1999. Diabetic neuropathy: scope of the syndrome. *Am.J.Med.*, 107, (2B) 2S-8S.

Gumy, L.F., Bampton, E.T., & Tolkovsky, A.M. 2008. Hyperglycaemia inhibits Schwann cell proliferation and migration and restricts regeneration of axons and Schwann cells from adult murine DRG. *Mol.Cell Neurosci.*, 37, (2) 298-311.

Guo, C., Quobatari, A., Shangguan, Y., Hong, S., & Wiley, J.W. 2004. Diabetic autonomic neuropathy: evidence for apoptosis in situ in the rat. *Neurogastroenterol.Motil.*, 16, (3) 335-345.

Hammes, H.P., Du, X., Edelstein, D., Taguchi, T., Matsumura, T., Ju, Q., Lin, J., Bierhaus, A., Nawroth, P., Hannak, D., Neumaier, M., Bergfeld, R., Giardino, I., & Brownlee, M. 2003. Benfotiamine blocks three major pathways of hyperglycemic damage and prevents experimental diabetic retinopathy. *Nat.Med.*, 9, (3) 294-299.

Han, D. 1997, Lipoic acid increases de novo synthesis of cellular glutathione by improving cystine utilization. *Biofactors*, 6, (3) 321-338.

Hansen, M.B. 2003a. Neurohumoral control of gastrointestinal motility. *Physiol Res.*, 52, (1) 1-30.

Hansen, M.B. 2003b. The enteric nervous system I: organisation and classification. *Pharmacol.Toxicol.*, 92, (3) 105-113.

Hansen, M.B. 2003c. The enteric nervous system II: gastrointestinal functions. *Pharmacol.Toxicol.*, 92, (6) 249-257.

Hattangady, N.G. & Rajadhyaksha, M.S. 2009. A brief review of in vitro models of diabetic neuropathy. *Int.J.Diabetes Dev.Ctries.*, 29, (4) 143-149.

Haupt, E., Ledermann, H., & Kopcke, W. 2005. Benfotiamine in the treatment of diabetic polyneuropathy--a three-week randomized, controlled pilot study (BEDIP study). *Int.J.Clin.Pharmacol.Ther.*, 43, (2) 71-77.

Heizmann, C.W. & Braun, K. 1992. Changes in Ca(2+)-binding proteins in human neurodegenerative disorders. *Trends Neurosci.*, 15, (7) 259-264.

Hinder, L.M., Vincent, A.M., Burant, C.F., Pennathur, S., & Feldman, E.L. 2012. Bioenergetics in diabetic neuropathy: what we need to know. *J.Peripher.Nerv.Syst.*, 17 Suppl 2, 10-14.

Houtkooper, R.H., Canto, C., Wanders, R.J., & Auwerx, J. 2010. The secret life of NAD+: an old metabolite controlling new metabolic signaling pathways. *Endocr.Rev.,* 31, (2) 194-223.

Huang, S., Heikal, A.A., & Webb, W.W. 2002a. Two-photon fluorescence spectroscopy and microscopy of NAD(P)H and flavoprotein. *Biophys.J.*, 82, (5) 2811-2825.

Huang, T.J., Sayers, N.M., Fernyhough, P., & Verkhratsky, A. 2002b. Diabetes-induced alterations in calcium homeostasis in sensory neurones of streptozotocin-diabetic rats are restricted to lumbar ganglia and are prevented by neurotrophin-3. *Diabetologia*, 45, (4) 560-570.

Huang, T.J., Price, S.A., Chilton, L., Calcutt, N.A., Tomlinson, D.R., Verkhratsky, A., & Fernyhough, P. 2003. Insulin prevents depolarization of the mitochondrial inner membrane in sensory neurons of type 1 diabetic rats in the presence of sustained hyperglycemia. *Diabetes*, 52, (8) 2129-2136.

Hugon, J., Hugon, F., Esclaire, F., Lesort, M., & Diop, A.G. 1996. The presence of calbindin in rat cortical neurons protects in vitro from oxidative stress. *Brain Res.*, 707, (2) 288-292.

Iacopino, A., Christakos, S., German, D., Sonsalla, P.K., & Altar, C.A. 1992. Calbindin-D28K-containing neurons in animal models of neurodegeneration: possible protection from excitotoxicity. *Brain Res.Mol.Brain Res.*, 13, (3) 251-261.

Ido, Y. 2007. Pyridine nucleotide redox abnormalities in diabetes. *Antioxid.Redox.Signal.*, 9, (7) 931-942.

Ido, Y., Kilo, C., & Williamson, J.R. 1997. Cytosolic NADH/NAD+, free radicals, and vascular dysfunction in early diabetes mellitus. *Diabetologia*, 40 Suppl 2, S115-S117.

Ilnytska, O., Lyzogubov, V.V., Stevens, M.J., Drel, V.R., Mashtalir, N., Pacher, P., Yorek, M.A., & Obrosova, I.G. 2006. Poly(ADP-ribose) polymerase inhibition alleviates experimental diabetic sensory neuropathy. *Diabetes*, 55, (6) 1686-1694.

Izbeki, F., Wittman, T., Rosztoczy, A., Linke, N., Bodi, N., Fekete, E., & Bagyanszki, M. 2008. Immediate insulin treatment prevents gut motility alterations and loss of nitrergic neurons in the ileum and colon of rats with streptozotocin-induced diabetes. *Diabetes Res.Clin.Pract.*, 80, (2) 192-198.

Jack, M.M., Ryals, J.M., & Wright, D.E. 2011. Characterisation of glyoxalase I in a streptozocin-induced mouse model of diabetes with painful and insensate neuropathy. *Diabetologia*, 54, (8) 2174-2182.

Jacobson, S. & Marcus, E. M. 2008. Neuroanatomy for the Neuroscientist. New York, USA: Springer Science, pp. 183-187.

Janig, W. & McLachlan, E.M. 1992. Specialized functional pathways are the building blocks of the autonomic nervous system. *J.Auton.Nerv.Syst.*, 41, (1-2) 3-13.

Jeyabal, P.V., Kumar, R., Gangula, P.R., Micci, M.A., & Pasricha, P.J. 2008. Inhibitors of advanced glycation end-products prevent loss of enteric neuronal nitric oxide synthase in diabetic rats. *Neurogastroenterol.Motil.*, 20, (3) 253-261.

Jobling, P. & Gibbins, I.L. 1999. Electrophysiological and morphological diversity of mouse sympathetic neurons. *J.Neurophysiol.*, 82, (5) 2747-2764.

Jobsis, F.F., O'Connor, M., Vitale, A., & Vreman, H. 1971. Intracellular redox changes in functioning cerebral cortex. I. Metabolic effects of epileptiform activity. *J.Neurophysiol.*, 34, (5) 735-749.

Kakehi, T. & Yabe-Nishimura, C. 2008. NOX enzymes and diabetic complications. *Semin.Immunopathol.*, 30, (3) 301-314.

Kalapos, M.P. 2008. The tandem of free radicals and methylglyoxal. *Chem.Biol.Interact.*, 171, (3) 251-271.

Kamiya, H., Zhangm, W., & Sima, A.A. 2005. Apoptotic stress is counterbalanced by survival elements preventing programmed cell death of dorsal root ganglions in subacute type 1 diabetic BB/Wor rats. *Diabetes*, 54, (11) 3288-3295.

Kann, O. & Kovacs, R. 2007. Mitochondria and neuronal activity. *Am.J.Physiol Cell Physiol*, 292, (2) C641-C657.

Karachalias, N., Babaei-Jadidi, R., Ahmed, N., & Thornalley, P.J. 2003. Accumulation of fructosyl-lysine and advanced glycation end products in the kidney, retina and peripheral nerve of streptozotocin-induced diabetic rats. *Biochem.Soc.Trans.*, 31, (Pt 6) 1423-1425.

Kasischke, K.A., Vishwasrao, H.D., Fisher, P.J., Zipfel, W.R., & Webb, W.W. 2004. Neural activity triggers neuronal oxidative metabolism followed by astrocytic glycolysis. *Science*, 305, (5680) 99-103.

Kihara, M., Schmelzer, J.D., Poduslo, J.F., Curran, G.L., Nickander, K.K., & Low, P.A. 1991. Aminoguanidine effects on nerve blood flow, vascular permeability, electrophysiology, and oxygen free radicals. *Proc.Natl.Acad.Sci.U.S.A*, 88, (14) 6107-6111.

King, R.H. 2001. The role of glycation in the pathogenesis of diabetic polyneuropathy. *Mol.Pathol.*, 54, (6) 400-408.

Kishi, Y., Schmelzer, J.D., Yao, J.K., Zollman, P.J., Nickander, K.K., Tritschler, H.J., & Low, P.A. 1999. Alpha-lipoic acid: effect on glucose uptake, sorbitol pathway, and energy metabolism in experimental diabetic neuropathy. *Diabetes*, 48, (10) 2045-2051.

Kishi, M., Tanabe, J., Schmelzer, J.D., & Low, P.A. 2002. Morphometry of dorsal root ganglion in chronic experimental diabetic neuropathy. *Diabetes*, 51, (3) 819-824.

Klimaschewski, L. 1997. VIP -- a 'very important peptide' in the sympathetic nervous system? *Anat.Embryol.(Berl)*, 196, (4) 269-277.

Korenaga, K., Micci, M.A., Taglialatela, G., & Pasricha, P.J. 2006. Suppression of nNOS expression in rat enteric neurones by the receptor for advanced glycation end-products. *Neurogastroenterol.Motil.*, 18, (5) 392-400.

Korsak, K., Silva, A.T., & Saffrey, M.J. 2012. Differing effects of NT-3 and GDNF on dissociated enteric ganglion cells exposed to hydrogen peroxide in vitro. *Neurosci.Lett.*, 517, (2) 102-6.

Krebs, H.A. 1967. The redox state of nicotinamide adenine dinucleotide in the cytoplasm and mitochondria of rat liver. *Adv.Enzyme Regul.*, 5, 409-434.

Kumar, S., Dunsby, C., De Beule, P.A., Owen, D.M., Anand, U., Lanigan, P.M., Benninger, R.K., Davis, D.M., Neil, M.A., Anand, P., Benham, C., Naylor, A., & French, P.M. 2007. Multifocal multiphoton excitation and time correlated single photon counting detection for 3-D fluorescence lifetime imaging. *Opt.Express*, 15, (20) 12548-12561.

Kunze, W.A. & Furness, J.B. 1999. The enteric nervous system and regulation of intestinal motility. *Annu.Rev.Physiol*, 61, 117-142.

La, S.M., Beltramo, E., Pagnozzi, F., Bena, E., Molinatti, P.A., Molinatti, G.M., & Porta, M. 1996. Thiamine corrects delayed replication and decreases production of lactate and advanced glycation end-products in bovine retinal and human umbilical vein endothelial cells cultured under high glucose conditions. *Diabetologia*, 39, (11) 1263-1268.

Lakowicz, J.R., Szmacinski, H., Nowaczyk, K., Berndt, K.W., & Johnson, M. 1992a. Fluorescence lifetime imaging. *Anal.Biochem.*, 202, (2) 316-330.

Lakowicz, J.R., Szmacinski, H., Nowaczyk, K., & Johnson, M.L. 1992b. Fluorescence lifetime imaging of free and protein-bound NADH. *Proc.Natl.Acad.Sci.U.S.A*, 89, (4) 1271-1275.

Langley, J.N. 1921. The Autonomic Nervous System. Cambridge University Press, UK, pp 1-94.

Leinninger, G.M., Edwards, J.L., Lipshaw, M.J., & Feldman, E.L. 2006. Mechanisms of disease: mitochondria as new therapeutic targets in diabetic neuropathy. *Nat.Clin.Pract.Neurol.*, 2, (11) 620-628.

Lichtman, J.W. & Conchello, J.A. 2005. Fluorescence microscopy. *Nat.Methods*, 2, (12) 910-919.

Lin, Z., Gao, N., Hu, H.Z., Liu, S., Gao, C., Kim, G., Ren, J., Xia, Y., Peck, O.C., & Wood, J.D. 2002. Immunoreactivity of Hu proteins facilitates identification of myenteric neurones in guinea-pig small intestine. *Neurogastroenterol.Motil.*, 14, (2) 197-204.

Lin, Z., Sandgren, K., & Ekblad, E. 2003. Increased expression of vasoactive intestinal polypeptide in cultured myenteric neurons from adult rat small intestine. *Auton.Neurosci.*, 107, (1) 9-19.

Lin, Z., Sandgren, K., & Ekblad, E. 2004. Increased expression of nitric oxide synthase in cultured neurons from adult rat colonic submucous ganglia. *Auton.Neurosci.*, 114, (1-2) 29-38.

Lincoln,J., Bokor,J.T., Crowe,R., Griffith,S.G., Haven,A.J., Burnstock,G. 1984. Myenteric plexus in streptozotocin-treated rats. Neurochemical and histochemical evidence for diabetic neuropathy in the gut. *Gastroenterology*, 86, (4) 654-661.

Lincoln, J. & Shotton, H.R. 2008. Diabetic autonomic neuropathy. *J.Tzu Chi Med*., 20, 161-168.

Loesch, A., Belai, A., Lincoln, J., & Burnstock, G. 1986. Enteric nerves in diabetic rats: electron microscopic evidence for neuropathy of vasoactive intestinal polypeptide-containing fibres. *Acta Neuropathol.*, 70, (2) 161-168.

Loffelhardt, S., Bonaventura, C., Locher, M., Borbe, H.O., & Bisswanger, H. 1995. Interaction of alpha-lipoic acid enantiomers and homologues with the enzyme components of the mammalian pyruvate dehydrogenase complex. *Biochem.Pharmacol.*, 50, (5) 637-646.

Low, P.A., Nickander, K.K., & Tritschler, H.J. 1997. The roles of oxidative stress and antioxidant treatment in experimental diabetic neuropathy. Diabetes, 46 Suppl 2, S38-S42.

Lukienko, P.I., Mel'nichenko, N.G., Zverinskii, I.V., & Zabrodskaya, S.V. 2000. Antioxidant properties of thiamine. *Bull.Exp.Biol.Med*., 130, (9) 874-876.

Lundgren, O. 2000. Sympathetic input into the enteric nervous system. *Gut*, 47 Suppl 4, iv33-iv35.

Macrae, I.M., Furness, J.B., Costa, M. (1986). Distribution of subgroups of noradrenaline neurons in the coeliac ganglion of the guinea-pig. *Cell Tissue Res*, 244,(1) 173-80.

Mann, P.T., Furness, J.B., & Southwell, B.R. 1999. Choline acetyltransferase immunoreactivity of putative intrinsic primary afferent neurons in the rat ileum. *Cell Tissue Res.*, 297, (2) 241-248.

Martinez-Cuesta, M.A., Massuda, H., Whittle, B.J., & Moncada, S. 1995. Impairment of nitrergic-mediated relaxation of rat isolated duodenum by experimental diabetes. *Br.J.Pharmacol.*, 114, (5) 919-924.

Mattson, M.P., Rychlik, B., Chu, C., & Christakos, S. 1991. Evidence for calcium-reducing and excito-protective roles for the calcium-binding protein calbindin-D28k in cultured hippocampal neurons. *Neuron*, 6, (1) 41-51.

McCormack, A.L., Atienza, J.G., Langston, J.W., & Di Monte, D.A. 2006. Decreased susceptibility to oxidative stress underlies the resistance of specific dopaminergic cell populations to paraquat-induced degeneration. *Neuroscience*, 141, (2) 929-937.

Mearin, F., Camilleri, M., & Malagelada, J.R. 1986. Pyloric dysfunction in diabetics with recurrent nausea and vomiting. *Gastroenterology*, 90, (6) 1919-1925.

Mehta, R., Shangari, N., & O'Brien, P.J. 2008. Preventing cell death induced by carbonyl stress, oxidative stress or mitochondrial toxins with vitamin B anti-AGE agents. *Mol.Nutr.Food Res.*, 52, (3) 379-385.

Melo, S.S., Arantes, M.R., Meirelles, M.S., Jordao, A.A., Jr., & Vannucchi, H. 2000. Lipid peroxidation in nicotinamide-deficient and nicotinamide-supplemented rats with streptozotocin-induced diabetes. *Acta Diabetol.*, 37, (1) 33-39.

Milner, P., Lincoln, J., & Burnstock, G. 1999, "The neurochemical organisation of the autonomic nervous system," *In Handbook of Clinical Neurology. The Autonomic Nervous System. Part 1. Normal Functions*, vol. 74 (30) O.Appenzeller, ed., pp. 87-120.

Miyauchi, Y., Shikama, H., Takasu, T., Okamiya, H., Umeda, M., Hirasaki, E., Ohhata, I., Nakayama, H., & Nakagawa, S. 1996. Slowing of peripheral motor nerve conduction was ameliorated by aminoguanidine in streptozocin-induced diabetic rats. *Eur.J.Endocrinol.*, 134, (4) 467-473.

Nagamatsu, M., Nickander, K.K., Schmelzer, J.D., Raya, A., Wittrock, D.A., Tritschler, H., & Low, P.A. 1995. Lipoic acid improves nerve blood flow, reduces oxidative stress, and improves distal nerve conduction in experimental diabetic neuropathy. *Diabetes Care*, 18, (8) 1160-1167.

Naidoo, V., Dai, X., & Galligan, J.J. 2010. R-type Ca(2+) channels contribute to fast synaptic excitation and action potentials in subsets of myenteric neurons in the guinea pig intestine. *Neurogastroenterol.Motil.*, 22, (12) e353-e363.

Nakama, K., Shichinohe, K., Kobayashi, K., Naito, K., Uchida, O., Yasuhara, K., & Tobe, M. 1985. Spontaneous diabetes-like syndrome in WBN/KOB rats. *Acta Diabetol.Lat.*, 22, (4) 335-342.

Negi, G., Kumar, A., Kaundal, R.K., Gulati, A., & Sharma, S.S. 2010. Functional and biochemical evidence indicating beneficial effect of Melatonin and Nicotinamide alone and in combination in experimental diabetic neuropathy. *Neuropharmacology*, 58, (3) 585-592.

Niacinamide.Monograph 2002. Niacinamide. Monograph. *Altern.Med.Rev.*, 7, (6) 525-529.

Nickander, K.K., McPhee, B.R., Low, P.A., & Tritschler, H. 1996. Alpha-lipoic acid: antioxidant potency against lipid peroxidation of neural tissues in vitro and implications for diabetic neuropathy. *Free Radic.Biol.Med.*, 21, (5) 631-639.

Niesner, R., Narang, P., Spiecker, H., Andresen, V., Gericke, K.H., & Gunzer, M. 2008a. Selective Detection of NADPH Oxidase in Polymorphonuclear Cells by Means of NAD(P)H-Based Fluorescence Lifetime Imaging. *J.Biophys.,* 2008, 602639.

Niesner, R.A., Andresen, V., & Gunzer, M. 2008b. Intravital two-photon microscopy: focus on speed and time resolved imaging modalities. *Immunol.Rev.*, 221, 7-25.

Nitti, M., Furfaro, A.L., Traverso, N., Odetti, P., Storace, D., Cottalasso, D., Pronzato, M.A., Marinari, U.M., & Domenicotti, C. 2007. PKC delta and NADPH oxidase in AGE-induced neuronal death. *Neurosci.Lett.*, 416, (3) 261-265.

Oates, P.J. 2002. Polyol pathway and diabetic peripheral neuropathy. *Int.Rev.Neurobiol.*, 50, 325-392.

Obrosova, I.G. 2002. How does glucose generate oxidative stress in peripheral nerve? *Int.Rev.Neurobiol.*, 50, 3-35.

Obrosova, I.G., Li, F., Abatan, O.I., Forsell, M.A., Komjati, K., Pacher, P., Szabo, C., & Stevens, M.J. 2004. Role of poly(ADP-ribose) polymerase activation in diabetic neuropathy. *Diabetes*, 53, (3) 711-720.

Obrosova, I.G., Drel, V.R., Pacher, P., Ilnytska, O., Wang, Z.Q., Stevens, M.J., & Yorek, M.A. 2005. Oxidative-nitrosative stress and poly(ADP-ribose) polymerase (PARP) activation in experimental diabetic neuropathy: the relation is revisited. *Diabetes,* 54, (12) 3435-3441.

Onorato,J.M.; Jenkins,A.J.; Thorpe,S.R.; Baynes,J.W. 2000. Pyridoxamine, an inhibitor of advanced glycation reactions, also inhibits advanced lipoxidation reactions. Mechanism of action of pyridoxamine. *J.Biol.Chem.*, 275, (28) 21177-21184.

Packer, L. 1994. Antioxidant properties of lipoic acid and its therapeutic effects in prevention of diabetes complications and cataracts. *Ann.N.Y.Acad.Sci.*, 738, 257-264.

Packer, L., Witt, E.H., & Tritschler, H.J. 1995. alpha-Lipoic acid as a biological antioxidant. *Free Radic.Biol.Med.*, 19, (2) 227-250.

Packer, L., Tritschler, H.J., & Wessel, K. 1997. Neuroprotection by the metabolic antioxidant alpha-lipoic acid. *Free Radic.Biol.Med.*, 22, (1-2) 359-378.

Papanas, N. & Ziegler, D. 2011. New diagnostic tests for diabetic distal symmetric polyneuropathy. *J.Diabetes Complications*, 25, (1) 44-51.

Parry, G.J. 1999. Management of diabetic neuropathy. *Am.J.Med.*, 107, (2B) 27S-33S.

Patterson, G.H., Knobel, S.M., Arkhammar, P., Thastrup, O., & Piston, D.W. 2000. Separation of the glucose-stimulated cytoplasmic and mitochondrial NAD(P)H responses in pancreatic islet beta cells. *Proc.Natl.Acad.Sci.U.S.A*, 97, (10) 5203-5207.

Pekiner, C., Cullum, N.A., Hughes, J.N., Hargreaves, A.J., Mahon, J., Casson, I.F., & McLean, W.G. 1993. Glycation of brain actin in experimental diabetes. *J.Neurochem.*, 61, (2) 436-442.

Pereira, R.V., de Miranda-Neto, M.H., da, S.S., I, & Zanoni, J.N. 2008. Vitamin E supplementation in rats with experimental diabetes mellitus: analysis of myosin-V and nNOS immunoreactive myenteric neurons from terminal ileum. *J.Mol.Histol.*, 39, (6) 595-603.

Phillips, R.J., Hargrave, S.L., Rhodes, B.S., Zopf, D.A., & Powley, T.L. 2004. Quantification of neurons in the myenteric plexus: an evaluation of putative pan-neuronal markers. *J.Neurosci.Methods*, 133, (1-2) 99-107.

Piston, D.W. & Knobel, S.M. 1999. Quantitative imaging of metabolism by two-photon excitation microscopy. *Methods Enzymol.*, 307, 351-368.

Piston, D.W., Fellers, T.J., and Davidson, M.W. 2012. Fundamentals and Applications in Multiphoton Excitation Microscopy. www.microscopyu.com/print/articles/fluorescence/multiphoton/multiphotonintro-print.html. Ref Type: Internet Communication

Pollak, N., Dolle, C., & Ziegler, M. 2007. The power to reduce: pyridine nucleotides--small molecules with a multitude of functions. *Biochem.J.*, 402, (2) 205-218.

Pop-Busui, R., Sima, A., & Stevens, M. 2006. Diabetic neuropathy and oxidative stress. *Diabetes Metab Res.Rev.*, 22, (4) 257-273.

Porter, A.J., Wattchow, D.A., Brookes, S.J.H., Costa, M. 1997. The neurochemical coding and projections of circular muscle motor neurons in the human colon. *Gastroenterology*, 113:1916–1923.

Powley, T.L. 2000. Vagal input to the enteric nervous system. *Gut*, 47 Suppl 4, iv30-iv32.

Price, D.L., Rhett, P.M., Thorpe, S.R., & Baynes, J.W. 2001. Chelating activity of advanced glycation end-product inhibitors. *J.Biol.Chem.*, 276, (52) 48967-48972.

Qu, Z.D., Thacker, M., Castelucci, P., Bagyánszki, M., Epstein, M.L., Furness, J.B. 2008. Immunohistochemical analysis of neuron types in the mouse small intestine. *Cell Tissue Res*, 334:147–161.

Quinson, N., Robbins, H.L., Clark, M.J., & Furness, J.B. 2001. Calbindin immunoreactivity of enteric neurons in the guinea-pig ileum. *Cell Tissue Res.*, 305, (1) 3-9.

Rabbani, N., Alam, S.S., Riaz, S., Larkin, J.R., Akhtar, M.W., Shafi, T., & Thornalley, P.J. 2009. High-dose thiamine therapy for patients with type 2 diabetes and microalbuminuria: a randomised, double-blind placebo-controlled pilot study. *Diabetologia*, 52, (2) 208-212.

Rabbani, N. & Thornalley, P.J. 2011. Emerging role of thiamine therapy for prevention and treatment of early-stage diabetic nephropathy. *Diabetes Obes.Metab*, 13, (7) 577-583.

Raff, M. C. 2002. Axonal self-destruction and neurodegeneration. *Science*, 296, (5569) 868-871.

Reed, L.J., DeBusk, B.G., Gunsalus, I.C., & Hornberger, C.S., Jr. 1951. Crystalline alpha-lipoic acid; a catalytic agent associated with pyruvate dehydrogenase. *Science*, 114, (2952) 93-94.

Risso, A., Mercuri, F., Quagliaro, L., Damante, G., & Ceriello, A. 2001. Intermittent high glucose enhances apoptosis in human umbilical vein endothelial cells in culture. *Am.J.Physiol Endocrinol.Metab*, 281, (5) E924-E930.

Rocheleau, J.V., Head, W.S., & Piston, D.W. 2004. Quantitative NAD(P)H/flavoprotein autofluorescence imaging reveals metabolic mechanisms of pancreatic islet pyruvate response. *J.Biol.Chem.*, 279, (30) 31780-31787.

Rosen, P., Nawroth, P.P., King, G., Moller, W., Tritschler, H.J., & Packer, L. 2001. The role of oxidative stress in the onset and progression of diabetes and its complications: a summary of a Congress Series sponsored by UNESCO-MCBN, the American Diabetes Association and the German Diabetes Society. *Diabetes Metab Res.Rev.*, 17, (3) 189-212.

Rubart, M. 2004. Two-photon microscopy of cells and tissue. *Circ.Res.*, 95, (12) 1154-1166.

Ruhl, A. 2005. Glial cells in the gut. *Neurogastroenterol.Motil.*, 17, (6) 777-790.

Russell, J.W. & Feldman, E.L. 1999. Insulin-like growth factor-I prevents apoptosis in sympathetic neurons exposed to high glucose. *Horm.Metab Res.*, 31, (2-3) 90-96.

Russell, J.W., Sullivan, K.A., Windebank, A.J., Herrmann, D.N., & Feldman, E.L. 1999. Neurons undergo apoptosis in animal and cell culture models of diabetes. *Neurobiol.Dis.*, 6, (5) 347-363.

Russell, J.W., Golovoy, D., Vincent, A.M., Mahendru, P., Olzmann, J.A., Mentzer, A., & Feldman, E.L. 2002. High glucose-induced oxidative stress and mitochondrial dysfunction in neurons. *FASEB J.*, 16, (13) 1738-1748.

Ryle, C. & Donaghy, M. 1995. Non-enzymatic glycation of peripheral nerve proteins in human diabetics. *J.Neurol.Sci.*, 129, (1) 62-68.

Ryle, C., Leow, C.K., & Donaghy, M. 1997. Nonenzymatic glycation of peripheral and central nervous system proteins in experimental diabetes mellitus. *Muscle Nerve*, 20, (5) 577-584.

Rühl A. 2005. Glial cells in the gut. *Neurogastroenterol Motil.*, 17, (6):777-90.

Saito, N., Kimura, M., Kuchiba, A., & Itokawa, Y. 1987. Blood thiamine levels in outpatients with diabetes mellitus. *J.Nutr.Sci.Vitaminol.(Tokyo)*, 33, (6) 421-430.

Salem, H.M. 1954. Glyoxalase and methylglyoxal in thiamine-deficient rats. *Biochem.J.*, 57, (2) 227-230.

Samsom, M. & Smout, A.J. 1997. Abnormal gastric and small intestinal motor function in diabetes mellitus. *Dig.Dis.*, 15, (4-5) 263-274.

Samsom, M., Roelofs, J.M., Akkermans, L.M., van Berge Henegouwen, G.P., & Smout, A.J. 1998. Proximal gastric motor activity in response to a liquid meal in type I diabetes mellitus with autonomic neuropathy. *Dig.Dis.Sci.*, 43, (3) 491-496.

Sandgren, K., Lin, Z., Fex, S.A., & Ekblad, E. 2003. Vasoactive intestinal peptide and nitric oxide promote survival of adult rat myenteric neurons in culture. *J.Neurosci.Res.*, 72, (5) 595-602.

Sang, Q. & Young, H.M. 1996. Chemical coding of neurons in the myenteric plexus and external muscle of the small and large intestine of the mouse. *Cell Tissue Res*, 284:39–53.

Sango, K., Horie, H., Sotelo, J.R., & Takenaka, T. 1991. A high glucose environment improves survival of diabetic neurons in culture. *Neurosci.Lett.*, 129, (2) 277-280.

Sango, K., Horie, H., Saito, H., Ajiki, K., Tokashiki, A., Takeshita, K., Ishigatsubo, Y., Kawano, H., & Ishikawa, Y. 2002. Diabetes is not a potent inducer of neuronal cell death in mouse sensory ganglia, but it enhances neurite regeneration in vitro. *Life Sci.*, 71, (20) 2351-2368.

Schafer, K.H. & Mestres, P. 1997. Human newborn and adult myenteric plexus grows in different patterns. *Cell Mol.Biol.(Noisy.-le-grand)*, 43, (8) 1171-1180.

Schemmel, K.E., Padiyara, R.S., & D'Souza, J.J. 2010. Aldose reductase inhibitors in the treatment of diabetic peripheral neuropathy: a review. *J.Diabetes Complications*, 24, (5) 354-360.

Schenes-Furry, J., Perrone-Bizzozero, N., & Jasmin, B.J. 2006. The RNA-binding protein HuD: a regulator of neuronal differentiation, maintenance and plasticity. *Bioessays*, 28, (8) 822-833.

Schmeichel, A.M., Schmelzer, J.D., & Low, P.A. 2003. Oxidative injury and apoptosis of dorsal root ganglion neurons in chronic experimental diabetic neuropathy. *Diabetes*, 52, (1) 165-171.

Schmid, U., Stopper, H., Heidland, A., & Schupp, N. 2008. Benfotiamine exhibits direct antioxidative capacity and prevents induction of DNA damage in vitro. *Diabetes Metab Res.Rev.*, 24, (5) 371-377.

Schmidt, R.E. & Plurad, S.B. 1986. Ultrastructural and biochemical characterization of autonomic neuropathy in rats with chronic streptozotocin diabetes. *J. Neuropathol. Exp. Neurol.*, 45, (5) 525-544.

Schmidt, R.E. & Cogswell, B.E. 1989. Tyrosine hydroxylase activity in sympathetic nervous system of rats with streptozocin-induced diabetes. *Diabetes*, 38, (8) 959-968.

Schmidt, R.E., Plurad, S.B., Parvin, C.A., & Roth, K.A. 1993. Effect of diabetes and aging on human sympathetic autonomic ganglia. *Am.J.Pathol.*, 143, (1) 143-153.

Schmidt, R.E., Dorsey, D.A., Beaudet, L.N., Reiser, K.M., Williamson, J.R., & Tilton, R.G. 1996. Effect of aminoguanidine on the frequency of neuroaxonal dystrophy in the superior mesenteric sympathetic autonomic ganglia of rats with streptozocin-induced diabetes. *Diabetes*, 45, (3) 284-290.

Schmidt, R.E. 1996. Neuropathology of human sympathetic autonomic ganglia. *Microsc.Res.Tech.*, 35, (2) 107-121.

Schmidt, R.E., Dorsey, D., Parvin, C.A., Beaudet, L.N., Plurad, S.B., & Roth, K.A. 1997. Dystrophic axonal swellings develop as a function of age and diabetes in human dorsal root ganglia. *J.Neuropathol.Exp.Neurol.*, 56, (9) 1028-1043.

Schmidt, R.E., Dorsey, D.A., Roth, K.A., Parvin, C.A., Hounsom, L., & Tomlinson, D.R. 2000. Effect of streptozotocin-induced diabetes on NGF, P75(NTR) and TrkA content of prevertebral and paravertebral rat sympathetic ganglia. *Brain Res.*, 867, (1-2) 149-156.

Schmidt, R.E. 2001. Neuronal preservation in the sympathetic ganglia of rats with chronic streptozotocin-induced diabetes. *Brain Res.*, 921, (1-2) 256-259.

Schmidt, R.E. 2002. Neuropathology and pathogenesis of diabetic autonomic neuropathy. *Int.Rev.Neurobiol.*, 50, 257-292.

Schmidt, R.E., Dorsey, D.A., Beaudet, L.N., Frederick, K.E., Parvin, C.A., Plurad, S.B., & Levisetti, M.G. 2003. Non-obese diabetic mice rapidly develop dramatic sympathetic neuritic dystrophy: a new experimental model of diabetic autonomic neuropathy. *Am.J.Pathol.*, 163, (5) 2077-2091.

Schmidt, R.E., Dorsey, D.A., Beaudet, L.N., Parvin, C.A., Zhang, W., & Sima, A.A. 2004. Experimental rat models of types 1 and 2 diabetes differ in sympathetic neuroaxonal dystrophy. *J.Neuropathol.Exp.Neurol.*, 63, (5) 450-460.

Sedeek, M., Montezano, A.C., Hebert, R.L., Gray, S.P., Di, M.E., Jha, J.C., Cooper, M.E., Jandeleit-Dahm, K., Schiffrin, E.L., Wilkinson-Berka, J.L., & Touyz, R.M. 2012.

Oxidative stress, nox isoforms and complications of diabetes-potential targets for novel therapies. *J.Cardiovasc.Transl.Res*., 5, (4) 509-518.

Semra, Y.K., Smith, N.C., & Lincoln, J. 2004. Comparative effects of high glucose on different adult sympathetic neurons in culture. *Neuroreport*, 15, (15) 2321-2325.

Semra, Y.K., Wang, M., Peat, N.J., Smith, N.C., Shotton, H.R., & Lincoln, J. 2006. Selective susceptibility of different populations of sympathetic neurons to diabetic neuropathy in vivo is reflected by increased vulnerability to oxidative stress in vitro. *Neurosci.Lett*., 407, (3) 199-204.

Semra, Y.K., Sherif, S., & Lincoln, J. 2009. NGF protects paravertebral but not prevertebral sympathetic neurons against exposure to high glucose in vitro. *Brain Res*., 1285, 164-173.

Shakil, A., Church, R.J., & Rao, S.S. 2008. Gastrointestinal complications of diabetes. *Am.Fam.Physician*, 77, (12) 1697-1702.

Shangari, N. & O'Brien, P.J. 2004. The cytotoxic mechanism of glyoxal involves oxidative stress. *Biochem.Pharmacol*., 68, (7) 1433-1442.

Shangari, N., Mehta, R., & O'Brien, P.J. 2007. Hepatocyte susceptibility to glyoxal is dependent on cell thiamin content. *Chem.Biol.Interact.*, 165, (2) 146-154.

Shay, K.P., Moreau, R.F., Smith, E.J., Smith, A.R., & Hagen, T.M. 2009. Alpha-lipoic acid as a dietary supplement: molecular mechanisms and therapeutic potential. *Biochim.Biophys.Acta*, 1790, (10) 1149-1160.

Shen, C.C., Huang, H.M., Ou, H.C., Chen, H.L., Chen, W.C., & Jeng, K.C. 2004. Protective effect of nicotinamide on neuronal cells under oxygen and glucose deprivation and hypoxia/reoxygenation. *J.Biomed.Sci.*, 11, (4) 472-481.

Shotton, H.R., Clarke, S., & Lincoln, J. 2003. The effectiveness of treatments of diabetic autonomic neuropathy is not the same in autonomic nerves supplying different organs. *Diabetes*, 52, (1) 157-164.

Shotton, H.R., Broadbent, S., & Lincoln, J. 2004. Prevention and partial reversal of diabetes-induced changes in enteric nerves of the rat ileum by combined treatment with alpha-lipoic acid and evening primrose oil. *Auton.Neurosci.*, 111, (1) 57-65.

Shotton, H.R. & Lincoln, J. 2006. Diabetes only affects nitric oxide synthase-containing myenteric neurons that do not contain heme oxygenase 2. *Brain Res.*, 1068, (1) 248-256.

Shotton, H.R., Adams, A., & Lincoln, J. 2007. Effect of aminoguanidine treatment on diabetes-induced changes in the myenteric plexus of rat ileum. *Auton.Neurosci.*, 132, (1-2) 16-26.

Shotton, H.R. 2008. Diabetic Autonomic Neuropathy in the Gastrointestinal Tract. PhD Thesis, University of London.

Shotton, H.R., Lincoln, J., & McGorum, B.C. 2011. Effects of Equine Grass Sickness on Sympathetic Neurons in Prevertebral and Paravertebral Ganglia. *J.Comp Pathol.*, 145, (1), 35-44.

Shuttleworth, C.W., Brennan, A.M., & Connor, J.A. 2003. NAD(P)H fluorescence imaging of postsynaptic neuronal activation in murine hippocampal slices. *J.Neurosci.*, 23, (8) 3196-3208.

Shuttleworth, C.W. 2010. Use of NAD(P)H and flavoprotein autofluorescence transients to probe neuron and astrocyte responses to synaptic activation. *Neurochem.Int.*, 56, (3) 379-386.

Singh, U. & Jialal, I. 2008. Alpha-lipoic acid supplementation and diabetes. *Nutr.Rev.*, 66, (11) 646-657.

Sinnreich, M., Taylor, B.V., & Dyck, P.J. 2005. Diabetic neuropathies. Classification, clinical features, and pathophysiological basis. *Neurologist.*, 11, (2) 63-79.

Skala, M.C., Riching, K.M., Bird, D.K., Gendron-Fitzpatrick, A., Eickhoff, J., Eliceiri, K.W., Keely, P.J., & Ramanujam, N. 2007a. In vivo multiphoton fluorescence lifetime imaging of protein-bound and free nicotinamide adenine dinucleotide in normal and precancerous epithelia. *J.Biomed.Opt.*, 12, (2) 024014.

Skala, M.C., Riching, K.M., Gendron-Fitzpatrick, A., Eickhoff, J., Eliceiri, K.W., White, J.G., & Ramanujam, N. 2007b. In vivo multiphoton microscopy of NADH and FAD redox states, fluorescence lifetimes, and cellular morphology in precancerous epithelia. *Proc.Natl.Acad.Sci.U.S.A*, 104, (49) 19494-19499.

Smith, T.K., Spencer, N.J., Hennig, G.W., & Dickson, E.J. 2007. Recent advances in enteric neurobiology: mechanosensitive interneurons. *Neurogastroenterol.Motil.*, 19, (11) 869-878.

Snell, R. S. 2010. Clinical Neuroanatomy. 7 ed. Baltimore, Philadelphia, USA: Lippincott Williams & Wilkins, pp. 397-426.

Spangeus, A., Suhr, O., & El-Salhy, M. 2000. Diabetic state affects the innervation of gut in an animal model of human type 1 diabetes. *Histol.Histopathol.*, 15, (3) 739-744.

Spangeus, A. & El-Salhy, M. 2001. Myenteric plexus of obese diabetic mice (an animal model of human type 2 diabetes). *Histol.Histopathol.*, 16, (1) 159-165.

Spencer, N.J. & Smith, T.K. 2001. Simultaneous intracellular recordings from longitudinal and circular muscle during the peristaltic reflex in guinea-pig distal colon. *J.Physiol*, 533, (Pt 3) 787-799.

Spencer, P.S. & Schaumburg, H.H. 1977a. Ultrastructural studies of the dying-back process. III. The evolution of experimental peripheral giant axonal degeneration. *J.Neuropathol.Exp.Neurol.*, 36, (2) 276-299.

Spencer, P.S. & Schaumburg, H.H. 1977b. Ultrastructural studies of the dying-back process. IV. Differential vulnerability of PNS and CNS fibers in experimental central-peripheral distal axonopathies. *J.Neuropathol.Exp.Neurol.*, 36, (2) 300-320.

Sreenan, S., Pick, A.J., Levisetti, M., Baldwin, A.C., Pugh, W., & Polonsky, K.S. 1999. Increased beta-cell proliferation and reduced mass before diabetes onset in the nonobese diabetic mouse. *Diabetes*, 48, (5) 989-996.

Srinivasan, S., Stevens, M., & Wiley, J.W. 2000. Diabetic peripheral neuropathy: evidence for apoptosis and associated mitochondrial dysfunction. *Diabetes*, 49, (11) 1932-1938.

Stevens, M.J., Obrosova, I., Cao, X., Van, H.C., & Greene, D.A. 2000. Effects of DL-alpha-lipoic acid on peripheral nerve conduction, blood flow, energy metabolism, and oxidative stress in experimental diabetic neuropathy. *Diabetes*, 49, (6) 1006-1015.

Stevens, M.J., Li, F., Drel, V.R., Abatan, O.I., Kim, H., Burnett, D., Larkin, D., & Obrosova, I.G. 2007. Nicotinamide reverses neurological and neurovascular deficits in streptozotocin diabetic rats. *J.Pharmacol.Exp.Ther.*, 320, (1) 458-464.

Stracke, H., Lindemann, A., & Federlin, K. 1996. A benfotiamine-vitamin B combination in treatment of diabetic polyneuropathy. *Exp.Clin.Endocrinol.Diabetes*, 104, (4) 311-316.

Stracke, H., Hammes, H.P., Werkmann, D., Mavrakis, K., Bitsch, I., Netzel, M., Geyer, J., Kopcke, W., Sauerland, C., Bretzel, R.G., & Federlin, K.F. 2001. Efficacy of benfotiamine versus thiamine on function and glycation products of peripheral nerves in diabetic rats. Exp.Clin.Endocrinol.Diabetes, 109, (6) 330-336.

Sud, D., Zhong, W., Beer, D.G., & Mycek, M.A. 2006. Time-resolved optical imaging provides a molecular snapshot of altered metabolic function in living human cancer cell models. *Opt.Express*, 14, (10) 4412-4426.

Sugimoto, K., Nishizawa, Y., Horiuchi, S., & Yagihashi, S. 1997. Localization in human diabetic peripheral nerve of N(epsilon)-carboxymethyllysine-protein adducts, an advanced glycation endproduct. *Diabetologia*, 40, (12) 1380-1387.

Sugimoto, K. & Yagihashi, S. 1997. Effects of aminoguanidine on structural alterations of microvessels in peripheral nerve of streptozotocin diabetic rats. *Microvasc.Res.,* 53, (2) 105-112.

Suji, G. & Sivakami, S. 2006. DNA damage by free radical production by aminoguanidine. *Ann.N.Y.Acad.Sci*., 1067, 191-199.

Suji, G. & Sivakami, S. 2007. DNA damage during glycation of lysine by methylglyoxal: assessment of vitamins in preventing damage. *Amino.Acids*, 33, (4) 615-621.

Szurszewski, J.H. 1981. Physiology of mammalian prevertebral ganglia. *Annu.Rev.Physiol*, 43, 53-68.

Tadrous, P.J. 2000. Methods for imaging the structure and function of living tissues and cells: 2. Fluorescence lifetime imaging. *J.Pathol*., 191, (3) 229-234.

Takahashi, T., Nakamura, K., Itoh, H., Sima, A.A., & Owyang, C. 1997. Impaired expression of nitric oxide synthase in the gastric myenteric plexus of spontaneously diabetic rats. *Gastroenterology*, 113, (5) 1535-1544.

Takahashi, T. 2003. Pathophysiological significance of neuronal nitric oxide synthase in the gastrointestinal tract. *J.Gastroenterol*., 38, (5) 421-430.

Tang, J., Wingerchuk, D.M., Crum, B.A., Rubin, D.I., & Demaerschalk, B.M. 2007. Alpha-lipoic acid may improve symptomatic diabetic polyneuropathy. *Neurologist*., 13, (3) 164-167.

Tankova, T., Koev, D., & Dakovska, L. 2004. Alpha-lipoic acid in the treatment of autonomic diabetic neuropathy (controlled, randomized, open-label study). *Rom.J.Intern.Med.*, 42, (2) 457-464.

The Diabetes Control and Complications Trial Research Group 1993. The effect of intensive treatment of diabetes on the development and progression of long-term complications in insulin-dependent diabetes mellitus. *N.Engl.J.Med.*, 329, (14) 977-986.

Theriault, M., Dort, J., Sutherland, G., & Zochodne, D.W. 1997. Local human sural nerve blood flow in diabetic and other polyneuropathies. *Brain*, 120 (Pt 7), 1131-1138.

Thiamine.Monograph 2003. Thiamine. Monograph. *Altern.Med.Rev.*, 8, (1) 59-62.

Thomas, P.K. 1997. Classification, differential diagnosis, and staging of diabetic peripheral neuropathy. *Diabetes*, 46 Suppl 2, S54-S57.

Thornalley, P.J., Yurek-George, A., & Argirov, O.K. 2000. Kinetics and mechanism of the reaction of aminoguanidine with the alpha-oxoaldehydes glyoxal, methylglyoxal, and 3-deoxyglucosone under physiological conditions. *Biochem.Pharmacol.*, 60, (1) 55-65.

Thornalley, P. J., Jahan, I., & Ng, R. 2001. Suppression of the accumulation of triosephosphates and increased formation of methylglyoxal in human red blood cells during hyperglycaemia by thiamine in vitro, *J.Biochem.*,129, (4) 543-549.

Thornalley, P.J. 2002. Glycation in diabetic neuropathy: characteristics, consequences, causes, and therapeutic options. *Int.Rev.Neurobiol.*, 50, 37-57.

Thornalley, P.J. 2003a. Glyoxalase I--structure, function and a critical role in the enzymatic defence against glycation. *Biochem.Soc.Trans.*, 31, (Pt 6) 1343-1348.

Thornalley, P.J. 2003b. Use of aminoguanidine (Pimagedine) to prevent the formation of advanced glycation endproducts. *Arch.Biochem.Biophys.*, 419, (1) 31-40.

Thornalley, P.J. 2005. Dicarbonyl intermediates in the maillard reaction. *Ann.N.Y.Acad.Sci.*, 1043, 111-117.

Thornalley, P.J., Babaei-Jadidi, R., Al, A.H., Rabbani, N., Antonysunil, A., Larkin, J., Ahmed, A., Rayman, G., & Bodmer, C.W. 2007. High prevalence of low plasma thiamine concentration in diabetes linked to a marker of vascular disease. *Diabetologia*, 50, (10) 2164-2170.

Timmermans, J-P., Barbiers, M., Scheuermann, D.W., Stach, W., Adriaensen, D., Mayer, B., De Groodt Lasseel, M.H.A. 1994. Distribution pattern, neurochemical features and projections of nitrergic neurons in the pig small intestine. *Ann Anat*, 176:515–525.

Tischler, M.E., Friedrichs, D., Coll, K., & Williamson, J.R. 1977. Pyridine nucleotide distributions and enzyme mass action ratios in hepatocytes from fed and starved rats. *Arch.Biochem.Biophys.*, 184, (1) 222-236.

Tolkovsky, A. 2002. Apoptosis in diabetic neuropathy. *Int.Rev.Neurobiol.*, 50, 145-159.

Tomlinson, D.R. 1999. Mitogen-activated protein kinases as glucose transducers for diabetic complications. *Diabetologia*, 42, (11) 1271-1281.

Tomlinson, D.R. & Gardiner, N.J. 2008a. Diabetic neuropathies: components of etiology. *J.Peripher.Nerv.Syst.*, 13, (2) 112-121.

Tomlinson, D.R. & Gardiner, N.J. 2008b. Glucose neurotoxicity. *Nat.Rev.Neurosci.*, 9, (1) 36-45.

Toth, C., Rong, L.L., Yang, C., Martinez, J., Song, F., Ramji, N., Brussee, V., Liu, W., Durand, J., Nguyen, M.D., Schmidt, A.M., & Zochodne, D.W. 2008. Receptor for advanced glycation end products (RAGEs) and experimental diabetic neuropathy. *Diabetes*, 57, (4) 1002-1017.

Tougas, G., Hunt, R.H., Fitzpatrick, D., & Upton, A.R. 1992. Evidence of impaired afferent vagal function in patients with diabetes gastroparesis. *Pacing Clin.Electrophysiol.*, 15, (10 Pt 2) 1597-1602.

Traverso, N., Menini, S., Cosso, L., Odetti, P., Albano, E., Pronzato, M.A., & Marinari, U.M. 1998. Immunological evidence for increased oxidative stress in diabetic rats. *Diabetologia*, 41, (3) 265-270.

Turk, Z. 2010. Glycotoxines, carbonyl stress and relevance to diabetes and its complications. *Physiol Res.*, 59, (2) 147-156.

UK Prospective Diabetes Study Group 1998. Intensive blood-glucose control with sulphonylureas or insulin compared with conventional treatment and risk of complications in patients with type 2 diabetes (UKPDS 33). *Lancet*, 352, (9131) 837-853.

Unlucerci, Y., Kocak, H., Seferoglu, G., & BekpInar, S. 2001. The effect of aminoguanidine on diabetes-induced inactivation of kidney Na(+),K(+)- ATPase in rats. *Pharmacol.Res.*, 44, (2) 95-98.

Valko, M., Leibfritz, D., Moncol, J., Cronin, M.T., Mazur, M., & Telser, J. 2007. Free radicals and antioxidants in normal physiological functions and human disease. *Int.J.Biochem.Cell Biol.*, 39, (1) 44-84.

Van Munster, E.B. & Gadella, T.W. 2005. Fluorescence lifetime imaging microscopy (FLIM). *Adv.Biochem.Eng Biotechnol.*, 95, 143-175.

Verkhratsky, A. & Fernyhough, P. 2008. Mitochondrial malfunction and Ca2+ dyshomeostasis drive neuronal pathology in diabetes. *Cell Calcium*, 44, (1) 112-122.

Vincent, A.M., Brownlee, M., & Russell, J.W. 2002. Oxidative stress and programmed cell death in diabetic neuropathy. *Ann.N.Y.Acad.Sci.*, 959, 368-383.

Vincent, A.M. & Feldman, E.L. 2004. New insights into the mechanisms of diabetic neuropathy. *Rev.Endocr.Metab Disord*., 5, (3) 227-236.

Vincent, A.M., Olzmann, J.A., Brownlee, M., Sivitz, W.I., & Russell, J.W. 2004a. Uncoupling proteins prevent glucose-induced neuronal oxidative stress and programmed cell death. *Diabetes*, 53, (3) 726-734.

Vincent, A.M., Russell, J.W., Low, P., & Feldman, E.L. 2004b. Oxidative stress in the pathogenesis of diabetic neuropathy. *Endocr.Rev*., 25, (4) 612-628.

Vincent, A.M., McLean, L.L., Backus, C., & Feldman, E.L. 2005a. Short-term hyperglycemia produces oxidative damage and apoptosis in neurons. *FASEB J.*, 19, (6) 638-640.

Vincent, A.M., Stevens, M.J., Backus, C., McLean, L.L., & Feldman, E.L. 2005b. Cell culture modeling to test therapies against hyperglycemia-mediated oxidative stress and injury. *Antioxid.Redox.Signal.*, 7, (11-12) 1494-1506.

Vincent, A.M., Perrone, L., Sullivan, K.A., Backus, C., Sastry, A.M., Lastoskie, C., & Feldman, E.L. 2007a. Receptor for advanced glycation end products activation injures primary sensory neurons via oxidative stress. *Endocrinology*, 148, (2) 548-558.

Vincent, A.M., Russell, J.W., Sullivan, K.A., Backus, C., Hayes, J.M., McLean, L.L., & Feldman, E.L. 2007b. SOD2 protects neurons from injury in cell culture and animal models of diabetic neuropathy. *Exp.Neurol*., 208, (2) 216-227.

Vincent, A.M., Hayes, J.M., McLean, L.L., Vivekanandan-Giri, A., Pennathur, S., & Feldman, E.L. 2009. Dyslipidemia-induced neuropathy in mice: the role of oxLDL/LOX-1. *Diabetes*, 58, (10) 2376-2385.

Vindedzis, S.A., Stanton, K.G., Sherriff, J.L., & Dhaliwal, S.S. 2008. Thiamine deficiency in diabetes - is diet relevant? *Diab.Vasc.Dis.Res*., 5, (3) 215.

Vinik, A.I., Maser, R.E., Mitchell, B.D., & Freeman, R. 2003. Diabetic autonomic neuropathy. *Diabetes Care*, 26, (5) 1553-1579.

Vlassara, H., Brownlee, M., & Cerami, A. 1981. Nonenzymatic glycosylation of peripheral nerve protein in diabetes mellitus. *Proc.Natl.Acad.Sci.U.S.A*, 78, (8) 5190-5192.

Voukali, E., Shotton, H.R., & Lincoln, J. 2011. Selective responses of myenteric neurons to oxidative stress and diabetic stimuli. *Neurogastroenterol.Motil.*, 23, (10) 964-e411.

Wada, R., Sugo, M., Nakano, M., & Yagihashi, S. 1999. Only limited effects of aminoguanidine treatment on peripheral nerve function, (Na+,K+)-ATPase activity and thrombomodulin expression in streptozotocin-induced diabetic rats. *Diabetologia*, 42, (6) 743-747.

Wada, R. & Yagihashi, S. 2005. Role of advanced glycation end products and their receptors in development of diabetic neuropathy. *Ann.N.Y.Acad.Sci.*, 1043, 598-604.

Wahlberg, G., Adamson, U., & Svensson, J. 2000. Pyridine nucleotides in glucose metabolism and diabetes: a review. *Diabetes Metab Res.Rev.*, 16, (1) 33-42.

Wakita, M., Nishimura, G., & Tamura, M. 1995. Some characteristics of the fluorescence lifetime of reduced pyridine nucleotides in isolated mitochondria, isolated hepatocytes, and perfused rat liver in situ. *J.Biochem.*, 118, (6) 1151-1160.

Walters, J.R., Bishop, A.E., Facer, P., Lawson, E.M., Rogers, J.H., & Polak, J.M. 1993. Calretinin and calbindin-D28k immunoreactivity in the human gastrointestinal tract. *Gastroenterology*, 104, (5) 1381-1389.

Wang, H.S. & McKinnon, D. 1995. Potassium currents in rat prevertebral and paravertebral sympathetic neurones: control of firing properties. *J.Physiol*, 485 (Pt 2), 319-335.

Wang, H.W., Gukassyan, V., Chen, C.T., Wei, Y.H., Guo, H.W., Yu, J.S., & Kao, F.J. 2008. Differentiation of apoptosis from necrosis by dynamic changes of reduced nicotinamide adenine dinucleotide fluorescence lifetime in live cells. *J.Biomed.Opt.*, 13, (5) 054011.

Watkins, C.C., Sawa, A., Jaffrey, S., Blackshaw, S., Barrow, R.K., Snyder, S.H., & Ferris, C.D. 2000. Insulin restores neuronal nitric oxide synthase expression and function that is lost in diabetic gastropathy. *J.Clin.Invest*, 106, (3) 373-384.

Weimer, L.H. 2010. Autonomic testing: common techniques and clinical applications. *Neurologist.*, 16, (4) 215-222.

Williams, S.K., Howarth, N.L., Devenny, J.J., & Bitensky, M.W. 1982. Structural and functional consequences of increased tubulin glycosylation in diabetes mellitus. *Proc.Natl.Acad.Sci.U.S.A*, 79, (21) 6546-6550.

Wood, J.D. 1994. Application of classification schemes to the enteric nervous system. *J.Auton.Nerv.Syst.*, 48, (1) 17-29.

Wood, J.D., Alpers, D.H., & Andrews, P.L. 1999. Fundamentals of neurogastroenterology. *Gut*, 45 Suppl 2, II6-II16.

Wood, J.D. 2007. Neuropathophysiology of functional gastrointestinal disorders. World *J.Gastroenterol.*, 13, (9) 1313-1332.

Wood, J.D. 2008. Enteric nervous system: reflexes, pattern generators and motility. *Curr.Opin.Gastroenterol.*, 24, (2) 149-158.

Worl, J., Mayer, B., & Neuhuber, W.L. 1994. Nitrergic innervation of the rat esophagus: focus on motor endplates. *J.Auton.Nerv.Syst.*, 49, (3) 227-233.

Wrzos, H.F., Cruz, A., Polavarapu, R., Shearer, D., & Ouyang, A. 1997. Nitric oxide synthase (NOS) expression in the myenteric plexus of streptozotocin-diabetic rats. *Dig.Dis.Sci.*, 42, (10) 2106-2110.

Wu, G., Fang, Y.Z., Yang, S., Lupton, J.R., & Turner, N.D. 2004. Glutathione metabolism and its implications for health. *J.Nutr.*, 134, (3) 489-492.

Yagihashi, S. & Sima, A.A. 1985. Diabetic autonomic neuropathy. The distribution of structural changes in sympathetic nerves of the BB rat. *Am.J.Pathol.*, 121, (1) 138-147.

Yagihashi, S., Kamijo, M., Baba, M., Yagihashi, N., & Nagai, K. 1992. Effect of aminoguanidine on functional and structural abnormalities in peripheral nerve of STZ-induced diabetic rats. *Diabetes*, 41, (1) 47-52.

Yan, S.D., Schmidt, A.M., Anderson, G.M., Zhang, J., Brett, J., Zou, Y.S., Pinsky, D., & Stern, D. 1994. Enhanced cellular oxidant stress by the interaction of advanced glycation end products with their receptors/binding proteins. *J.Biol.Chem.*, 269, (13) 9889-9897.

Yang, J., Klaidman, L.K., Nalbandian, A., Oliver, J., Chang, M.L., Chan, P.H., & Adams, J.D., Jr. 2002. The effects of nicotinamide on energy metabolism following transient focal cerebral ischemia in Wistar rats. *Neurosci.Lett.*, 333, (2) 91-94.

Yang, S.H., Sharrocks, A.D., & Whitmarsh, A.J. 2003. Transcriptional regulation by the MAP kinase signaling cascades. *Gene*, 320, 3-21.

Yenilmez, A., Ozcifci, M., Aydin, Y., Turgut, M., Uzuner, K., & Erkul, A. 2006. Protective effect of high-dose thiamine (B1) on rat detrusor contractility in streptozotocin-induced diabetes mellitus. *Acta Diabetol.*, 43, (4) 103-108.

Ying, W. 2008. NAD+/NADH and NADP+/NADPH in cellular functions and cell death: regulation and biological consequences. *Antioxid.Redox.Signal.*, 10, (2) 179-206.

Yorek, M.A., Coppey, L.J., Gellett, J.S., Davidson, E.P., & Lund, D.D. 2004. Effect of fidarestat and alpha-lipoic acid on diabetes-induced epineurial arteriole vascular dysfunction. *Exp.Diabesity.Res.*, 5, (2) 123-135.

Yoshida, M.M., Schuffler, M.D., & Sumi, S.M. 1988. There are no morphologic abnormalities of the gastric wall or abdominal vagus in patients with diabetic gastroparesis. *Gastroenterology*, 94, (4) 907-914.

Yu, T., Robotham, J.L., & Yoon, Y. 2006. Increased production of reactive oxygen species in hyperglycemic conditions requires dynamic change of mitochondrial morphology. *Proc.Natl.Acad.Sci.U.S.A*, 103, (8) 2653-2658.

Zandecki, M., Vanden, B.P., Depoortere, I., Geboes, K., Peeters, T., Janssens, J., & Tack, J. 2008. Characterization of myenteric neuropathy in the jejunum of spontaneously diabetic BB-rats. *Neurogastroenterol.Motil.*, 20, (7) 818-828.

Zherebitskaya, E., Akude, E., Smith, D.R., & Fernyhough, P. 2009. Development of selective axonopathy in adult sensory neurons isolated from diabetic rats: role of glucose-induced oxidative stress. *Diabetes*, 58, (6) 1356-1364.

Ziegler, D., Schatz, H., Conrad, F., Gries, F.A., Ulrich, H., & Reichel, G. 1997. Effects of treatment with the antioxidant alpha-lipoic acid on cardiac autonomic neuropathy in NIDDM patients. A 4-month randomized controlled multicenter trial (DEKAN Study). Deutsche Kardiale Autonome Neuropathie. *Diabetes Care*, 20, (3) 369-373.

Ziegler, D. 2001. Diagnosis and treatment of diabetic autonomic neuropathy. *Curr.Diab.Rep.*, 1, (3) 216-227.

Ziegler, D., Nowak, H., Kempler, P., Vargha, P., & Low, P.A. 2004. Treatment of symptomatic diabetic polyneuropathy with the antioxidant alpha-lipoic acid: a meta-analysis. *Diabet.Med.*, 21, (2) 114-121.

Ziegler, D., Low, P.A., Litchy, W.J., Boulton, A.J., Vinik, A.I., Freeman, R., Samigullin, R., Tritschler, H., Munzel, U., Maus, J., Schutte, K., & Dyck, P.J. 2011. Efficacy and Safety of Antioxidant Treatment With {alpha}-Lipoic Acid Over 4 Years in Diabetic Polyneuropathy: The NATHAN 1 Trial. *Diabetes Care*, 34, (9) 2054-60.

Zigmond, R.E. & Sun, Y. 1997. Regulation of neuropeptide expression in sympathetic neurons. Paracrine and retrograde influences. *Ann.N.Y.Acad.Sci.*, 814, 181-197.

Zipfel, W.R., Williams, R.M., & Webb, W.W. 2003. Nonlinear magic: multiphoton microscopy in the biosciences. *Nat.Biotechnol.*, 21, (11) 1369-1377.

Zochodne, D.W. 2007. Diabetes mellitus and the peripheral nervous system: manifestations and mechanisms. *Muscle Nerve*, 36, (2) 144-166.

Zochodne, D.W., Verge, V.M., Cheng, C., Sun, H., & Johnston, J. 2001. Does diabetes target ganglion neurones? Progressive sensory neurone involvement in long-term experimental diabetes. *Brain*, 124, (Pt 11) 2319-2334.

Zucker, L.M. 1965. Hereditary obesity in the rat associated with hyperlipemia. *Ann.N.Y.Acad.Sci.*, 131, (1) 447-458.